CHARACTERISATION OF TOMATO MADS-BOX GENES INVOLVED IN FLOWER AND FRUIT DEVELOPMENT

A thesis presented in partial fulfilment of the requirements for the degree of

Doctor of Philosophy

in

Plant Biology

at

Massey University, Palmerston North, New Zealand

CHARLES AMPOMAH-DWAMENA

2001

Abstract

MADS-box genes encode transcription factors that are involved in various aspects of plant development, by regulating target genes that control morphogenesis. Over the last decade, plant MADS-box genes have been studied extensively to reveal their control of floral development, especially in the model plants *Arabidopsis* and *Antirrhinum*. Their functions are however, not restricted to the flower but are involved in various aspects of plant development (Rounsley et al., 1995; Jack, 2001). By virtue of their extensive roles in the flower, these genes are expected to function in fruit development, which is a progression from flower morphogenesis. The aim of this study was to examine the role of MADS-box genes during flower and fruit development.

Two new members of the tomato MADS-box gene family, *TM10* and *TM29* were identified. *TM29* was isolated from a young fruit cDNA library by screening with homologous MADS-box fragments and *TM10* was amplified by polymerase chain reaction from fruit cDNA templates. These genes were characterised by sequence and RNA expression patterns and their functions examined using molecular genetic techniques. Sequence analyses confirmed that both genes belong to the MADS-box family.

TM29 shows 68% amino acid sequence identity to *Arabidopsis* SEP1 MADS-box protein. *TM29* expression pattern showed similarities as well as differences to *SEP1* (Flanagan and Ma, 1994). *TM29* is expressed in shoot, inflorescence and floral meristems unlike *SEP1*, which is expressed exclusively in floral meristems (Flanagan and Ma, 1994). *TM29* is expressed in all the four whorls of the flower. During floral

organ development, it is highly expressed at early stages of the organ primordium but decreases as the organ differentiates and matures. In the mature flower bud, *TM29* is expressed in the anther and ovary pericarp. During fruit development, *TM29* is expressed from anthesis ovary to fruit of 14 days post-anthesis with its transcript localised to the pericarp and placenta.

TM10 showed 64% amino acid identity to *Arabidopsis* AGL12, across the entire sequence. This notwithstanding, *TM10* expression differed from *AGL12*. *TM10* was expressed in shoot tissues of tomato and was not detected in roots. In contrast, the *AGL12* gene transcript was only present in the roots of *Arabidopsis* (Rounsley et al., 1995). Expression was detected in leaves, shoot growing tips, floral buds and fruit. During fruit development, *TM10* is expressed in anthesis ovary and in fruits at different growth stages.

The functions of *TM29* and *TM10* were examined by transgenic techniques and phenotypes generated were consistent with their spatial and temporal gene expression patterns. *TM29* transgenic phenotypes suggested it might be involved in the control of sympodial growth, transition to flowering, proper development of floral organs, parthenocarpic fruit development and maintenance of floral meristem identity. *TM10* affected apical dominance and flowering time, development of floral organs and parthenocarpic fruit development.

HortResearch

Massey University
Institute of Molecular
BioSciences

Acknowledgements

I give thanks and honour to the One and True God, from whom all blessings flow, for his guidance and protection during my studies towards this thesis.

I am very grateful to HortResearch for funding this research project and also to the Institute of Molecular BioSciences, Massey University for the support I received.

I am indebted to my supervisors, **Dr. Bruce Veit**, **Dr Jialong-Yao**, **Dr Bret Morris** for their advice and critical assessments which contributed in no small measure to the project and this thesis. I also thank **Prof. Paula Jameson** who readily agreed to be my Chief Supervisor during the difficult phase of this PhD (when my three supervisors "deserted" me) and showed concern for my general well-being.

For people at HortResearch, particularly members of the defunct Gene Transfer and Expression Group and the Plant Development Group, I want to thank you all for your contributions. I give special thanks to Andrew Gleave, Dan Cohen and Bart Janssen for their advice and help; to Julie Nichols for taking good care of the plants in the glasshouse, Martin Heffer and Sharlene Cookson for the beautiful photographs and posters, Paul

Sutherland and Anna Henderson for the Scanning Electron Microscopy work. Thank you Lesley Beuning and Ross Atkinson, I appreciate your encouragement during this study. My gratitude goes to Dr Richard Newcomb, who as the Science Capability Leader of the Plant Health and Development Group supported my research project to the very end.

I also thank family and friends for their support and encouragement; to my wife Mercy for enduring the long hours I spent away from home studying; to Kofi, Florence and those on their way, Daddy says thanks. I thank my mum Florence for coming to help look after the kids; this no doubt offered me more time to spend on my studies. My gratitude to Yeboah and Leigh Asiamah for their genuine friendship and hospitality, which was instrumental to my "**Coming to Auckland**" expedition. Thank you for your friendship. To all members of Hope, Auckland, many thanks for your prayers, best wishes and support for my family. I am grateful to all my friends in Christchurch, Massa Frank and Auntie B, Charles and Anne, Freddie Ghanaman and family, the Yamoahs, Ama Nketiah, the Reveleys and all those who consistently kept us in their thoughts and prayers.

Note: The genetic experimentation in this project was conducted with approval from the appropriate authority (Protocol No. GMO 00-HRA 037).

Table of contents

List of figures

List of tables

List of Abbreviations

µg	microgram
µl	microlitre
µM	micromolar
A_{260}	absorbance at 260 nm
BA	Benzyl aminopurine
bp	basepairs
CaMV	Cauliflower mosaic virus
cm	centimetres
CTAB	cethyltrimethylammonium bromide
CTP	cytidine-5-triphosphate
cv	cultivar
d.p.a	days post-anthesis
dCTP	deoxycytidine-5-triphosphate
DEPC	diethylpyrocarbonate
DIG	digoxigenin
DMSO	dimethyl sulphoxide
DNA	deoxyribonucleic acid
dNTP	deoxy-nucleotide triphosphate
DTT	dithiothreitol
E. coli	*Escherichia coli*
EDTA	ethylene diaminetetraacetic acid
g	gram
GA	gibberellic acid
IBA	indoyl butyric acid
IPTG	isopropylthiogalactoside
kb	kilobasepairs
l	litre
LB	Luria Bertani
mg	milligram
mins	minutes

ml	millilitre
mM	millimolar
MOPS	N morpholino propane-sulfonic acid
mRNA	Messenger RNA
NAA	naphthalene acetic acid
ng	nanogram
nm	nanometer
nptII	neomycin phosphotransferase II
OD	optimal density
Oligo	Oligonucleotide
ORF	open reading frame
PBS	phosphate buffered saline
PCR	polymerase chain reaction
pH	-logarithm $[H^+]$
RACE	rapid amplification of cDNA ends
RNase	ribonuclease
RT-PCR	Reverse transcriptase-PCR
s	seconds
SDS	sodium dodecyl sulphate
TAE	Tris acetate ethylene diaminetetraacetic acid
T-DNA	transfer-DNA
TE	Tris ethylene diaminetetraacetic acid
Tris	tris(hydroxymethyl)aminomethane
UTR	untranslated region
UV	ultraviolet
V	Volts
v	volume
X-gal	5-bromo-4-chloro-3-indoyl-ß-D-galactopyranoside
Z	zeatin

CHAPTER 1 INTRODUCTION

1.1 MADS-box genes

MADS-box genes are a super-family of genes found in fungi, plants and animals that encode transcription factors with a highly conserved domain called the MADS-box or the MADS domain. The acronym "**MADS**" is acquired from the first four isolated members of this family, namely, ***M****inichromosome maintenance 1* (***M****CM1*; from yeast), *AGAMOUS* (*AG*; from *Arabidopsis thaliana*), ***D****EFICIENS* (***D****EF*; from *Antirrhinum majus*) and ***S****erum response* factor (***S****RF*; from humans) (Schwarz-Sommer *et al.*, 1990; Shore and Sharrocks, 1995). The MADS domain is a 56-58 amino acid motif involved in DNA binding and dimerization in these transcription factors (Krizek and Meyerowitz, 1996; Davies *et al.*, 1999; Figure 1.1).

Figure 1.1 Alignment of the MADS-box sequence motif of the first four members of the MADS-box family: MCM1, AG, DEF and SRF.

MADS-box genes function as part of key regulatory mechanisms that control important developmental pathways (Mouradov *et al.*, 1998; Alvarez-Buylla *et al.*, 2000). The *MCM1* is an essential gene in yeast, required to regulate mating-type specific genes and also to support the growth and maintain the viability of the cell (Passmore *et al.*, 1988; Acton *et al.*, 2000). The SRF is a nuclear protein, in animals that binds to the serum response element, which is required for transient transcriptional activation of genes in response to growth factors (Norman *et al.*, 1988). The *AG* and *DEF* genes are involved in genetic control of flower development; mutations in these genes cause homeotic transformations of floral organs. (Sommer *et al.*, 1990; Yanofsky *et al.*, 1990). In general, two distinct MADS-box sequences are identified in animals and fungi: the SRF-like and MEF2 (myocyte enhancer factor 2)-like classes (Shore and Sharrocks, 1995; Alvarez-Buylla *et al.*, 2000). The MEF2 proteins are a group of MADS-box transcription factors that play a key role in myogenesis and morphogenesis of muscle cells (Huang *et al.*, 2000).

1.1.1 The structure of MADS-box proteins

The general structure of the proteins encoded by MADS-box genes comprises the core DNA binding MADS domain and a poorly conserved C-terminal region, which carry a transcriptional activation domain (Huang *et al.*, 2000). The SRF protein has the MADS-box and a so-called "**SAM**" (SRF, **A**G and **M**CM1) domain adjacent to the c-terminus of the MADS-box. MEF2 has a DNA binding core with two sub-domains: the first part is a 56 amino acid portion representing the MADS-box and the second part is MEF2 domain of 29 residues (Huang *et al.*, 2000). Extensive X-ray crystallography studies indicate the structure of the MADS-box in SRF, MCM1 and MEF2 are very similar (Pellegrini *et al.*, 1995; Tan and Richmond, 1998; Huang *et al.*, 2000; Figure1.2). Due to the high level of amino acid sequence identity within the MADS-domain, these structures are used as prototypes for the rest of the MADS-box family.

SRF, MCM1 and MEF2 proteins bind DNA as homodimers. They have a compact layered structure of three distinct units stacked above the other with each unit in the monomer interacting with the same motif in the other subunit (Figure 1.2). The primary DNA-binding element of MADS-box proteins is an antiparallel coiled-coil of two α-helices, one from each monomer and makes contact with the phosphate backbone of the DNA (Pelligrini *et al.*, 1995). The second structural motif is a four-stranded antiparallel ß-sheet on top of the coiled-coil and forms the central element of the dimerization surface. The third structural component is an irregular helical-coiled structure followed by a short α-helix folded over the ß-sheet. In MEF2, the third component differs from that of SRF and MCM1 in that the α-helix precedes the random coiled structure (Huang *et al.*, 2000; Figure 1.2).

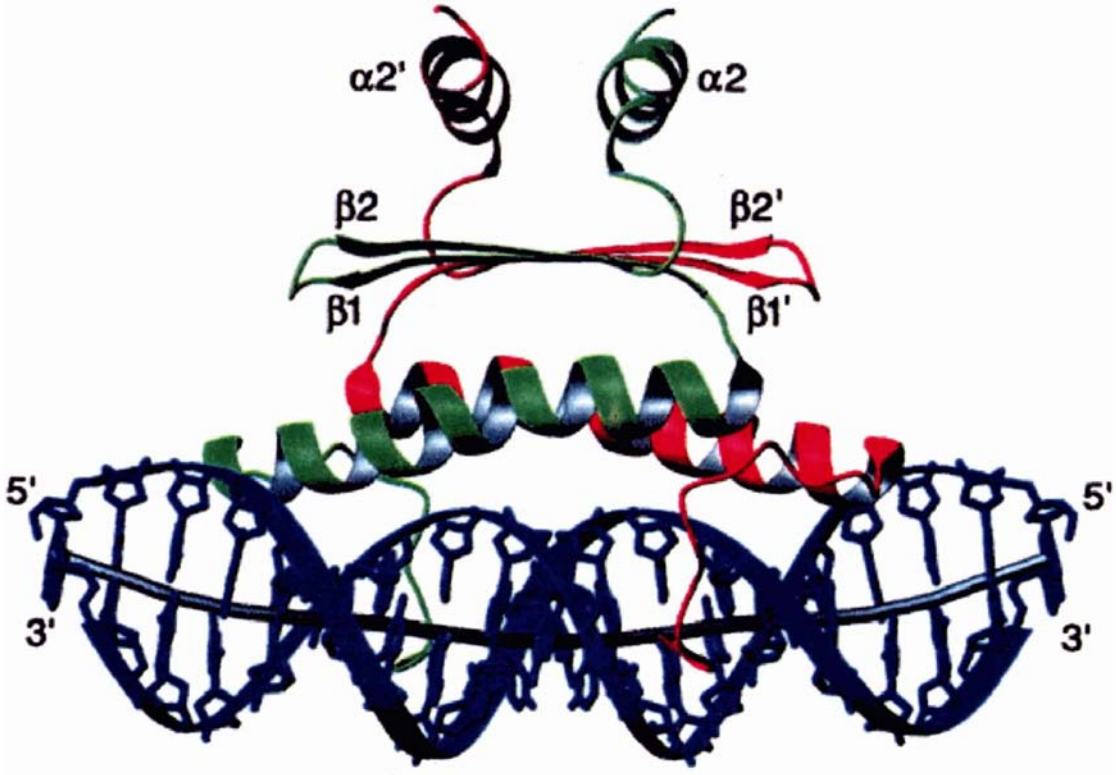

Figure 1.2. A representation of the crystal structure of the myocyte enhancer factor 2 (MEF2) bound to DNA (Huang *et al.*, 2000). The two MEF2 monomers are represented in red and green, the double-stranded DNA in blue. The antiparallel coiled-coil of the α-helices makes contact with the phosphate DNA backbone. The second structural motif is a four-stranded ß-sheet. The third structure is a short α-helix followed by a helically coiled structure.

Plant MADS-box proteins differ in structure to those in animals and fungi. The majority of plant MADS-box proteins have, in addition to the MADS domain, the moderately conserved K domain. This domain is characterised by a conserved regular spacing of hydrophobic residues, which are proposed to allow for the formation of an amphipathic helix and mediate in protein-protein interactions (Ma *et al.*, 1991; Pneuli *et al.*, 1991). The short intervening (I) region joins the K domain to the MADS-box and followed by the variable C-terminal region. The plant MADS-box genes are therefore unique with respect to the **MIKC** structure.

Although, none of the plant MADS-box genes have their structure determined by x-ray crystallography the high level of sequence similarities among these proteins suggests plant MADS-box proteins would have similar crystal structures as those described for the SRF, MCM1 and MEF2 proteins. However, because of the presence of the second conserved domain (K domain) it is also possible that the plant proteins may display different structures.

1.1.2 The domains in plant MADS-box proteins

The distinct regions of plant MADS-box proteins are individually significant to the functions of these proteins. In *AGAMOUS* and other closely related proteins, there is a short terminal region (N) that precedes the MADS-box (Figure 1.3). Studies have revealed the significance of these regions.

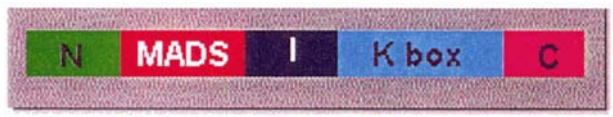

Figure 1.3. The structure of plant MADS-box proteins. The MADS domain (56-58 amino acids) is preceded by an amino terminal extension (N) in the case of AG and related proteins. The intergenic (I) region, the K-box and a carboxyl terminal region follow the conserved MADS domain.

The MADS domain is the most conserved of all the regions in MADS-box proteins. This domain is required for DNA binding and dimerization (Riechmann *et al.*, 1996). The highly conserved nature of the MADS-box in the diverse organisms suggests that their basic features of structure and function have been conserved among members of this family. Plant MADS-box proteins bind to their targets either as homodimers or as heterodimers (Eagea-Cortines *et al.*, 1999). The ability to form dimers is therefore, essential to the functions of these proteins. Truncated AG proteins which lacked part or all of the MADS domain fail to bind DNA or form dimers (Mizukami *et al.*, 1996). This is consistent with the SRF, MCM1 and MEF2 MADS domain, which are required in DNA binding and dimerization (Pellegrini *et al.*, 1995; Huang *et al.*, 2000).

The conserved nature of the MADS domain in this gene family also, suggests that the regions other than the MADS-box have the responsibility of conferring specificity to their binding properties. In experiments involving domain swapping of MADS-box proteins, chimeric gene constructs which had the MADS domain of APETALA3 (AP3)

and PISTILLATA (PI) replaced with that of AG caused the same phenotypes as the AP3, PI proteins respectively (Krizek and Meyerowitz, 1996). This indicated the MADS domain may not be required to confer functional specificity, at least in the contexts of some plant MADS-box proteins.

The intervening (I) region varies both in sequence and length (27 to 42 amino residues) among MADS-box proteins (Riechmann and Meyerowitz, 1997). The I-region is an essential part of the minimal DNA binding domain and a key molecular determinant for specificity in protein dimerization (Riechmann *et al.*, 1996; Riechmann *et al.*, 1997). The MADS domain together with the I-region can sufficiently form dimers and bind DNA *in vitro*. In a deletion analysis of AG protein the MADS domain with only the I-region formed dimers and was able to bind DNA *in vitro* (Mizukami *et al.*, 1996). The variation within the I-region among MADS-box proteins may also define the specificity attached to the function of each MADS-box protein. In a domain swapping experiment to determine the functional specificity of MADS domain proteins, the I-region (also referred to as the linker L) was a defining factor in conferring specificity to the proteins (Krizek and Meyerowitz, 1996).

The K-box was named for its similarity to the coiled-coil segment of keratin and is predicted to form amphipathic α-helices (Ma *et al.*, 1991; Pneuli *et al.*, 1991). It may mediate protein-protein interactions and also promote dimerization through interactions between K-boxes of different proteins. The role of the K-box in protein interactions was observed in the deletion studies of MADS-box proteins. In a yeast two-hybrid screening, a partial fragment consisting of the K-box and C-region of AG protein was able to interact with certain MADS-box proteins, AGAMOUS-LIKE (AGL) 2, AGL4, AGL6 and AGL9 (Fan *et al.*, 1997), confirming the function of the K domain during protein interactions. This result is however, qualified by other results that show that in certain contexts the K-box can be dispensable. The removal of the K-box from AGL2 protein did not affect heterodimerization with other MADS-box proteins (Huang *et al.*, 1996; Mizukami *et al.*, 1996). In *Arabidopsis* APETALA1 (AP1) and AG proteins, domain swapping outside the MADS domain does not affect functional specificity of these two proteins (Krizek and Meyerowitz, 1996).

The significance of the K-box *in vivo* is indicated by the ectopic expression of truncated MADS-box genes. The expression of an AG construct encoding protein lacking the K-

domain and C region did not cause conversion of perianth organ to reproductive organs, as is the case with ectopic expression of full-length AG construct; rather, this truncated construct resulted in a dominant-negative mutant phenotype (Mizukami *et al.*, 1996). The implication here is the K-box and C-region may be required for the *in vivo* function of MADS-box proteins.

The C-terminal region is the most variable segment of the MADS-box proteins both in sequence and in length (Reichmann and Meyerowitz, 1997). The C-terminal region of some MADS-box proteins has been suggested to act as a transcriptional activation domain, citing the glutamine-rich regions present in some C-terminal regions (Reichmann and Meyerowitz, 1997). A truncated AG protein consisting of the K and C regions was able to activate transcription of Gal4 in yeast, suggesting the presence of an activation domain (Ma *et al.*, 1991; Fan *et al.*, 1997). This is in agreement with the C-terminal region of MEF2 protein, which carries a transcriptional activation domain (Huang *et al.*, 2000). The C-region may play important functions *in vivo* (Mizukami *et al.*, 1996).

1.1.3 MADS-box proteins are transcription factors

MADS-box proteins SRF and MCM1 are known transcription factors that are involved in DNA binding, DNA bending, activation of transcription and interaction with other proteins. The SRF protein binds DNA *in vitro* and able to activate the transcription of serum response element *in vitro* (Norman *et al.*, 1988). Similarly, the MCM1 protein binds to DNA *in vitro* and has been shown to activate gene expression *in vivo* (Acton *et al.*, 2000). In general, proteins with the MADS domain sequence are considered as transcription factors (Riechmann and Meyerowitz, 1997). The most significant features of transcription factors are their DNA binding and ability to recognise a promoter target sequence (Schwechheimer *et al.*, 1998).

In vitro sequence selection has been used to determine DNA recognition sequences of MADS-box proteins. The SRF and MCM1 recognise a consensus sequence $CC(A/T)_6GG$ referred to as the CArG box (Pellegrini *et al.*, 1995; Acton *et al.*, 2000), to

which plant MADS-box proteins also bind with a certain level of sequence specificity (Huang *et al.*, 1995; Huang *et al.*, 1996; Mizukami, *et al.*, 1996). The MCM1 and SRF proteins recognise $CC(A/T)_6GG$ while MEF2 recognise $CTA(A/T)_4TAG$ (Pollock and Treisman, 1991). AG and AGL1 proteins recognise $CC(A/T)_4NNGG$ while AGL2 and AGL3 binds $CC(A/T)_4T(A/G)G$ (Huang *et al.*, 1993; Huang *et al.*, 1995; Huang *et al.*, 1996).

1.1.4 MADS-box proteins form complexes

MADS-box proteins interact to bind DNA as dimers *in vitro*, which may be between monomers of the same proteins to form homodimers or between different protein species to form heterodimers. The SRF and MEF2 proteins both form homodimers to bind DNA *in vitro* (Pellegrini *et al.*, 1995; Huang *et al.*, 2000). The *Arabidopsis* MADS-box proteins APETALA3 (AP3) AND PISTILLATA (PI) form heterodimers (Riechmann *et al.*, 1996). In *Antirrhinum*, the MADS-box protein SQUAMOSA (SQUA) homodimerise *in vitro* while DEFICIENS (DEF) and GLOBOSA (GLO) form heterodimers to bind CArG box sequences (Egea-Cortines *et al.*, 1999). However, it is possible that larger complexes may be formed by MADS-box factors to control events *in vivo*. SQUA, DEF and GLO formed a DNA binding complex in yeast to bind DNA with this complex displaying greater binding affinity than the separate homo- or heterodimers formed by these proteins (Egea-Cortines *et al.*, 1999). The formation of higher complexes is supported by recent reports, which found the PI and AP3 MADS-box proteins form a heterodimer to interact with *AG* and *SEP3* proteins (Honma and Goto, 2001; Theißen and Saedler, 2001).

1.2 Plant MADS-box genes

Plants appear to have a large family of MADS-box genes and with the completed sequence of the *Arabidopsis* genome, it is now known that there are at least 80 MADS-box genes in *Arabidopsis* (Alvarez-Buylla *et al.*, 2000; Riechmann *et al.*, 2000; Jack, 2001a). The first characterised plant MADS-box gene was *AGAMOUS* in *Arabidopsis* (Yanofsky *et al.*, 1990). Its structural similarity with well characterised regulatory factors such as SRF and MCM1 suggested it functions as a transcriptional regulator. More members isolated afterwards were identified as regulators of floral organ identity (Mandel *et al.*, 1992; Bradley *et al.*, 1993; Davies *et al.*, 1999). However, they have since been found to control additional developmental processes such as meristem identity, root development, fruit characteristics and flowering time (Rounsley *et al.*, 1995; Carmona *et al.*, 1998; Zhang and Forde, 1998). In addition to angiosperms, MADS-box genes can be found in gymnosperms and ferns. These three plant divisions represent seeded and non-seeded plants, and suggest the diversity of function of MADS-box genes (Becker *et al.*, 2000).

1.2.1 MADS-box genes in angiosperms

Angiosperms are the large class of flowering plants that bear seed in enclosed carpel. They fall into two main groups: the monocotyledonous and dicotyledonous plants. The MADS-box gene family in these plants has been the subject of intense studies. Most of these studies, however, have centred on the model plant *Arabidopsis* with suggestions that homologues of these genes in other plants may have similar characteristics. The majority of the angiosperm MADS-box proteins show sequence similarity to the MEF2 protein; this group also carries the typical **MIKC** structure. Recently, a small number of MADS-box genes with SRF-like sequences have been isolated in plants. This group

lacks the K domain due to the absence of conserved residues that predict the coiled-coil structure (Alvarez-Buylla *et al.* 2000). In animals and fungi, both the SRF and the MEF2-type proteins lack the K domain. The presence of the coiled-coil K-domain in the majority of plant MADS-box proteins suggests that the K domain is significant to the developmental processes in plants.

The MADS-box gene family in angiosperms is divided into well-defined clades whose members share sequence homology, similar expression patterns and related functions. Following the observation that MADS-box genes control specific functions in flower development, the major floral homeotic genes were found to be grouped into phylogenetic clades that define the various floral organ identity functions (Purugganan *et al.*, 1995). Such gene clades included genes from different plant species indicating MADS-box genes (from different plant species) with similar functions are more similar to each other than they are to other MADS-box genes having different functions (Purugganan *et al.*, 1995; Ma and dePamphilis, 2000).

The gene clades that defined the floral organ identity functions included the *AP1/AGL9* group that involved members such as *APETALA1*, *CAULIFLOWER* (*CAL*), *SQUA*, which control floral meristem identity and specifies the identity of sepals. Similarly, the *AP3/PI* clade contain members involved in specifying the identity of petals and stamens while the *AGAMOUS* (*AG*) clade included *Antirrhinum PLENA* (*PLE*) which controls carpel identity (Lawton-Rauh *et al.* 2000). Subsequent to the identification of more MADS-box genes in *Arabidopsis*, more gene groups have been described. Based on these precedents, newly isolated MADS-box genes are often assigned putative functions based on sequence similarity (Kater *et al.*, 1998; Perl-Treves *et al.*, 1998) and in some cases genes with redundant functions can be predicted (Liljegren *et al.*, 2000).

However, this linkage between functional and sequence similarity is not strictly followed. The *Arabidopsis AGL1* gene has high sequence similarity with *AG* but these two genes have different expression patterns and play different roles in *Arabidopsis* (Yanofsky *et al.*, 1990; Flanagan *et al.*, 1996; Liljegren *et al.*, 2000). Similarly, within the *AP1* clade, *AGL3* is expressed in leaves and stems (Rounsley *et al.*, 1995). The *AP3/PI* clade includes the *SHORT VEGETATIVE PHASE* (*SVP*) gene which is not involved in petal and stamen identity but expressed in inflorescence meristems, stems and leaves and controls flowering time (Hartmann *et al.*, 2000). Subsequent to the

identification of more MADS-box genes in *Arabidopsis*, seven new clades have been described (Alvarez-Buylla *et al.*, 2000b).

1.2.2 MADS-box genes in gymnosperms

MADS-box genes have been identified in gymnosperms. Gymnosperms and angiosperms together constitute spermatophytes, or seed plants. Gymnosperms are characterised by strobili (cones), which are morphologically distinct from flowers (Theissen *et al.*, 2000). They produce 'naked seeds', which are not enclosed in carpel but are formed from ovules borne on the adaxial surface of ovuliferous scales. The ovuliferous scale develops from a primordium within the axil of a sterile bract. MADS-box studies in gymnosperms have focused on conifers and gnetophytes. Studies in conifers have shown that there are at least 27 MADS-box genes in *Picea mariana* (Rutledge *et al.*, 1998).

The MADS-box genes in gymnosperms have similar structure (**MIKC**) to those in angiosperms. MADS-box genes isolated from *Pinus radiata*, *Picea abies*, *Picea mariana* and *Gnetum gnemon* have sequence similarities to MADS-box genes in angiosperms. Phylogenetic analyses of these genes from gymnosperms put them into same gene clades with members from angiosperms (Mouradov *et al.*, 1998; Rutledge *et al.*, 1998; Tandre *et al.*, 1998; Becker *et al.*, 2000). Also, gymnosperm MADS-box genes have similar expressions to their homologues in angiosperms. The spatial expression of an *AG* homologue (*SAG1*) in *Picea mariana*, was found to be cone specific. Transcripts were detected in the tapetal layer in male cones and in the developing ovuliferous scales in female cones (Rutledge *et al.*, 1998). These reproductive structures (cones) are the equivalent of stamen and carpel in *Arabidopsis*, in which *AG* is expressed. Similarly, the *PI/AP3*-like genes in *Pinus radiata* are found to be specific to the male strobili (Mouradov *et al.*, 1999); while the *PI/AP3* genes are involved in specification of petal and stamen identities in *Arabidopsis*. The expression characteristics of these genes in gymnosperms can therefore be related to their counterparts in angiosperms and suggest that their functions have been conserved. Like the MADS-box genes in angiosperms, the expression of MADS-box genes in gymnosperms can also be found in vegetative structures. At least three of the MADS-

box genes identified in *Gnetum gnemon* were expressed in vegetative structures (Rounsley *et al.*, 1995; Becker *et al.*, 2000).

The conservation of function between gymnosperms and angiosperms is observed when genes from gymnosperms are overexpressed in *Arabidopsis*. Heterologous expression of *SAG1* in *Arabidopsis* caused homeotic conversions of sepals to carpels and petals to stamens (Rutledge *et al.*, 1998). Similarly, overexpression of *DAL2* (an *AG* homologue) from *Picea abies* in *Arabidopsis*, caused similar homeotic conversions (Tandre *et al.*, 1998). These developmental alterations are similar to those caused by ectopic expression of *AG* in *Arabidopsis* (Mizukami and Ma, 1992) and suggest a certain level of conservation in gene activity among the MADS-box genes of angiosperms and gymnosperms. The initial analyses of identified members of the MADS-box family in gymnosperms, indicate conservation of gene structure, expression and function with angiosperms despite the morphological divergence between the structures present in these two plant divisions.

1.2.3 MADS-box genes in ferns

Ferns are primitive vascular plants with very simple reproductive structures that lack all accessory floral organs. They produce naked sporangia on the abaxial surface of leaves. The sporangium contains spore mother cells that form the haploid reproductive spores (Hasebe *et al.*, 1998). Ferns do not form ovules or seeds and do not aggregate their sporophylls into flower-like structures. Despite these structural variations, the MADS-box genes identified in ferns share similar characteristics with those in angiosperms and gymnosperms. Members identified so far have the **MIKC** domain structure (Munster *et al.*, 1997; Hasebe *et al.*, 1998). This is an indication that the fern MADS-box proteins are under similar functional constraints as those of seed plants (Munster *et al.*, 1997). Some members of the fern MADS-box gene family display certain features typical of angiosperm MADS-box genes. The members of the CMADS1 subfamily display additional amino terminal residues, which is seen with the *AG* group of MADS-box genes in angiosperms (Yanofsky *et al.*, 199[illegible]; Hasebe *et al.*, 1998). Despite some sequence similarities, the fern MADS-box genes do not group into same phylogenetic clades with MADS-box genes from gymnosperms and angiosperms (Baum, 1998;

Theissen *et al.*, 2000). Phylogenetic analyses show that the MADS-box genes from ferns form a separate clade and do not cluster with any MADS-box gene group in seed plants (Hasebe *et al.*, 1998; Theissen *et al.*, 2000) meaning they cannot be described as orthologues of MADS-box genes in seed plants. It is suggested, therefore, that the fern and seed plant MADS-box genes share a common ancestor from which members of both groups were independently derived by gene duplications, sequence diversification and fixation (Munster *et al.*, 1997; Hasebe *et al.*, 1998).

1.3 MADS-box genes in vegetative development

In addition to their known roles in reproductive development, there is some evidence suggesting that MADS-box genes have functions in vegetative development. Such indications come from their diverse expression patterns in vegetative tissues. MADS-box genes are expressed in embryo tissues and suggest they may be involved in the early events of plant life cycle. The *Arabidopsis AGL15* gene is expressed in octant stage embryos (Heck *et al.*, 1995). Similarly, transcripts of the *AGL2* and *MdMADS4* accumulate in embryos of developing seeds (Flanagan and Ma, 1994; Sung et al., 2000). Though the functions of these genes in the embryo are not clearly illustrated, these expression patterns suggest they may be involved in regulating events in embryo development.

The expressions of some MADS-box genes are specific to shoot or root tissues suggesting their involvement in vegetative development. The *Arabidopsis AGL3* is expressed in shoot tissues but not found in roots (Huang *et al.*, 1995); the *AGL11* and *AGL13* are expressed in rosette leaves of *Arabidopsis* suggesting that they may control the development of these tissues (Rounsley *et al.*, 1995). The *AGL12*, *AGL14* and *AGL17* genes are expressed in roots but are not detected in other organs (Rounsley *et*

al., 1995). Also, *AGL16* and *AGL19* transcripts are localised to specific tissues in roots with *AGL16* expressed in the epidermal cells while *AGL19* is expressed in the columella and lateral root cap (Alvarez-Buylla *et al.*, 2000a). These genes may regulate the response of root growth to environmental stimuli similar to the nitrate inducible *ANR1* MADS-box gene of *Arabidopsis*. *ANR1* was found to control the response of root growth to nitrate rich zones (Zhang and Forde, 1998).

In *Solanum tuberosum*, the expression of *STMADS11* was detected in all the vegetative parts of the plant (Carmona *et al.*, 1998). Similarly, *STMADS16* was expressed in stems and its overexpression in tobacco affected vegetative growth (Garcia-Maroto *et al.*, 2000). In petunia, overexpression of the *FLORAL BINDING PROTEIN 20* (*FBP20*) conferred leaf-like characteristics to floral organs, suggesting a role in maintaining vegetative identity (Ferrario *et al.*, 2000). These examples give indications that MADS-box genes are involved in vegetative development and more studies will illustrate the roles played by these genes.

1.4 MADS-box genes and flower development

Plant MADS-box genes are widely known for their functions in flower development. The first isolated members, *AGAMOUS* and *DEFICIENS* both function to specify floral organ identity. Subsequently, a large number of MADS-box genes have been identified, especially in *Arabidopsis thaliana*, with most studies focussed on the roles of these genes in flower development.

1.4.1 Stages of plant reproductive phase

The reproductive phase of flowering plants involves at least three initial steps: transition to flowering, initiation of individual flowers and floral patterning (Ma *et al.*, 1994). The transition to flowering involves a switch from the vegetative phase, during which shoots and leaves are produced, to the reproductive phase, where flowers are initiated. In general, the transition to flowering is influenced by developmental programs and pathways that respond to environmental cues. Four pathways are known to influence flowering time; these are the photoperiod pathway, vernalization promotion pathway, the gibberellic acid promotion pathway, and the autonomous pathway (Levy and Dean, 1998; Blazquez, 2000; Figure 1.4). The photoperiod and vernalization promotion pathways mediate signals from the environment, light and temperature respectively. The gibberellin pathway is responsive to GA biosynthesis whereas the autonomous pathway controls flowering irrespective of environmental conditions (Wilson *et al.*, 1992; Blazquez *et al.*, 1998; Pineiro and Coupland, 1998).

1.4.2 MADS-box genes regulate the switch to reproductive phase

There are at least five MADS-box genes involved in the regulation of flowering time in *Arabidopsis*: *SUPPRESSOR OF OVEREXPRESSION OF CO 1* (*SOC1*), *SHORT VEGETATIVE PHASE* (*SVP*), *FLOWERING LOCUS C* (*FLC*), *FLOWERING LOCUS M* (*FLM*) and *FRUITFULL* (*FUL*). These genes either promote or repress flowering. *SOC1* and *FUL* act to promote flowering (Bonhomme *et al.*, 2000; Samach *et al.*, 2000) whereas *FLC*, *FLM* and *SVP* are inhibitors of flowering (Sheldon *et al.*, 2000; Scortecci *et al.*, 2001).

SOC1 acts as an integrator of the autonomous, photoperiod and vernalization floral promotion pathways in *Arabidopsis* (Araki, 2001; Lee *et al.*, 2000; Figure 1.4). *SOC1* expression responds positively to long-day photoperiods. Loss of *SOC1* function suppresses early flowering phenotype of *Arabidopsis* plants overexpressing the *CONSTANS* gene, which normally promotes flowering under long days (Samach *et al.*, 2000). Also, *SOC1* expression is downregulated by a mutation in *FCA*, a gene that is

involved in both the vernalisation and autonomous flowering pathways, suggesting that *FCA* positively regulates *SOC1* (Samach *et al.*, 2000; Lee *et al.*, 2000). These observations support the suggestion that *SOC1* integrates the photoperiod, vernalisation and autonomous floral promotion pathways. Interestingly, the GA pathway may also regulate the expression of *SOC1*. GA_3 application on wild type *Arabidopsis* plants caused an increase in *SOC1* expression (Borner *et al.*, 2000).

FLC is involved in the vernalisation and autonomous pathways in *Arabidopsis*. Mutations in *FLC* result in early flowering, thus indicating that the role of the wild type *FLC* is to repress flowering (Michaels and Amasino, 1999). Vernalisation or cold treatment promotes flowering in late-flowering *Arabidopsis* plants, possibly through a direct effect on *FLC* transcripts and protein. This is supported by a strong negative correlation between *FLC* transcripts and vernalisation (Sheldon *et al.*, 2000). However, vernalisation may not affect flowering solely through *FLC*. This is because *flc* null mutants still respond to cold treatment by flowering early suggesting the presence of *FLC*-dependent and *FLC*-independent vernalisation pathways in *Arabidopsis* (Michaels and Amasino, 2001).

SVP and *FLM* are recently identified MADS-box genes that repress flowering in *Arabidopsis* by acting independent of environmental factors (Hartmann *et al.*, 2000; Scortecci *et al.*, 2001). *FLM* is 70% identical to *FLC* and also controls flowering in a dosage-dependent manner as *FLC*. However, unlike *FLC* the autonomous or vernalisation pathway does not influence its expression. Both *SVP* and *FLM* have similar expression patterns but the pathways in which they repress flowering is not yet clear. Since MADS-box proteins form functional DNA binding complexes with other proteins it is suggested that SVP, FLM and FLC proteins may interact to control flowering (Scortecci *et al.*, 2001). MADS-box genes are therefore important players in the genetic pathways regulating the transition to flowering in plants.

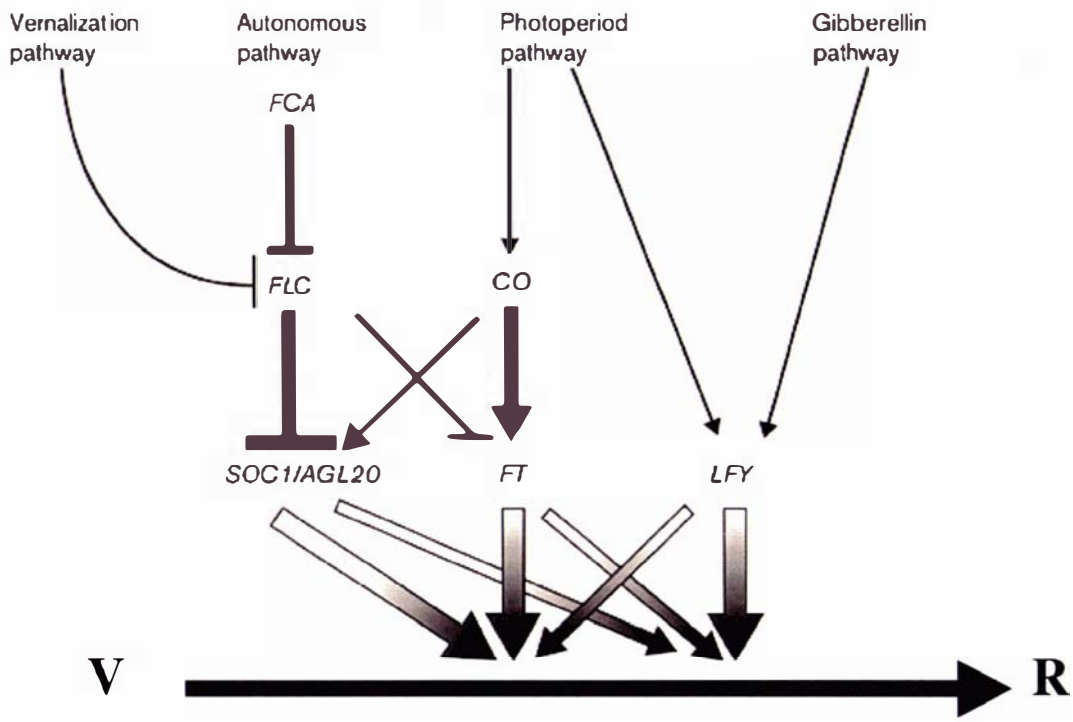

Figure 1.4. A model shows the integrative role of *AGL20/SOC1* and the interaction of flowering pathways in *Arabidopsis*. [Figure adapted from Araki, T (2001)]. The horizontal line represents the vegetative (V) to reproductive (R) transition. Arrows indicate promotion, and T-bars indicate repression. In the autonomous pathway, *FCA* represses *FLC*, and *FLC* represses *AGL20/SOC1*. *AGL20/SOC1* acts as a floral activator. Vernalization also promotes flowering by activating *AGL20* expression through the repression of *FLC*. Photoperiod pathway gene *CONSTANS* (*CO*) promote flowering by activating *SOC1* and also through other factor(s).

1.4.3 MADS-box genes control floral meristem identity

The reproductive phase in plants is characterised by the formation of inflorescence and floral meristems (Araki, 2001). So-called floral meristem identity genes control the formation of floral meristems on the flanks of the inflorescence meristems. Two *Arabidopsis thaliana* MADS-box genes that co-ordinate this function are *APETALA1* (AP1) and *CAULIFLOWER* (*CAL*). Similarly, *AP1* orthologue *SQUAMOSA* is responsible for conferring floral meristem identity in *Antirrhinum majus*. Mutations in *AP1* result in the production of secondary flowers in the axils of the first whorl organs of primary flowers and this may be reiterated in secondary flowers resulting in tertiary flowers (Mandel *et al.*, 1992). This arrangement resembles inflorescence and indicates a partial conversion of the floral meristem into inflorescence meristem. A similar function is observed with *SQUA* in *Antirrhinum*, whose loss of function mutation results in excessive formation of bracts and malformed flowers (Huijser *et al.*, 1992). The *AP1* homologue in pea, *PEAM4* also influence inflorescence to flower transformation, suggesting that this function of *AP1* is conserved. *AP1* interacts with other floral meristem identity genes such as *LEAFY* (*LFY*) and *CAL*, in the specification of floral meristem fate (Weigel *et al.*, 1992; Shannon and Meeks-Wagner, 1993; Liljegren *et al.*, 1999).

1.4.4 Floral meristem development

Floral meristems are determinate structures that differentiate to form flowers, producing floral organs in precisely defined positions within concentric whorls. A typical angiosperm flower consists of sepals, petals, stamens and carpels in four concentric whorls. In *Arabidopsis*, the floral organs initiate and develop sequentially from the sepals to the gynoecium (Hill and Lord, 1988; Smyth *et al.*, 1990). In maize and other monocots, the flower structure is distinct from the dicot flower; different male (tassel) and female (ear) inflorescences are formed on the maize plant, which produce staminate and pistillate florets. However, despite the morphological differences, early development of both types of florets are remarkably similar. Each floret develops as a bisexual flower from a floral meristem, producing a series of organs: lemma, palea,

lodicules, stamen and a central gynoecium (Dellaporta and Calderon-Urrea, 1994; Irish, 1996). The monocot floret is thus similar to the dicot flower; the lemma is considered a bract, with the palea and lodicule, the structural equivalents of sepal and petal, respectively (Ambrose *et al.*, 2000; McSteen *et al.*, 2000).

The identity and position of the floral organs are a result of interactions between different genes whose functions are required for the proper development of these organs. Extensive genetic studies of homeotic flower mutants identified genes that control floral organ identity (Schwarz-Sommer *et al.*, 1990; Bowman *et al.*, 1991; Coen and Meyerowitz, 1991; Bowman *et al.*, 1993). This led to the formulation of the **ABC** model of floral organ specification, which explained the complex interactions among floral organ identity genes (Weigel and Meyerowitz, 1994; Figure 1.5). MADS-box genes form a large part of this model, an indication of their centrality to the floral program (Weigel and Meyerowitz, 1994; Mena *et al.*, 1995; Mena *et al.*, 1996; Mizukami *et al.*, 1996; Ma, 1998; Ambrose *et al.*, 2000).

1.4.5 The ABC theory of floral organ identity

The **ABC** model in general, attempts to explain the genetic interactions that culminate in the specification of the different floral organs in a flower. The **ABC** model predicts that homeotic genes controlling flower development fall into three classes, which uniquely, or in combination with other genes, determine formation of specific floral organs in an overlapping two-whorl pattern (Weigel and Meyerowitz, 1994; Coen and Meyerowitz, 1991; Figure 1.5). The class A genes are involved in specifying the identity of sepals (the first whorl organ) and in combination with genes belonging to class B, they determine petal formation. Class C genes together with class B genes are necessary for the formation of stamens and class C genes alone control carpel identity.

In *Arabidopsis*, the A- function is performed by *APETALA1* (*AP1*) and *APETALA2* (*AP2*). Flowers of *ap1* and *ap2* mutant plants have their sepals transformed into ovule bearing carpels or bracts with suppressed petal formation (Jofuku *et al.*, 1994; Mandel *et al*; 1992a). The B function is performed by *AP3* and *PISTILLATA* (*PI*) genes; *ap3/pi* mutant flowers have petals transformed to sepals and stamen to carpels (Goto and

Meyerowitz, 1994; Jack *et al.*, 1992). Mutations in the C function gene, *AGAMOUS* (*AG*) result in the absence of stamens and carpels and an indeterminate flower phenotype (Yanofsky *et al.*, 1990). AP1, AP3, PI, and AG are MADS domain proteins while AP2 belongs to a different family of DNA binding proteins, which has a novel 68 amino acid repeated motif called the AP2 domain (Jofuku *et al.*, 1994; Okamuro *et al.*, 1997). Homologues of these MADS-box genes have been isolated from other species and in some cases their functions determined to be similar to their *Arabidopsis* counterparts. This suggests the roles of these genes are largely conserved across species (Schwarz-Sommer *et al.*, 1990; Bradley *et al.*, 1993; Kim *et al.*, 1998; Rutledge *et al.*, 1998; Yu *et al.*, 1999).

The validity of the **ABC** model was tested in studies that looked at ectopic expression of the **ABC** genes. The A function represses the C function in the first and second whorls and the C function in turn represses the A in the third and fourth whorls. In *ag* mutants, the A function genes are ectopically expressed in the third and fourth whorls; their subsequent interactions with B genes result in the stamens replaced by petals (Yanofsky *et al.*, 1990). According to predictions from the **ABC** model, sepals would replace the fourth whorl, however in *ag* flowers, a new mutant flower replaces the fourth whorl. Ectopic expression of B genes in wild type flower results in petals in the first two whorls and stamens in the third and fourth whorls, according to the **ABC** model. The expression of *AP3* under a constitutive promoter resulted in petaloid sepals and stamens in the first and fourth whorls respectively (Jack *et al.*, 1994). The ectopic expression of *AG* is illustrated by the phenotype of *apetala2* flower, which displays carpelloid sepals, staminoid petals in the first and second whorls respectively (Drews *et al.*, 1991). Similarly, the expression of *AG* in wild type *Arabidopsis*, under a constitutive promoter resulted in carpelloid sepals, staminoid petals in the first and second whorls respectively (Mizukami and Ma, 1992). Taken together, the ectopic expression of the **ABC** genes further validates the model and suggests that the **ABC** genes are sufficient to specify floral organ identity. Triple mutants that carry mutations in A, B and C functions have a conversion of floral organs into leaf-like organs (Weigel and Meyerowitz, 1994). However, ectopic expressions of these genes are not able to convert vegetative leaves to floral organs. The **ABC** genes are therefore, only sufficient in the context of the flower and possibly involved other organ identity factors.

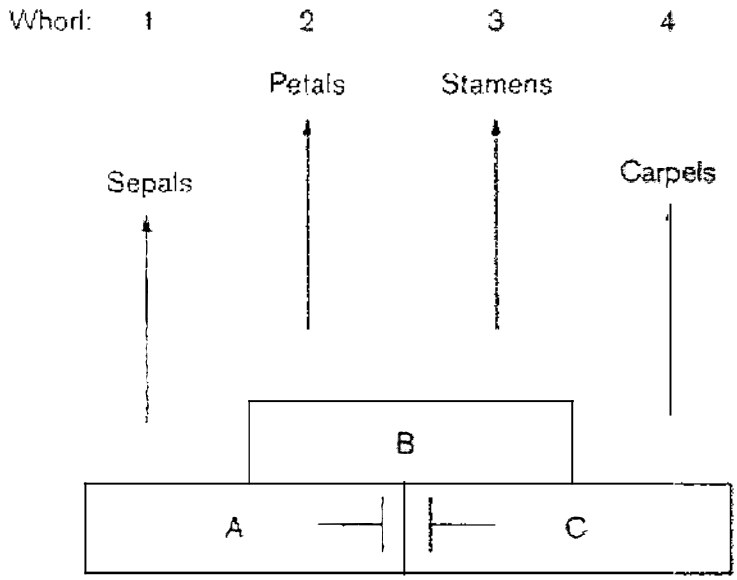

Figure 1.5. Schematic representation of the ABC model of floral organ identity (credit: Theißen, 2001a). The organ identity functions (A, B, C) combinatorially specify the identity of the different types of organs in the four whorls of a typical angiosperm flower. The activities of A and C are mutually antagonistic; the A function is repressed (denoted by T-bar) in the inner two whorls by the C-function and the C function is also repressed by the A function in the first two whorls.

1.4.6 Variations to the ABC theory

1.4.6.1 Changes to two-whorl expression pattern

One cardinal observation of the **ABC** theory was that the expression pattern of the genes correlated strongly with their domain of function. These **ABC** genes were therefore expressed in adjacent whorls. Further characterisation found that this was not always the case; the expression patterns of some MADS box genes in the floral organs did not resemble the two-whorl pattern described for the **ABC** genes. In *Arabidopsis*, *AGL1* was expressed only in the carpel (Ma *et* al., 1991). A MADS-box gene identified as the ortholog of *AGAMOUS* in *Panax ginseng* (*GAG2*) was observed to be expressed in the three inner whorls of flowers, (Kim *et al.*, 1998). The expression of two other tomato MADS-box genes, *TM5* and *TM6* were found in the inner three whorls of the tomato flower while *TM16* was expressed in all the four whorls (Pneuli *et al.*, 1994a). These differences reflected hidden facets of the floral program and gave early indications of added complexity to the **ABC** model.

1.4.6.2 The D organ identity function

The **ABC** model was extended to cover a D-function component responsible for ovule identity (Figure 1.6). Initially, the ovules were considered as integral part of the carpel and therefore under the control of the C-function. However, experiments in *Petunia hybrida* supported a separate D- function responsible for the specification of ovule identity.

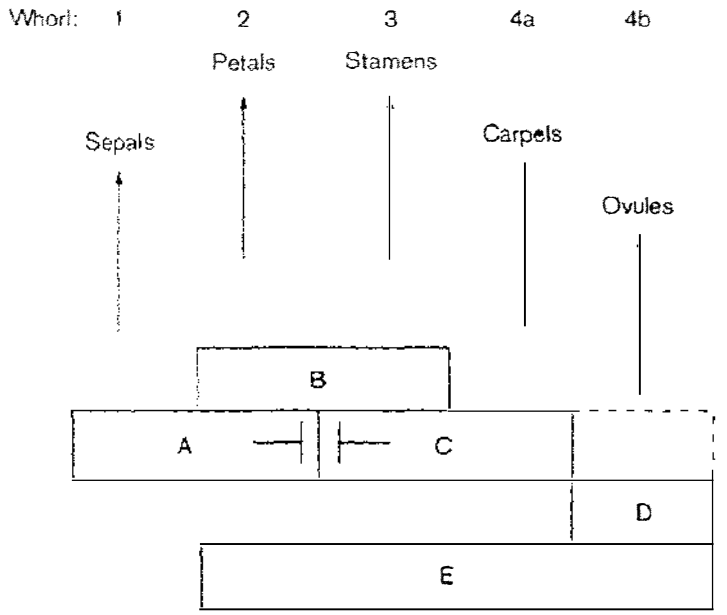

Figure 1.6. A representation of the **ABCDE** model of organ identity functions in Arabidopsis (credit: Theißen, 2001a). This is a modification of the ABC model; the D function is responsible for specifying ovule identity. The involvement of the C function in ovule identity is unclear and represented by dashed line. The E function is required for the activities of the B, C and possibly D organ identity genes.

The MADS-box genes encoding *FLORAL BINDING PROTEIN* (*FBP*) 7 and *11* are expressed in the centre of the developing carpel of *Petunia hybrida*, and later in the ovules. The inhibition of these genes by co-suppression resulted in the homeotic conversion of ovules into vestigial structures (Angenent *et al.*, 1995; Colombo *et al.*, 1997). Overexpression of *FBP11* caused ovule-like structures to be formed on the abaxial and adaxial surfaces of sepals (Colombo *et al.*, 1995). Since *agamous* flower mutants lack carpels and associated ovules, it suggests *AG* functions to control both carpel and ovule identity. So far, this proposed D organ identity function has not been extensively studied as other components of the **ABC** model. Judging from the *ag* phenotype which causes the complete replacement of the carpel, and the suggestion that *AG* promotes ovule identity (Western and Haughn, 1999), the D-function appears integral to the C-function.

1.4.6.3 The E organ identity function

Recent studies into MADS-box genes using reverse genetics has identified another group of floral organ identity genes whose activity bear directly on the **ABC** functions and offer candidates for the missing factors required to convert vegetative leaves to flowers. Pelaz *et al.*, (2000) found that the MADS-box genes *AGL2*, *AGL4* and *AGL9* are floral organ identity genes that redundantly control the B and C functions in *Arabidopsis*. These three genes are closely related with high sequence homology (Flanagan and Ma, 1994; Mandel and Yanofsky, 1998). While, the single mutants of these genes displayed subtle phenotypes, the triple mutant flower displayed homeotic conversion of petals and stamens into sepals and the fourth whorl replaced by a similar flower (Pelaz *et al.*, 2000; Pelaz *et al.*, 2001a). The *AGL2*, *AGL4* and *AGL9* have subsequently been renamed as *SEPALLATA* (*SEP*) 1, *SEP2* and *SEP3* and classified as E organ identity genes (Figure 1.6). The sepallata flower phenotype is similar to that seen in double mutants of B and C organ identity functions (Bowman *et al.*, 1991), suggesting the E-function is required for the proper functions of B and C genes. The equivalent of the *SEP* genes in other species may have similar functions. In tomato, plants expressing antisense RNA of *TM5* (orthologous with *SEP3*) have flowers with partial transformations of the inner whorls (Pneuli *et al.*, 1994a). In petunia,

cosuppression of *FBP2* (a *SEP3* orthologue) generated sepalloid flowers (Angenent *et al.*, 1994).

The *SEP* genes may not function completely redundantly. For instance, unlike *SEP1* and *SEP2*, the *SEP3* gene has a different expression pattern, produces subtle changes in the flower and has been shown to interact with *AP1* to promote flower development (Mandel and Yanofsky, 1998; Pelaz *et al.*, 2001a). In other species there are indications the functions of the *SEP*-like genes may not completely overlap. Using cossupression and antisense studies, the individual *SEP*-like genes in tomato, petunia and *Gerbera* produced significant phenotypes in transgenic plants (Angenent *et al.*, 1994; Pneuli *et al.*, 1994a; Kotilainen *et al.*, 2000).

The *SEP* genes together with the B and C organ identity genes are sufficient to convert vegetative leaves to floral organs. In a recent ground breaking experiment, ectopic expressions of *PI*, *AP3*, with *SEP3* converted cauline leaves of *Arabidopsis* into petaloid organs. Also, the ectopic expression of *PI*, *AP3*, *AG* with *SEP3* transformed cauline leaves into staminoid organs (Honma and Goto, 2001). Though these were not sufficient to convert rosette leaves to floral organs, it has been shown that ectopic expression of *AP1*, *PI*, *AP3* and *SEP3* is sufficient to convert rosette leaves into petals (Pelaz *et al.*, 2001b). The *SEP* genes have therefore been established as the missing link in the conversion of vegetative leaves to floral organs by the **ABC** genes.

1.4.7 Floral meristem reversion

Indeterminate growth of floral meristem results in flowers with extra whorls, increased number of floral organs or double flower phenotype. These indeterminate phenotypes are attributed to unregulated cell division in the floral meristems (Clark *et al.*, 1993). The *AG* gene controls determinate growth of the floral meristem in *Arabidopsis*. Mutation in *AG* or expression of antisense *AG* RNA in *Arabidopsis* result in indeterminate flower phenotype (Yanofsky *et al.*, 1990; Mizukami and Ma, 1995). Similarly, the *AG* homologues in tomato (Pneuli *et al.*, 1994b) and *Gerbera* (Yu *et al.*, 1999) have been shown to also regulate determinate growth of their floral meristems. The *AP1* gene also controls determinate growth in Arabidospsis flower. *ap1* flowers

display the indeterminate features of inflorescence meristem (Irish and Sussex, 1990; Mandel *et al.*, 1992b).

Unlike indeterminate growth of floral meristems, floral meristem identity can revert to inflorescence or shoot meristem identity. This is a genetic switch resulting in the growth of shoot within flowers, a development known as floral meristem reversion (Okamuro *et al.*, 1996). Floral meristem reversion can be induced in the flowers of *Arabidopsis ag-1* mutants by growing them under short-day light conditions, also, in double mutants of *ag* and *constans* (*co*) grown under long-day inductive conditions (Okamuro *et al.*, 1996; Mizukami and Ma, 1997). Double mutants of *clavata1* and *ap1* also caused cells in the central region of flowers to revert to inflorescence meristem (Clark *et al.*, 1993). In, *Impatiens balsamina*, flowers revert to vegetative shoot growth upon placement in non-inductive conditions and when photo-induced leaves are removed (Pouteau *et al.*, 1997; Pouteau *et al.*, 1998ab). These reversions to shoot growth suggest the identity of the floral meristem must be maintained during flower development.

The control of floral reversion is largely unknown. In *Arabidopsis*, floral reversion seems to be limited by *AG*, but only under non-inductive conditions (Okamuro *et al.*, 1996; Mizukami and Ma, 1997). Since *AG* also functions to control determinate growth of the flower, there is a suggestion that the pathways controlling determinate growth and maintenance of floral meristem identity are related. However, unlike its determinate function, *AG* role in floral reversion is required only under short-day conditions (Okamuro *et al.*, 1996). In *Impatiens*, the transcription patterns of floral meristem identity genes *Imp-FLO*, *Imp-FIM* and *Imp-SQUA*, orthologues of *Antirrhinum FLORICAULA*, *FIMBRIATA* and *SQUAMOSA* cannot explain this phenomenon. *Imp-FLO* is expressed continuously in vegetative and floral tissues under both inductive and non-inductive conditions (Pouteau *et al.*, 1997; Pouteau *et al.*, 1998ab). Leaf removal experiments and photoperiod treatments in *Impatiens* have suggested that a lack of persistent induced state in the leaves is responsible for floral reversion (Poteau *et al.*, 1997; Pouteau *et al.*, 1998b; Tooke and Battey, 2000). The photo-induced signal transmitted via the leaves is responsible for maintaining the flowering program and is required to reach the meristem continuously during flower development to prevent reversion to vegetative growth. These experiments are yet to be clearly repeated in other

plant species (Hempel *et al.*, 2000). More studies will be required to fully explain the molecular basis of floral reversion.

1.5 MADS-box genes and fruit development

MADS-box genes, are implicated in events that suggest they play important roles during fruit development. These include fruit growth characteristics, proper growth of tissues, seed development, fruit dehiscence and fruit abscission.

1.5.1 Stages in fruit development

1.5.1.1 Fruit set

Fruit development is a progression of the events of flower development. The various floral organs formed during flower morphogenesis progress differently in the later stages of development. In most flowers, events at anthesis lead to the transfer of pollen to the ovary. Pollination of the flower stimulates the initial growth of tissues towards fruit formation and triggers a series of developmental events that eventually result in fertilisation. These events include the senescence and abscission of floral organs, growth and development of the ovary and ovule development in anticipation of fertilisation (Ho and Hewitt, 1986; O'Neill, 1997). While the sepals often delay in senescence and remain on the flower for a longer period, the petals and stamens senesce shortly after anthesis. The senescence of the petals and stamens is hastened by increase in ethylene production, which is triggered by pollination (O'Neill, 1997). The ovary

subsequently develops into fruit. In other flower types, the ovary develops together with other parts of the flower, hypanthium in pomes, to form the fruit (Pratt, 1998).

The first phase of fruit development involves initial ovary development, fertilisation and fruit set. Fruit set is associated with increase in sink strength, activation of carbohydrate import, metabolism and increase in hormone levels in tissues forming fruit (Mapelli *et al.*, 1979; Bungler-Kibler and Bangerth, 1983; Takeno *et al.*, 1992; Lee *et al.*, 1997ab). Fertilisation of the ovules increases the levels of hormones such as auxins and gibberellins which are hypothesised to play important roles in processes required for ovary development (Nitsch, 1970). The role of hormones in fruit set is evident in the effects of growth regulators on ovaries, which can lead to parthenocarpic fruit development (Ozga and Reinecke, 1999).

Parthenocarpy is an alternative pathway of fruit production, which leads to the formation of seedless fruit. Parthenocarpy may be caused by genetic factors, induced through application of exogenous hormones or introduced by genetic engineering to increase hormone accumulation. Several mutations inducing natural parthenocarpy, *pat-2*, *pat-3* and *pat-4* have been described in tomato (Mazzucato *et al.*, 1998; Fos *et al.*, 2001). These genes may induce parthenocarpy by increasing the levels of endogenous hormones. In all three tomato *pat* mutants, the levels of gibberellins are significantly higher than the wild type ovaries (Fos and Garcia-Martinez, 2000; Fos *et al.*, 2001). Though other hormones were not examined, these results suggest that increased giberrellic acid (GA) content may, at least partially, be responsible for parthenocarpy. This observation is consistent with previous observations that GA application induces parthenocarpic fruit development (Gustafson, 1960; Bunger-Kibler and Bangerth, 1983; Cano-Medrano and Darnell, 1997). Also, the application of an inhibitor of GA biosynthesis, paclobutrazol, reduces the development of seeded wild type tomato fruits (Fos and Garcia-Martinez, 2000).

Auxins have similar stimulatory effect on fruit development and the fertilised ovules are a major source of this hormone. The application of exogenous auxins can stimulate fruit growth in the absence of fertilisation or seed development (Kagan-Zur *et al.*, 1992; Aznar *et al.*, 1995; Ozga and Reinecke, 1999). Consistent with this, parthenocarpy has been induced via genetic engineering to increase auxin production in fruit. The auxin biosynthetic gene (*iaaM*) from *Pseudomonas syringae* when introduced into tobacco

and eggplant successfully induced parthenocarpic fruit development in these plants (Rotino *et al.*, 1997; Ficcadenti *et al.* 1999). The *iaaM* gene product synthesises indole-3-acetamide which is converted to indole-3-acetic acid in transgenic plants (Kawaguchi *et al.*, 1991; Gaudin *et al.*, 1994).

1.5.1.2 Fruit growth

Fruit growth is described by sigmoid-shaped curves comprising initial period of slow growth, which is the cell division phase followed by a rapid cell expansion phase and then a ripening phase. Some fruits exhibit double sigmoid growth curves with two rapid growth phases occurring within its life cycle. While the growth pattern of tomato and apple follows a single sigmoidal curve kiwifruit and peach have double sigmoid growth curves (Masia *et al.*, 1992; Lewis *et al.*, 1996; Gandar *et al.*, 1996).

The duration of the cell division phase varies from one species to another, however, as a proportion of the entire fruit growth period, it is of a short duration in most species (Marcellis and Hofman-Eijer, 1993b; Carno-Medrano and Darnell, 1997). In tomato, cell division occurs during the first 10 to14 days after anthesis while cell expansion continues for the next 6 to 7 weeks (Bunger-Kibler and Bangerth, 1983; Ho and Hewitt, 1986; Varga and Bruinsma, 1986; Gillaspy *et al.*, 1993). While cell division may be restricted during fruit growth, cell expansion continue from ovary development to fruit maturity (Marcelis and Hofman-Eijer, 1993a). Both the cell division and cell expansion phases significantly influence the final fruit size (Bunger-Kibler and Bangerth, 1983; Narita and Gruissem, 1989; Marcelis, 1993; Marcelis and Hofman-Eijer, 1993b).

1.5.1.3 Fruit ripening

Ripening marks an important phase in fruit development where growth is reduced and fruit undergoes biochemical, physiological and structural changes (Rhodes, 1970; Brady *et al.*, 1987). Fruits are classified broadly as climacteric or non-climacteric, depending on the presence or absence of a rise in respiration rate associated with ethylene production during ripening (Lincoln *et al.*, 1987). Ethylene is required for the ripening of climacteric fruits. In tomato plants in which ethylene synthesis is inhibited or in the *Never Ripe* mutant, which is insensitive to ethylene, fruit ripening is impaired (Lanahan *et al.*, 1994; Giovannoni, 2001). Ethylene activates the expression of ripening-related

genes. The exposure of unripe tomato fruit to ethylene activates the expression of genes involved in ripening (Lincoln *et al.*, 1987; Gonzalez-Bosch *et al.*, 1996). The ripening process in non-climacteric fruits is similar to climacteric fruits; it is associated with biochemical changes and the expression of ripening related genes (Manning, 1998; Nam *et al.*, 1999; Itai *et al.*, 2000). However, the increase in respiration rate and the associated rise in ethylene production is absent from climacteric fruits. There is a general understanding that ethylene is not required for ripening of non-climacteric fruit, though ethylene can induce the expression of specific RNAs in non-climacteric fruit (Alonso *et al.*, 1995; Lelievre *et al.*, 1997; Giovannoni, 2001). This suggests the presence of ethylene-independent regulation of ripening.

1.5.2 Evidence of MADS-box genes in fruit development

The study of MADS-box genes in regulating fruit development has not been extensive as in flower development. However, there are observations suggesting that MADS-box genes control events in fruit development. The *AG* gene of *Arabidopsis* (Yanofsky *et al.*, 1990) and its orthologues in other plant species such as *PLE* of *Antirrhinum* (Davies *et al.*, 1999) and *TAG1* of tomato (Pneuli *et al.*, 1994), are responsible for specifying carpel identity. The products of these genes are therefore required for carpel development, which is the precursor of fruit. Mutations in these genes cause complete loss of carpel identity and fruit development.

MADS-box genes may hold the key to parthenocarpic fruit development. In a recent finding, the *PI* homologue in apple (*MdPI*) was responsible for the parthenocarpic fruit development in apple mutants. A transposon insertion in *MdPI* produces the typical loss of B function mutant flower, with sepal in the first two whorls and carpels in the inner two whorls. This ultimately produced pathenocarpic fruit (Yao *et al.*, 2001). It was therefore suggested that the absence of the *PI* function removed a repressor of parthenocarpy in apple. This newly identified *PI* function may not be present in all plant species since apple fruit is a pome derived from sepals, petals and stamen tissues (Yao *et al.*, 2001; Surridge, 2001).

The *FRUITFULL (AGL8)* MADS-box gene of *Arabidopsis* is necessary for cellular differentiation in the mature silique (Mandel and Yanofsky, 1995; Gu *et al.*, 1998). *ful* mutant siliques fail to elongate after fertilization, producing short compact fruits. *FUL* may regulate the transcription of gene required for cellular differentiation during fruit development. Similarly, the *SHATTERPROOF1* (*SHP1*) and *SHP2* MADS-box genes (previously AGL1, AGL5) are required for fruit dehiscence in *Arabidopsis* siliques (Liljegren *et al.*, 2000). *SHP1* and *SHP2* redundantly control dehiscence zone differentiation and lignification of cells and are negatively regulated by *FUL* (Ferrandiz *et al.*, 2000). In tomato, the *JOINTLESS* MADS-box gene controls the formation of abscission zone in flower and fruit pedicel required for shedding fruits (Mao *et al.*, 2000).

The *TAG1* MADS-box gene of tomato may be involved in lycopene accumulation and cell wall softening associated with ripening. Tomato sepals incubated at low temperatures became swollen, red and succulent and were associated with increase in *TAG1* expression. Fruits with ectopic expression of *TAG1* RNA also displayed succulent sepals when incubated at low temperatures (Ishida *et al.*, 1998). *TAG1* may regulate events during tomato fruit ripening.

The number of isolated MADS-box genes expressed in fruit tissues continues to increase. These include apple *MdMADS1-MdMADS4*, preferentially expressed in floral organs and young fruits of apple (Sung and An, 1997), *MdMADS5-MdMADS11* expressed in different parts of the apple fruit (Yao *et al.*, 1999). These reports together give strong indications that the members of the MADS-box family are involved in regulating events in fruit development. However, more genetic and molecular studies of these genes will help understand how this gene family regulates such events in fruit development.

1.6 Aims of this study

The overall aim of this research project was to study the roles of MADS-box genes in flower and fruit development. This study formed part of the Fruit formation and Development project at the Horticulture and Food Research Institute of New Zealand, Auckland. At the beginning of this study, most investigations on MADS-box genes were centred on flower development in the model plant species *Arabidopsis*. The objectives of this study were therefore, to:

- Identify new MADS-box genes in tomato which may be involved in flower and fruit development
- Characterise these genes by analysing their sequence and expression patterns
- Examine gene functions using transgenic techniques

CHAPTER 2 MATERIALS AND METHODS

2.1 Organisms and reagents used

Bacterial strains, source and genotype

Escherichia coli strain DH10B, (Gibco BRL, Maryland, USA) F⁻ *mcr*A Δ(*mrr*⁻*hsd*RMS-*mcr*BC) Φ80d*lac*ZΔM15 Δ*lac*X74 *deo*R *rec*A1 *end*A1 *ara*Δ139 ▶(*ara leu*)7697 *gal*U *gal*K1⁻ *rps*L *nup*G

E. coli strain DH5α, (Gibco BRL): F⁻ Φ80d*lac*ZΔM15 Δ(*lac*ZYA-*arg*F)U169 *deo*R *rec*A1 *end*A1 *hsd*R17(r_k^-, m_k^+) *pho*A *sup*E44 λ⁻ *thi*-1 *gyr*A96 *rel*A1

Agrobacterium tumefaciens strain LBA4404 (Gibco BRL): disarmed Ti Plasmid pAL4404 with only *vir* and *ori* region of the Ti plasmid.

Table 2.1 Vectors used in this study

Vectors	Source or reference
λ Uni-ZAP XR	Stratagene, CA, USA
pGEM-T Easy	Promega, Madison, USA
pART7	Gleave, (1992)
pART27	Gleave, (1992)
pART69	Yao, unpublished

2.1.2 Primers

Table 2.2 General primers

Name	Sequence (5' - 3')
M13 forward primer	GTAAAACGACGGCCAGT
M13 reverse primer	GGAAACAGCTATGACCATG
P35S-1	GTC ACT TCA TCA AAA GGA CAG

Table 2.3 Primers for *TM29* analysis

Name	Sequence (5' - 3')[a]
ITM-03	GCA ATT AAC CCT CAC TAA AGG GGG TAC CAA AAG TGC AGC T'
ITM-04	GCT AAT ACG ACT CAC TAT AGG GGG TTC ACA ACG TTC ACC T'
TM29-GM1	GAT CTA AGA GTT AGC CAA GA
TM29-GM2	GGT TCA CAA CGT TCA CCT
TM29-P1	CTC CCA TCC TAA AGT TGT TCA
TM29-P2	TGA GGA TGT TGC TGC TGA CCA
TM29-P3	TGG GTA ATC TCA TGA CAT GCA
TM29-P4	TCA AGA ACC TTG TTA GCC TCA
TM29-P5	GCT TTT GCT GGG CAT ATA G
TM29-P6	TTG TGA CTA GAG CGT CCA
TM29-P7	TCC ATT TGC CAA CTT ACC
TM29-P8	AGC TGC TTT GCT GCA ATG

[a] Underlined primer sequence in ITM-03 and ITM-04 are promoter-binding sequences of T3 and T7 RNA polymerases, respectively.

Table 2.4 Primers for *TM10* analysis

Name	Sequence (5'-3')*
3' anchor primer	GAG AGA GAA CTA GTC TCG AGT
DEG-1	ATG GGS MGN GGN AAR RT
DEG-2	ACY TCN GCR TCR CAN A
NotI primer adapter	GAC TAG TTC TAG ATC GCG AGC GGC CGC CC $(T)_{15}$
ITM-01	GCA ATT AAC CCT CAC TAA AGG GGA AGC ATG CAA GGG CTG A
ITM-02	GCT AAT ACG ACT CAC TAT AGG GGT TCA TCT CTC CAA AGT G
TM10-P1	ATG GGG CGG GGG AAG GTT CAA
TM10-P2	ATG GGG CGG GGG AAG GTT CAA ATG AAG AGG

* M= A/C, N=A/T/C/G , R=A/G , Y= C/T, S=C/G

Table 2.5 Buffer compositions

Buffer name	Composition
1X Saline	8.5 g/l NaCl
Church and Gilbert buffer	0.5 M sodium phosphate, 1 mM EDTA (pH 8), 7% SDS (w/v)
Detection buffer 1	100 mM Tris-HCl, 150 mM NaCl, pH 7.5
Detection buffer 2	Buffer 1, 0.5% (w/v) blocking reagent
Detection buffer 3	Buffer 1, 1% bovine serum albumin, 0.3% (v/v) Triton X-100
Detection buffer 4	Buffer 3, 0.5% (v/v) Anti-digoxigenin-alkaline phosphate (Roche Molecular Biochemicals, Mannheim, Germany)
Detection buffer 5	100 mM Tris-HCl, 100 mM NaCl, 50 mM $MgCl_2$, pH 9.5
Detection buffer 6	Buffer 5, 0.375 mg/ml nitro blue tetrazolium chloride, 0.2 mg/ml 5-Bromo-4-chloro-3-indoyl phosphate, toluidine salt
Fixative solution	4% paraformaldehyde in PBS (pH 11)
***In situ* hybridisation buffer**	0.3 M NaCl, 0.01 M Tris-HCl (pH 6.8), 0.1 M $NaH_2P●_4$, 5 mM EDTA, 50% deionised formamide, 12.5% dextran sulfate, 1X Denhardt's solution, 20 µg of tRNA
Ligase 10X buffer	300 mM Tris-HCl, 100 mM $MgCl_2$, 100 mM DTT, 10 mM ATP
mRNA buffer 1	0.5 M NaCl, 20 mM Tris-HCl, pH 7.5
MRNA buffer 2	0.1 M NaCl, 20 mM Tris-HCl, pH 7.5
NTE	0.5 M NaCl, 10 mM Tris-HCl (pH 7.5), 1 mM EDTA
PBS	130 mM NaCl, 7 mM Na_2HPO_4, 3 mM $NaH_2P●_4$
RNA loading buffer	50% glycerol, 1 mM EDTA, 0.4% bromophenol blue
RNA sample buffer	2.2M formaldehyde, 50% (v/v) deionised formamide, 50mM MOPS (pH 7.0), 1mM EDTA
SSC	150 mM NaCl, 1.5 mM Na_3 citrate, pH 7.0
TAE	4 mM Tris-acetate (pH 6.7), 0.1 mM EDTA

2.2 Growth media

2.2.1 Bacterial media

LB (1 litre): 10 g tryptone, 5 g yeast extract, 5 g NaCl

LB Agar: 15 g of bacteriological agar in 1 litre of LB

YM (1 litre): 0.4 g yeast extract, 10 g mannitol, 0.1 g NaCl, 0.2 g $MgSO_4.7H_2O$, 0.5 g K_2HPO_4

YM Agar: 15 g of bacteriological agar in 1 litre of YM broth

S.O.C (1 litre): 20 g tryptone, 5 g yeast extract, 0.6 g NaCl, 0.2 g KCl, 2 g $MgCl.6H_2O$, 2.5 g $MgSO_4.7H_2O$, 3.6 g glucose

Table 2.6 Plant growth media

Media composition (1 litre)	Reference
Murashige and Skoog (MS) macro salts (1X) 1.65 g NH_4NO_3, 1.9 g KNO_3, 0.4 g $CaCl_2.2H_2O$, 0.17 g KH_2PO_4, 0.37 g $MgSO_4.7H_2O$, 40 mg FeEDTA	Murashige and Skoog, (1962)
MS micro salts (1X) 6.2 mg H_3BO_3, 22.3 mg $MnSO_4.4H_2O$, 8.6 mg $ZnSO_4.7H_2O$, 0.83 mg KI, 0.25 mg $Na_2MoO_4.2H_2O$, 0.025 mg $CuSO_4.5H_2O$, 0.025 mg $CoCl_2.6H_2O$	Murashige and Skoog (1962)

KCMS, cocultivation medium 1X MS macro and micro salts, 100 mg inositol, 1.3 mg thiamine-HCl, 200 mg KH_2PO_4, 200 mg of 2, 4 dichlorophenoxyacetic acid, 100 mg kinetin, 2.7 g phytagel (Sigma), pH 5.8	Fillati *et al.*, 1987
1Z regeneration medium 1X MS macro and micro salts, 1mg zeatin 100 mg inositol, 20 g sucrose, 2.7 g phytagel, pH 5.8	Fillati *et al.*, 1987
2Z regeneration medium 1Z medium plus additonal 1 mg zeatin	Fillati *et al.*, 1987
MSSV medium 1X MS macro and micro salts, 1X Nitsch vitamins, 30 g sucrose	Fillati *et al.*, 1987

2.3 Bacteria transformation procedures

2.3.1 *E. coli* transformation

2.3.1.1 Heat-shock transformation method

Competent *E coli* DH5α cells were transformed by the heat-shock method. 50 μl aliquots of DH5α cells are placed in chilled microcentrifuge tubes and mixed with DNA

(plasmid or ligation reaction). The cell and DNA mixture is incubated on ice for 30 minutes, heat-shocked in a 42°C water bath for 45 seconds and immediately placed on ice for 2 minutes. 900 ml of S.O.C medium was added and incubated at 37°C for 1 hour shaking at 225 rpm. Cells were selected on LB plates containing appropriate antibiotic at 37°C overnight.

2.3.1.2 Electroporation method

DH10B Electromax cells (Gibco BRL) were transformed using electroporation. Frozen cells were thawed on ice and aliquots of 20 μl mixed with DNA in sterile microcentrifuge tubes. The cell and DNA mixture is placed in chilled micro-electroporation chambers and electroporated at voltage setting of 400 V, which delivers up to 2.5 kV with the voltage booster. Cells are then removed from micro-electroporation chamber and immediately added to 1 ml of LB medium, incubated at 37°C for 1 hour with shaking at 225 rpm. Cell cultures are plated on LB plates containing appropriate antibiotics for selecting transformed and incubated at 37°C overnight.

2.3.2 *Agrobacterium* transformation

Competent ElectroMAX *Agrobacterium tumefaciens* LBA4404 cells (Life Technologies/Invitrogen) were transformed by electroporation. Cells were transferred into chilled disposable micro-electroporation chamber and electroporated with the Gibco BRL Cell-Porator and Voltage Booster at 400 V (2.5 kV with voltage booster). Cells were added to 1 ml of YM medium at room temperature and incubated at 28°C for 3 hours, shaking at 225 rpm. Transformed cells are then selected on plates of YM media supplemented with appropriate antibiotics incubated at 28°C for 48-72 hours.

2.4 Nucleic acid isolation

2.4.1 Genomic DNA preparation

Genomic DNA was isolated from selected plant tissues using the CTAB method (Doyle and Doyle, 1990). Fresh tissues were ground in pre-heated CTAB isolation buffer. Samples were incubated at 60°C for 30 minutes with gentle swirling. Equal volume of chloroform-isoamylalcohol (24:1) was added and mixed thoroughly to form an emulsion. Samples were centrifuged at 11,000xg for 10 minutes. Aqueous phase was removed and two-third volume of cold isopropanol added. Samples were chilled on ice for 5 minutes and centrifuged at 5,000xg for 10 minutes to precipitate DNA. DNA pellet was washed with 70% ethanol and dried in a dessicator for 20 minutes. DNA was dissolved in distilled water and treated with RNAse.

For purified genomic DNA used for sequencing, DNA was isolated using Qiagen DNeasy Plant DNA isolation kit (Qiagen GmbH, Germany) following manufacturer's protocol.

2.4.2 Total RNA isolation

For preparation of RNA from plant tissues, samples were picked and quickly frozen in liquid nitrogen (-95°C). Total RNA was isolated using Trizol reagent (Gibco BRL, Gaithersburg, MD, USA) according to manufacturer's instructions. Tissues were homogenised in Trizol reagent using 1 ml of reagent per 100 mg of tissue. Samples were then incubated at room temperature for 5 minutes and 0.2 ml of chloroform added per 1 ml of Trizol reagent used. Tubes were shaken vigorously by hand and incubated further at room temperature for 3 minutes. This was followed by centrifugation at

12,000xg for 10 minutes at 8°C. RNA pellet was washed with 70% ethanol and dried at 37°C for 10 minutes. RNA was dissolved in diethylpyrocarbonate (DEPC)-treated RNase-free water. RNA concentrations were determined by Spectrophotometer readings at λ=260nm (A_{260}). 1 A_{260} was equivalent to 40 µg/ml RNA.

2.4.3 Messenger-RNA purification

Messenger RNA (mRNA) was purified from total RNA using the Messagemaker Reagent Assembly (Life Technologies). Poly(A)$^+$ RNA was selected from total RNA using oligo(dT) cellulose suspension. Total RNA was made to a concentration of 0.5 mg/l, denatured by heating at 65°C for 5 minutes and chilled on ice. 200 µl of 5M NaCl was added to 2 ml of the total RNA (1 mg) followed by 200 mg of oligo(dT) cellulose. The mixture was incubated at 37°C for 10 minutes for hybridization of oligo(dT) to poly(A)$^+$ RNA.

The oligo(dT) cellulose/RNA suspension was transferred to a filter syringe and the liquid containing unbound RNA expelled into a clean RNAse-free tube. The oligo(dT) cellulose in the filter was washed with 5 ml of Buffer 1 followed by Buffer 2. The poly(A)$^+$ RNA was eluted from the filter syringe with 2 ml of RNAse-free distilled water. A second poly(A)$^+$ selection was performed on this eluted sample following the first selection procedure. The mRNA was precipitated by adding 50 µg glycogen/ml, 0.1 volume of 7.5 M ammonium acetate and two volumes of -20°C ethanol. The mixture was incubated overnight at -20°C and then centrifuged at 5,000xg for 20 minutes. The pellet was washed with 75% ethanol and precipitated by centrifuging at 2,600xg for 10 minutes. The mRNA pellet was then air-dried and dissolved in RNAse-free distilled water.

2.4.4 cDNA synthesis

The SuperScript II reverse transcriptase system (Gibco BRL) was used for cDNA synthesis using the purified mRNA. 5 µg of mRNA was used as template for the first

strand cDNA synthesis. 2 µl of *NotI* primer-adadpter [0.5 µg/µl] was added to a 1.5-ml microcentrifuge tube and 5 µg mRNA in 8 µl total volume added. The primer/mRNA mixture was heated to 70°C for 10 minutes and quick-chilled on ice. The contents were collected to the bottom by brief centrifugation; 4 µl of 5X first strand buffer, 2 µl of 0.1 M DTT and 1 µl of 10 mM dNTP mix were added to the tube and contents mixed gently. The tube was placed at 37°C to equilibrate the temperature before adding 5 µl of SuperScript II RT [200 U/µl]. The reaction mixture was incubated at 37°C for 1 hour.

The second strand was synthesised by adding 30 µl 5X second strand buffer, 3 µl of 10 mM dNTP mix, 10 units of *E. coli* DNA ligase, 40 units of *E. coli* DNA polymerase, 2 units of *E. coli* RNAse H and DEPC-treated water to a final volume of 150 µl. The reaction mix was incubated at 16°C for 2 hours; after which 10 units of T4 DNA polymerase was added to reaction and further incubated for 5 minutes. Following this, 10 µl of 0.5 M EDTA was added to terminate reaction. The reaction was treated with 150 µl of phenol:chloroform:isoamyl alcohol (25:24:1), vortexed thoroughly and centrifuged for 5 minutes at 14,000xg for phase separation. 140 µl of the upper aqueous phase was transferred to a fresh 1.5 ml microcentrifuge tube, 70 µl of 7.5 M ammonium acetate added and well mixed before adding 0.5 ml of -20°C absolute ethanol. Mixture was vortexed thoroughly and centrifuged at 14,000xg for 20 minutes to pellet cDNA. The supernatant was carefully removed and pellet washed with 0.5 ml of 70% ethanol. The cDNA pellet was dried at 37°C for 10 minutes.

2.4.5 PCR to amplify MADS-box fragments using degenerate primers

MADS-box DNA fragments were amplified from flower and fruit cDNA templates using degenerate PCR primers, DEG-1, DEG-2. These primers were designed based on the conserved amino acid residues MGRGKV/I and LCDAEV in the MADS domain. These were expected to amplify a 145 basepairs DNA fragment. The PCR conditions were as follows: initial denaturation at 94°C for 5 minutes; followed by 30 cycles of 94°C for 1 minute, 55°C for 30 seconds and 72°C for 30 seconds plus a final extension at 72°C for 5 min.

The 145-bp fragment was gel purified and used in a ligation reaction with the pGEM-T Easy vector. The pGEM-T vector system takes advantage of the template-independent addition of single adenosine to the 3' end of PCR products by enzymes such as Taq DNA polymerase (Doyle, 1996). 10 nanograms (ng) of the 145-bp fragment was added to 50 ng of the pGEM-T vector (3 kb size) in a total volume of 10 µl including 1 µl of supplied ligase buffer. Reaction was incubated at 4°C overnight. The ligation was used to transform *E. coli* strain DH5α competent cells (Gibco BRL) using a standard heat shock treatment.

2.4.5.1 PCR for longer fragment of *TM10*

The longer fragment of *TM10* was amplified from cDNA templates in a 3' rapid amplification of cDNA ends (RACE) reaction (Ohara *et al.*, 1989). Overlapping gene specific primers TM10-P1 and TM10-P2 were used in combination with the 3' anchor primer in primary and secondary reactions respectively. The sequence of the 3' anchor primer is based on the *NotI* primer-adapter used for cDNA synthesis. The amplification reaction was set up usng the Expand High Fidelity PCR System (Roche, Mannheim, Germany) according to the manufacturer's instructions. The amplification conditions were as follows: initial denaturation at 94°C for 2 minutes, 30 cycles of 94°C for 30 seconds, 50°C for 30 seconds, 72°C for 1 minute and a final elongation step at 72°C for 5 minutes. A 1:100 fold dilution of the primary PCR product was used as template for the secondary PCR. These reactions resulted in a 0.9-kb DNA fragment of *TM10*.

2.5 Sequence analyses

2.5.1 DNA sequencing

Sequence data were generated at the DNA Sequencing Facility, University of Waikato, Hamilton, New Zealand on an ABI Prism 377 DNA Sequencer (Applied Biosystems). Sequencing reactions were performed using dye terminator chemistry. Template and primers were prepared at required purity (http://sequence.bio.waikato.ac.nz), free of contaminating salts, solvents, RNA, proteins and chelating agents.

2.5.1.1 *TM29* genomic sequence

The genomic DNA fragment of *TM29* was amplified by PCR using primers TM29-GM1 and TM29-GM2. A 4-kb DNA fragment was obtained and cloned into pGEM-T Easy vector.

The ligation reaction was set up in a total volume of 10 µl containing 1 µl of supplied ligase (pGEM-T Easy vector system, Promega, Madison, USA), 50 ng of pGEM-T vector, 200 ng of *TM29* DNA fragment and 3 units of T4 DNA ligase. The reaction was incubated at 4°C overnight. Competent *E. coli* DH10B Electromax cells (Gibco BRL) were transformed with 1 µl of the ligation reaction using Gibco BRL Cell porator, as described previously (Section 2.3). Transformed colonies were selected on LB media containing 100 mg/l ampicillin and 40 µg/l of X-gal, for blue and white colony screening.

The cloned *TM29* fragment was sequenced on both strands using the M13 forward and M13 reverse primers. Internal fragments were successively sequenced with following primer pairs: TM29-P1, TM29-P2; TM29-P3, TM29-P4; TM29-P5, TM29-P6; TM29-P7, TM29-P8. Overlapping sequences were then assembled using the FRAGMENT ASSEMBLY SYSTEM (GCG Version 9; Genetics Computer Group, WI, USA).

2.5.1.2 cDNA sequencing and mapping

The *TM29* and *TM10* cDNA fragments were sequenced using the M13 forward and M13 reverse primers. The cDNA sequences were analysed using the MAP program (GCG software). Mapped DNA sequences were manually edited to display the positive strand with protein translations below.

2.5.2 Secondary structure prediction

Predicted protein sequences were analysed by PSIPRED, a protein structure prediction based on position-specific scoring matrices (Jones, 1999). Residues were predicted as α-helices, ß-strands or coils.

2.5.3 Phylogenetic analysis

Sequences used in the analysis were retrieved from the GenBank database (Appendix A), except for *TM29* and *TM10* sequences. Amino acid sequences from the MADS-box, I- and K- regions were used in phylogenetic analysis. Multiple sequence alignment of the sequences was created by the progressive pairwise method PILEUP (Feng and Doolittle, 1987; GCG version 9). A matrix of pairwise distances between the aligned sequences was created and corrected with Kimura protein distance correction method (Kimura, 1983). The neighbour-joining method (Saitou and Nei, 1987; Thompson, *et al.*, 1994) was used to cluster the sequences in a pairwise fashion and an unrooted phylogenetic tree was reconstructed with GrowTree (GCG version 9) and plotted with the TREEVIEW software (Page, 1996).

2.6 Nuclei acid hybridisation

2.6.1 Preparation of radio-labelled probes

2.6.1.1 Labelling DNA probes

The gene-specific DNA probes were prepared from cDNA fragments of MADS-box genes, which were completely without the conserved MADS-box region so as to reduce cross hybridising to other MADS-box sequences. 50 ng of cDNA fragment was radioactively labelled with ^{32}P-dCTP using the Megaprime DNA labelling system RPN 1604 (Amersham Pharmacia Biotech, England, UK). DNA template was denatured at 100°C for 5 minutes in the presence of random nonamer primers. A reaction mix was prepared on ice containing 4 µl each of unlabelled nucleotides dATP, dGTP and dTTP, 10 µl of the reaction buffer and 2 units of DNA polymerase I Klenow fragment. 5 µl of α-^{32}P dCTP with specific activity 3000Ci/mmol was added to the mixture and the reaction incubated at 37°C for 1 hour. Unincorporated nucleotides were removed using a spin column containing sephadex-G50. The probe was then denatured in 0.1 M NaOH at room temperature for 20 minutes and added to the hybridisation buffer and the blot.

2.6.1.2 RNA probes

Sense and antisense RNA transcripts were detected in transgenic plants using gene-specific RNA probes. Probes were generated by in vitro transcription using T3 and T7 RNA polymerases (Roche) respectively.

DNA fragments were first amplified by PCR using gene-specific primers carrying T3 and T7 promoter sequences at their 5' ends. The PCR fragment which was without MADS-box conserved region was then used as template in transcription reactions with α-^{32}P CTP to generate radioactively labelled RNA probes. The reaction was set up in a

final volume of 20 µl. This included 4µl of 5X transcription buffer, 2 µl of 100 mM DTT, 20 units of RNAse inhibitor, 0.5 mM each of ATP, GTP and UTP, 12 µM of CTP (Promega), 5µl of α-^{32}P CTP (400Ci/mmol, 10 mCi/ml; Amersham), 1 mg of DNA template and 20 units of RNA polymerase. Reaction was incubated at 37°C for 60 minutes. Unincorporated nucleotides were removed from labelling reaction by passing through a sephadex G-50 column. These probes were used to hybridise to RNA blots.

2.6.2 DNA blot hybridisation

Tomato genomic DNA (20 µg) was digested separately with *Eco*RI, *Hin*dIII and *Xba*I at 37°C for 6 hours. The digests were separated on electrophoretic gel (1% agarose in 1X TAE buffer). The separated fragments were transferred onto Hybond-N$^+$ membrane (Amersham) in a Southern blot transfer with 0.4 M NaOH buffer, for 16 hours. The membrane was fixed by baking at 80°C for 2 hours.

Hybridisation was performed as described previously by Church and Gilbert (1984) with some modifications. The blot was pre-hybridised in Church and Gilbert buffer containing 0.1 mg/ml herring sperm DNA, for one hour. Then a radioactively labelled gene-specific probe was added and allowed to hybridise at 65°C for 15 hours in a Hybaid oven. The hybridised blot was washed successively at 65°C in solutions containing 2X SSC and 0.1% SDS for 30 minutes, 1X SSC + 0.1% SDS for 30 minutes and 0.1X SSC + 0.1% SDS for 10 minutes. Hybridisation signals were visualised with Storm 840 Phosphor-Imaging system (Molecular Dynamics, CA, USA) and analysed with the ImageQuant software (Molecular Dynamics).

2.6.3 RNA blot hybridisation

For blot analysis, RNA (10 or 20 µg) was denatured in RNA sample buffer at 70°C for 5 minutes, quenched on ice and 2 µl of RNA loading buffer added to each sample (Doyle, 1996). Samples were loaded into 1% agarose gel prepared with RNase-free 1X TAE buffer containing 5 µg/ml ethidium bromide. Samples were electrophoresed at 100 volts

until bromophenol blue dye has migrated two-thirds the length of the electrophoretic gel. The gel was visualised and photographed under ultraviolet transillumination (302 nm). RNA samples were transferred to Hybond N^+ membrane following standard procedure (Sambrook *et al.*, 1989) using an RNAse-free 0.05 M NaOH buffer. Hybridisation and washing conditions were the same as described for the DNA blot hybridisation above. To re-probe blots, the previous probes were stripped with 0.1% SDS at 100°C for 5 minutes.

2.6.4 Reverse transcriptase-PCR

To detect rare gene transcripts and to determine semi-quantitative levels of gene expression, reverse transcriptase PCR (RT-PCR) was performed with the Titan One-Tube RT-PCR System, (Roche) which combines the first and second strand synthesis in one reaction. The reaction mix had a final concentration of 0.2 mM dNTPS, 0.4 µM of each primer, 5 mM DTT, 10 units of RNase inhibitor, 1X RT-PCR buffer with 1.5 mM $MgCl_2$ and 1 µl of supplied enzyme mix. The first strand synthesis was catalysed by AMV reverse transcriptase at 50°C for 30 minutes. This was directly followed by PCR amplification by Taq DNA polymerase and Pwo DNA polymerase at the following conditions: 94°C for 2 minutes, 25 cycles of 94°C for 30 seconds, 58°C for 30 seconds and 68°C for 1 minute and a final elongation at 68°C for 5 7 minutes.

PCR products were electrophoresed at 100 V in 1% agarose gel and transferred onto Hybond N^+ membrane as described previously. The membrane was then hybridised with a gene specific probe according to Southern hybridisation procedure described.

2.6.5 RNA *in situ* hybridisation

The methods for labelling RNA probes, tissue preparation and *in situ* hybridisation followed that described by Jackson (1992). All solutions were prepared with distilled deionised water treated with 0.1% diethylpyrocarbonate (Sambrook *et al.*, 1989).

2.6.5.1 Tissue preparation

1. Tissues were fixed in 4% formaldehyde in phosphate buffered saline (PBS) by infiltration under vacuum and kept at 4°C overnight.

2. Tissue samples were passed through 85% saline for 30 mins, then 50%, 70%, 85%, 95%, 100% ethanol solutions for 90 minutes each and kept at 4°C overnight.

3. Tissues were then passed through 100% ethanol for 2 hours, 1:1 ethanol/histoclear for 1 hour, 100% histoclear for 1 hour and then 1:1 histoclear/wax at 50°C overnight.

4. Tissues were placed in wax at 50°C overnight and then embedded in blocks of wax.

5. Embedded tissues were sectioned to 8μm thickness with ultra-microtome (Leica Microsystems). Ribbons of sections were floated on sterile RNase free water at 42°C until the ribbon flattens out. These were then mounted on positively charged glass slides (BDH, Dorset, UK) and left at 40°C overnight.

2.6.5.2 Pre-hybridisation treatment

1. Slides with sections were placed in slide racks and dipped into fresh Histoclear solutions for 10 minutes to dewax.

2. Slides were passed through ethanol dilution series: 100% ethanol for 1 minute (twice), then 95%, 85%, 70%, 50% and 30% alcohol solutions containing 1X saline for 30 seconds each.

3. They were then dipped into 1X PBS solution for 2 minutes followed by 0.2% (w/v) glycine in PBS for 2 minutes.

4. Sections were then permeabilized with 20 μg/ml Proteinase K in proteinase buffer at 37°C for 30 minutes followed by treatment in freshly prepared 4% paraformaldeyde at room temperature for 10 minutes.

5. Sections were then incubated in freshly prepared 0.25% acetic anhydride in 0.1 M triethanolamine buffer for 10 minutes.

6. Slides were passed up through the alcohol series to the first 100% ethanol and then washed in fresh 100% ethanol before drying.

2.6.5.3 Preparation of DIG-labelled RNA probes

Digoxigenin (DIG)-labelled sense and antisense probes were generated with T3 and T7 RNA polymerases respectively by in vitro transcription using the DIG nucleic acid detection kit (Roche). PCR fragments with T3 and T7 promoter sites were used as templates. 1 μg of template was added to a 20 μl reaction mix of 1X transcription buffer, 40 units of RNA polymerase, 1 mM each of ATP, CTP, GTP plus 0.65 mM UTP and 0.35 mM DIG-11-UTP, 50 U of RNase inhibitor. The reaction was incubated at 37°C for 2 hours. DNA template was removed by adding 40 units of RNase-free DNAse I to the reaction and incubated at 37°C for 40 minutes. The labelled RNA was hydrolysed with 40 mM $NaHCO_3$ and 60 mM Na_2CO3 at 60°C for 2 hours. RNA was precipitated by adding a tenth volume of 10% acetic acid, 100 μg transfer-RNA (SIGMA), 0.48 μM LiCl, twice volume of 100% ethanol. The solution was left at -20°C overnight and centrifuged at 13,000 rpm for 10 minutes. RNA pellet was washed with 70% ethanol, dried at 37°C for 10 minutes and dissolved in RNAse-free water to a final concentration of 1 μg/μl.

2.6.5.4 Hybridisation

1. The sense and antisense RNA probes in 50% formamide were denatured at 80°C for 2 minutes cooled on ice and given a quick spin to collect contents.

2. *In situ* hybridisation buffer was added to give a final mix of 1 part probe in 50% formamide and 4 parts hybridisation buffer.

3. 150 μl of hybridisation mix was added to each slide of sections and then covered with cover slips avoiding air bubbles.

4. Slides were put on a platform inside a sealed container with paper soaked in 2X SSC, 50% formamide and placed in a hybridisation oven at 50°C overnight. A beaker of water was placed in the oven to prevent drying of tissues.

2.6.5.5 Post-hybridisation washing

1. Slides were placed in a glass rack and washed by dipping into 1X SSC for 10 minutes in the fume hood (cover slips were removed from slides at this step) followed by two fresh solutions of NTE buffer at room temperature for 5 minutes each.

2. Slides were then treated with 20 µg/ml RNAse A in NTE buffer at 37°C for 30 minutes followed by two washes in NTE buffer for 5 minutes each.

3. Slides were incubated in 1X SSC at room temperature for 10 minutes and then 0.2X SSC at 55°C for 60 minutes.

2.6.5.6 Immunological detection

1. Slides were placed in a rack and incubated in detection buffer 1 for 5 minutes, detection buffer 2 for 1 hour, buffer 3 for 1 hour.

2. Slides were placed on a tray and covered with buffer 4 (containing anti-DIG-alkaline phosphate) for 1 hour.

3. Slides were then washed four times in detection buffer 3 for 10 minutes each.

4. They were equilibriated in detection buffer 1 and buffer 5 for 5 minutes each and then incubated in detection buffer 6 containing NBT and BCIP for 24-48 hours as described by Coen *et al.* (1990).

2.6.5.7 Photography

Slides were air-dried in fume hood, mounted with toluene-based acrylic resin medium (Probing & Structure, Qld, Australia). These were dried in the fume hood overnight (~16 hours). Photographs were taken under Olympus Vanox AHT3 light microscope with RS Photometrics camera (Kodak, NY, USA).

2.7 Transformation prodedures

2.7.1 Transformation vectors

Three vectors were used to clone cDNA fragments for transformation of plants (Figure 2.1). cDNA fragments were cloned into a primary cloning vector, pART7. The expression cartridge of pART7 comprises the 35S promoter of a cauliflower mosaic virus (CaMV), a multiple cloning site and the octopine synthase gene (OCS) 3'-untranslated region (Gleave, 1992; Appendix B). The binary vector pART27 has a transfer-DNA (T-DNA) comprising of a β-galactosidase (*lac*Z') region with a unique *Not*I site immediately 3' of the right T-DNA border (RB), a chimaeric kanamycin resistance gene (nopaline synthase promoter (PNOS)-neomycin phosphotransferase (NPTII)-nopaline synthase terminator (NOS3'))) as plant selectable marker and a left T-DNA border (LB, Appendix C). The binary vector, pART69 is a derivative of pART27 and carries a ß-glucuronidase (GUS) gene driven by the mannopine synthase (MAS) promoter and CaMV (5'-7') terminator, immediately 3' to the T-DNA right border (Langridge *et al.*, 1989, Yao, unpublished).

2.7.1.1 Cloning of *TM29* cDNA

The *TM29* cDNA (1.2 kb) was cloned into the *Bam*HI site of the pART7 vector, between the CaMV 35S promoter and OCS 3' untranslated region. The cloning of the *Bam*HI cDNA insert into pART7 resulted in two vectors, pT729S (sense) and pT729AS (antisense), with the cDNA in sense or antisense orientation to the 35S promoter, respectively.

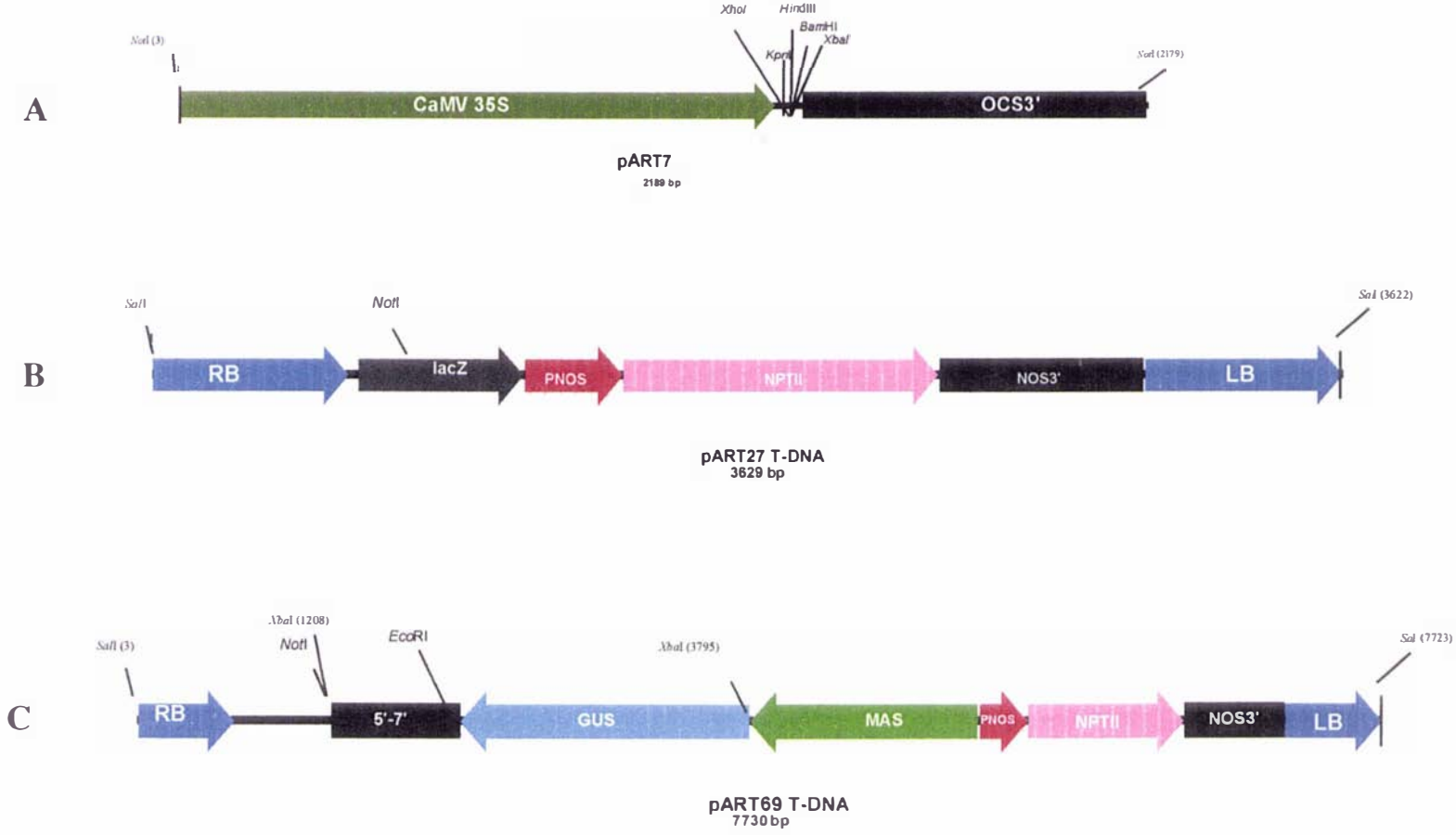

Figure 2.1. Schematic diagrams of cloning vectors used in this study. **A.** The expression catridge of pART7 primary cloning vector (Gleave, 1992). **B.** The T-DNA region of pART27 binary vector (Gleave 1992). **C.** T-DNA of pART69 vector (Yao, unpublished). For abbreviations in figure refer to Section 2.7.1 (Page 54).

The orientations were confirmed using *Xba*I enzyme. A third vector pT729PAS was constructed by cloning a 0.7kb cDNA fragment (comprising part of the I-region, the K-box, the C- and 3-' untranslated region) in antisense orientation to the 35S promoter in pART7.

The *Not*I 35S-cDNA-OCS fragment of each construct was introduced into the *Not*I cloning site of pART69 (Yao, unpublished) to yield three vectors, p69S (sense), p69AS (antisense) and p69PAS (partial antisense). These vectors containing the *TM29* sequences were transformed into *Agrobacterium tumefaciens* strain LBA4404 cells by electroporation.

2.7.1.2 Cloning of *TM10* cDNA

*Eco*RI recognition site was introduced into the 5' and 3' ends of the *TM10* cDNA by PCR. The *TM10* cDNA fragment was digested with the *Eco*RI enzyme and cloned into the *Eco*RI site of pART7 vector (Gleave, 1992). This cloning procedure resulted in the *TM10* cDNA cloned in either sense or antisense orientations to the 35S promoter, yielding two vectors pART70S and pART70AS respectively. A 2.7kb *Not*I fragment, including the 35S promoter, the *TM10* insert fragment and the OCS 3' untranslated region from each vector was cloned into the *Not*I site in the *Agrobacterium* binary vector, pART27 (Gleave, 1992) to obtain pART270S and pART270AS vectors (sense and antisense transformation vectors respectively).

2.7.2 Plant transformation

Agrobacterium cells carrying transformation vectors were used in separate experiments to transform tomato and tobacco tissues.

2.7.2.1 Tomato transformation

Tomato transformation experiments were carried out using the cultivar, Microtom following the method by Meissner *et al.*, (1997). Cotyledons from 7-9 day old seedling

were used as explants for transformation. Explants were prepared by slicing off the tip and the base of cotyledons. These were pre-cultured overnight on KCMS medium supplemented with 100 μM acetosyringone, with an overlay of sterilised Whatmann filter paper. Explants were placed with their adaxial surface to the filter paper.

Agrobacterium cells carrying the individual transgene vectors were cultured in YM medium supplemented with 100 mg/l of spectinomycin, at 28°C for two days. The cells were re-cultured in fresh YM medium with antibiotic and allowed to grow overnight up to OD_{600} of 1.5-2.0. The *Agrobacterium* cells were precipitated by centrifugation and resuspended in KCMS to an OD_{600} of 0.8.

The pre-cultured explants were transferred to a beaker containing 10 ml of the *Agrobacterium* cells in KCMS and incubated for 5 minutes with gentle swirling. The explants were then blotted on sterile filter paper and co-cultivated on the KCMS incubation medium at 23-24°C for two days. This was followed by their transfer to selective regeneration medium (2Z) consisting of MS salts and vitamins, 2 mg/l zeatin, 100 mg/l myo-inositol, 20 g sucrose, 2.7 g of phytagel supplemented with 100 mg/l kanamycin and 200 mg/l carbenicillin. Ten explants were put on each Petri dish containing 25 ml of medium. Subsequent transfers to fresh regeneration medium were done every two weeks until shoots were distinguishable. Explants with shoots were moved to pottles with shoot regeneration medium (1Z) containing 1 mg/l zeatin. Dead tissues were trimmed or removed to maintain healthy explants. Regenerated shoots at about 1-cm length were then transferred to MSSV medium supplemented with 1 mg/l indoyl butyric acid and 50 mg/l kanamycin. Rooted plants were transferred to soil in the glasshouse.

2.7.2.2 Tobacco transformation

Tobacco (*Nicotiana tabacum* cv Samson) was used as a heterologous host to examine the effects of ectopic expression of tomato MADS-box genes. Transformation procedure was similar to the one used for tomato, with certain modifications. Leaf disks from tobacco plants growing in tissue culture were used as explants. Leaf disks were inoculated with *Agrobacterium* cells carrying the vector p69S and pART270S and co-

cultivated on medium containing 1X MS salts and vitamins, 30 g/l sucrose, 0.1 mg/l NAA, 1 mg/l BA and 2.7 g/l phytagel, pH 5.8 before autoclaving. These were kept at 23-24°C for two days.

Co-cultivated explants were transferred to selection medium consisting of the co-cultivation medium supplemented with 100 mg/l kanamycin and 200 mg/l carbenicillin. Regenerating shoots were sub-cultured onto MS basal medium with 100 mg/l kanamycin and 200 mg/l carbenicillin. Shoots at 3-cm height were rooted on MS medium with 1 mg/l indol-butyric acid and transferred to soil in containment glasshouse.

2.7.2.3 Plant growth conditions

Transgenic and wild type tomato and tobacco plants were grown in potting mix of peat: loam: sand (2:1:1) in 10 cm diameter pots under glasshouse conditions at 23 ± 1 °C. Sodium vapor lamps (3000-5000 lux) were used to supplement natural light for a total of 16/8 hours light/dark (Atkinson *et al.*, 1998). For short-day treatment, plants were placed in a growth chamber, with 8 hours of light supplied by cool white flourescent bulbs (120 μmol m^{-2} s^{-1}) and a temperature of 24 ± 0.5 °C. Plants were watered regularly with normal tap-water.

2.8 Analyses of transgenic plants

2.8.1 Polymerase Chain Reaction (PCR) to confirm transgenic plants

To confirm the presence of the T-DNA constructs in the transformed tomato and tobacco plants, PCRs were performed with Taq DNA polymerase (Roche). Genomic DNA was isolated from young leaf tissues of transgenic plants as described previously (section 2.4.1).

A 35S promoter sense primer, P35S-1 was used in combination with *TM29* specific primer ITM-04 to amplify a 1.45 kb DNA fragment from the sense transformed plants. As an internal control, this primer combination did not give any fragment from the full and partial antisense lines or the non-transgenic plants. P35S-1 and ITM-03 amplified a 1.6 kb DNA fragment from both the full and partial antisense transformed plants.

For *TM10* transformed plants, P35S-1 was used in combination with ITM-02 primer to amplify a 1.1 kb fragment. PCR conditions were as follows: initial denaturation at 95°C for 2 minutes, 25 cycles of 95°C for 30 seconds; 58°C for 1 minute and 72°C for 1 minute plus a final extension at 72°C for 5 minutes.

2.8.2 Measurement of floral organ and fruit size

The length and width of each floral organ was measured under a stereo microscope. The mean of 3-5 flowers picked at the same stage was calculated for each line. Floral organs were separated with forceps and the length of each organ was measured along the mid-section from the apex to the point of attachment on the flower. The width was measured

at the widest portion of each organ. The diameter of each fruit was measured at the equatorial section picked at the breaker stage. The mean of five to six fruits was calculated for each plant studied

2.8.3 Scanning electron microscopic analyses

Plant samples were fixed in a 50% ethanol, 0.9 M glacial acetic acid and 3.7% formaldehyde for 15 hours and dried in a BalTec CPD 030 critical point drier. Samples were dissected under stereo microscope by removing some parts, to reveal the organs to be examined. These were mounted onto stubs and coated with gold in a Polaron E5100 sputter coater. Specimens were examined in a scanning electron microscope (Philips PSEM 505).

2.8.4 Tissue preparation and staining

To observe the early developmental stages of ectopic inflorescence, 8 μm tissue sections of ovary at 0-6 days post-anthesis (d.p.a) were prepared from the AS/45 transgenic line, which has a severe phenotype, using the method described previously (Jackson 1992). For staining, tissues were dewaxed in Histoclear (National Diagnostics), rehydrated through serial dilutions of ethanol and allowed to dry as described by O'Brien and McCully (1981). Tissues were stained in 0.01% toluidine blue (pH 4.5) and photographed as described previously.

2.8.5 GA treatment

For gibberellin treatment, GA_3 was either sprayed on whole plant produced from cuttings or was applied directly to flowers using a paintbrush.

Control and transgenic plants from vegetative cuttings were grown until they had three fully expanded leaves. Plant lines were sprayed generously twice a week for 4 weeks with 100 μM GA_3 (Sigma) and 0.02% Tween 20 (Wilson *et al.*, 1992). As a control, plants were sprayed with 0.02% Tween 20 in water. In a second treatment, individual inflorescence of 5-6 flowers was tagged and GA_3 applied to them using fine-tip paintbrush. As control, flowers on same plant were treated with 0.02% Tween 20. Flowers and fruits on these plants were observed for phenotypic changes.

CHAPTER 3

A Tomato MADS-box gene involved in flower and fruit development

3.1 INTRODUCTION

In plants, MADS-box genes are well known for their regulatory roles in flower development, functioning as homeotic genes in the specification of floral organs and controlling the spatial expression of other genes (Yanofsky *et al.*, 1990; Mandel *et al.*, 1992; Bradley *et al.*, 1993; Davies *et al.*, 1999). Fruit development is a progression from the events of flower morphogenesis and there are indications from expression patterns and genetic analyses that MADS-box genes play important functions during this process (Yao *et al.*, 1999; Sung *et al.*, 2000). The *AGL8* MADS-box gene in *Arabidopsis* controls cellular differentiation during fruit development (Gu *et al.*, 1998). The tomato *AGAMOUS1* is also implicated in the fruit ripening process (Ishida *et al.*, 1998). Recently the *PISTILLATA* homologue in apple, *MdPI* has been implicated in parthenocarpic fruit development (Yao *et al.*, 2001).

To further study the involvement of MADS-box genes in flower and fruit development, tomato (*Lycopersicon esculentum* Mill.) was chosen as a model system. *Tomato MADS-box gene 29* was obtained from a fruit cDNA library and its expression pattern determined in vegetative, floral and fruit tissues. Further experiments were carried out to examine its functions by transgenic methods. In this chapter, the characteristics of *TM29* and its potential functions in flower and fruit development are analysed.

3.2 RESULTS

The cDNA clone of *TM29* was isolated from a primary cDNA library constructed with mRNA extracted from young tomato fruit (1-7 days post-anthesis) in the λ Uni-Zap XR vector (Stratagene, CA, USA) (Kvarnheden *et al.* 2000; Yao, unpublished). The cDNA of *TM29* was sequenced on both strands using an ABI Prism Model 377 with M13 forward and reverse primers and also with custom-designed primers based on internal sequences. The length of the isolated *TM29* cDNA was 1231-bp comprising of an open reading frame (292-1029) encoding 246 amino acid residues, a 5' untranslated region (1-291) and a 3' region terminated by poly-A tail (1030-1231) (Figure 3.1).

CTAAAGTTAAAACAATGAATCCCTAAAGAAGATAGGAAGAAATGCCATAGATAAAAACAA
CCCATGTTCACTTTTTCTCTCTCTAAACATTGAAATTCAACCAAAACAAAAAACAAAAGT
TGATAAGAATCCTTTCTTTCTTTCTTTGTGTGTGTGTGTGTCTAGCTAGGGTTTGCATTT
CTTTCACAATTTTGGTTGTTTCAGTAGGAGAGAAAAGAGGATCTAAGAGTTAGCCAAGAG
*AAGAAATTAGTGAGAAAATAAAGTAGAAAAAGATCATCAGAGGAAGGAGGG***ATGGGTAGA**
M G R

GGAAGAGTTGAGCTGAAGAGGATAGAAAACAAGATAAATAGACAAGTCACTTTGCAAAG
G R V E L K R I E N K I N R Q V T F A K

AGGAGAAATGGATTGCTCAAAAAAGCTTATGAACTATCTGTGCTTTGTGATGCTGAAGTT
R R N G L L K K A Y E L S V L C D A E V

GCTCTACTCGTTTTCTCTAATCGTGGAAAACTCTATGAATTCTGCAGCACAAACAATATG
A L L V F S N R G K L Y E F C S T N N M

CTCAAAACACTTGATAGGTACCAAAAGTGCAGCTATGGAACATTGGAAGTCAATCGATCA
L K T L D R Y Q K C S Y G T L E V N R S

ATCAAAGATAATGAGCAAAGCAGCTATAGGGAATACTTGAAACTCAAAGCCAAATATGAG
I K D N E Q S S Y R E Y L K L K A K Y E

TCGCTGCAGCGATATCAAAGACACCTTCTTGGAGATGAGTTGGGGCCTCTGACTATAGAT
S L Q R Y Q R H L L G D E L G P L T I D

GATCTTGAGCATCTTGAAGTCCAACTAGATACTTCCCTCAAACACATTAGGTCCACCAGG
D L E H L E V Q L D T S L K H I R S T R

ACACAAATGATGCTTGATCAGCTTTCTGATCTTCAAACTAAGGAGAAATTGTGGAATGAG
T Q M M L D Q L S D L Q T K E K L W N E

GCTAACAAGGTTCTTGAAAGAAAGATGGAAGAAATATATGCTGAAAACAACATGCAACAA
A N K V L E R K M E E I Y A E N N M Q Q

GCATGGGGTGGTGGTGAGCAAAGTCTCAATTATGGTCAGCAGCAACATCCTCAATCTCAG
A W G G G E Q S L N Y G Q Q Q H P Q S Q

GGTTTCTTCCAACCTCTAGAGTGCAACTCTTCCTTGCAAATTGGGTACGATCCAATAACA
G F F Q P L E C N S S L Q I G Y D P I T

ACTTCAAGCCAAATAACAGCAGTAACAAATGCCCAAAACGTGAATGGTATGATACCTGGT
T S S Q I T A V T N A Q N V N G M I P G

TGGATGCTG*TGAATGAAAAAGTCCTTTATCTTCAGCTTTGCATAAAAGCATATGAAGTAT*
W M L *
ATTTCTATAATAATAAAGGAAAACTCCAGTACCTTTATTTTCAGCAAAATACCCTAATTA
AGGTGAACGTTGTGAACCATTTTCTTTGCATAAAAACAAACTTGTTTGCTTGGAAATGTT
TTATTTTATTCAAAAAAAAAAAAAAAAAAA

Figure 3.1. Nucleotide sequence of the positive strand of TM29 cDNA and derived amino acid sequence below. The 5' untranslated region (UTR) and the 3' UTR have been italicized, before and after the coding region respectively. The positions of introns are marked with ▼. The * marks the translational stop codon.

3.2.1 *TM29* is a tomato MADS-box gene and groups to the *SEP1* subfamily

The conceptual TM29 protein was analysed for sequence similarity with members of the MADS-box family. TM29 has the 4 regions typical of plant MADS-box genes (i.e. the MADS-box (M), intergenic region (I), K box and a carboxyl (C)-terminal region; Figure 3.2; Ma *et al.*, 1991; Krizek and Meyerowitz, 1996; Mizukami *et al.*, 1996; Riechmann *et al.*, 1996; Riechmann and Meyerowitz, 1997). The proportion of each amino acid residue in TM29 protein was compared to tomato TM5, *Arabidopsis* SEPALLATA (SEP) 1, SEP2 and SEP3 MADS-box proteins using the program COMPOSITION from the GCG package (Version 9; Genetics Computer Group, Madison, WI). The percentage of each amino acid in TM29 was very similar to those of SEP1 and SEP2 proteins compared to the AGAMOUS protein (Table 3.1).

For detailed comparisons, each of the four domains of TM29 protein was compared to those of other MADS-box proteins. Sequences from each domain were analysed by BESTFIT (GCG) to calculate percentage similarity. TM29 showed high degree of sequence similarity with the selected sequences within the MADS-box region (Table 3.2). In the I-region and the K-box, there was high sequence similarity to SEP1 and SEP2. Within the most-variable C-terminal region, there was no significant identity between TM29 and TM5 or SEP3; however, a certain level of identity was observed between TM29 and DEFH49, FBP2, SEP1 and SEP2 (Table 3.2). When TM29 was aligned with MADS-box sequences to compare residues, conserved amino residues were observed among the closely related sequences in all four domains (Figure 3.2). TM29 shared a motif **PGWML** with SEP1, SEP2 and DEFH49 at the C terminus, which distinguished them from other MADS-box proteins (Figure 3.2).

Table 3.1. Amino acid composition (%) of TM29 and other MADS-box proteins

Amino acid	Letter code	TM29	TM5	SEP1	SEP2	SEP3	AG
Alanine	A	4.0	5.8	4.8	3.6	4.7	5.5
Cysteine	C	1.6	2.2	2.0	2.4	1.6	1.0
Aspartic acid	D	4.0	2.2	3.6	3.6	4.0	3.2
Glutamic acid	E	8.0	8.0	8.0	8.0	8.3	7.5
Phenylalanine	F	2.0	1.8	1.2	1.2	2.4	1.2
Glycine	G	6.2	5.3	7.6	9.2	5.9	5.5
Histidine	H	1.6	1.0	1.6	2.8	2.0	1.2
Isoleucine	I	4.0	5.0	3.8	4.4	3.2	6.8
Lysine	K	6.9	8.0	6.8	6.8	5.2	6.0
Leucine	L	12.7	16.5	12.9	12.8	14.4	8.8
Methionine	M	3.2	4.0	3.6	2.8	2.8	2.5
Asparagine	N	6.9	5.0	6.8	5.6	5.5	8.4
Proline	P	2.0	1.3	2.8	2.4	4.0	3.5
Glutamine	Q	8.5	8.0	8.8	8.8	9.5	8.0
Arginine	R	6.0	8.9	6.5	6.4	8.0	8.4
Serine	S	7.0	7.5	6.0	6.8	6.8	10.8
Threonine	T	5.5	3.1	3.6	2.4	3.5	3.5
Valine	V	4.0	2.2	3.6	4.4	3.2	3.6
Tryptophan	W	1.2	1.0	1.1	0.8	0.5	0
Tyrosine	Y	4.5	3.1	4.8	4.8	4.4	4.5

Table 3.2. Identity (%) between TM29 and selected MADS-box proteins

[a]	[b] MADS-box	I region	K domain	C terminus
TM29	100 (58)	100 (31)	100 (67)	100 (90)
SEP1	96 (58)	59 (31)	70 (67)	42 (88)
SEP2	96 (58)	67 (31)	68 (67)	32 (94)
SEP3	96 (58)	50 (34)	65 (67)	* (92)
TM5	94 (58)	50 (32)	70 (67)	* (67)
FBP2	96 (58)	50 (32)	71 (67)	28 (84)
DEFH49	96 (58)	67 (31)	85 (67)	41 (91)

* No significant identity. [a] For sequence accession numbers, refer to Appendix A.

[b] Numbers in parentheses refer to length of amino acids compared.

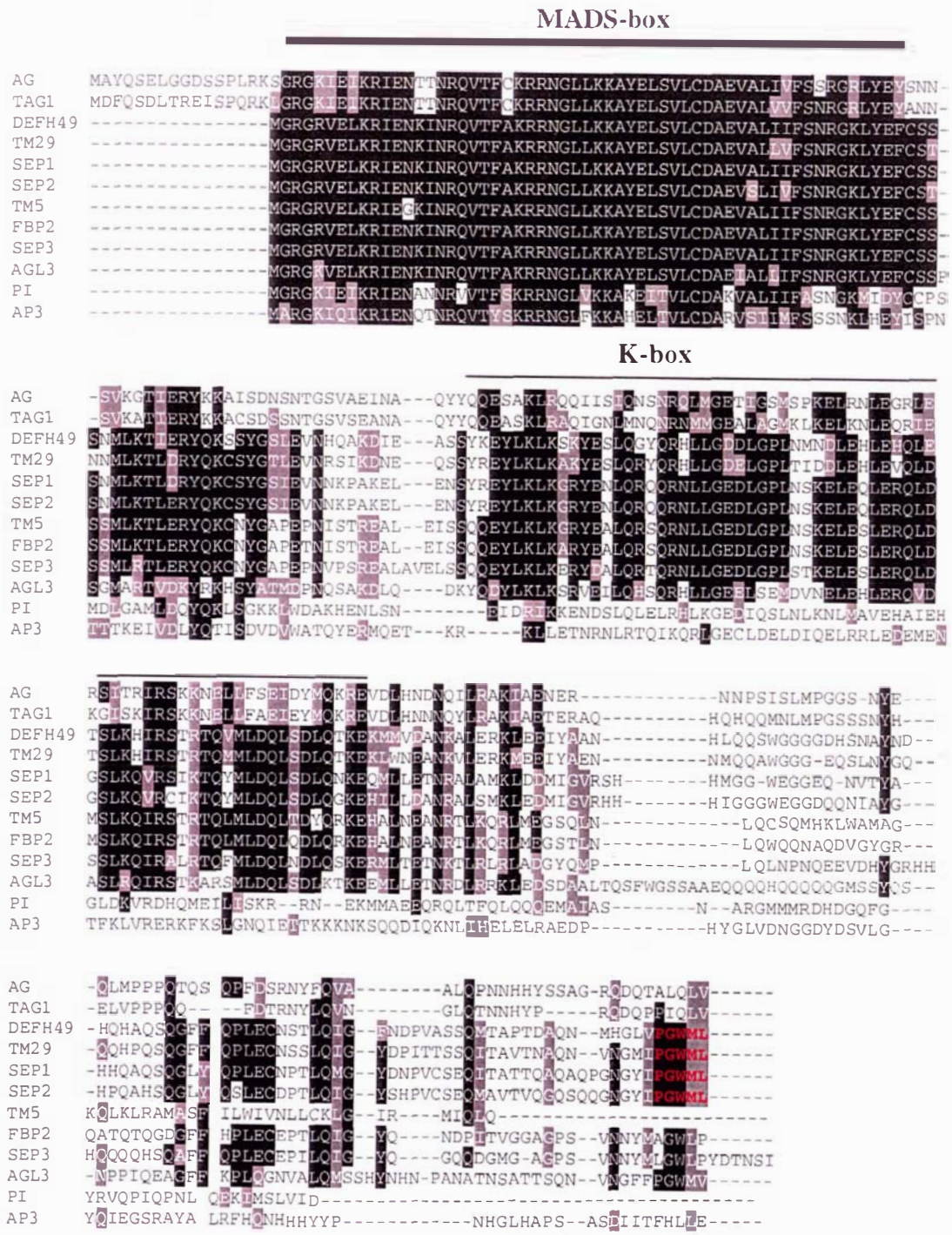

Figure 3.2. Sequence alignment of selected MADS-box proteins using clustal W analyses. Conserved residues are shaded in black; gaps were introduced to achieve maximum alignment. Bold and thin lines indicate the MADS-box and the K-box, respectively. The C-terminal of TM29 displays residues that are conserved among members of the SEP1 subfamily (shown in red).

Over the entire protein sequences, TM29 shows 78% amino acid sequence identity to DEFH49, an *Antirrhinum majus* MADS-box gene, 68% and 66% identity to SEP1 and SEP2 of *Arabidopsis*, respectively (Ma *et al.*, 1991; Davies *et al.*, 1996). Among the known MADS-box proteins in tomato, the Tomato MADS-box 5 (TM5) (Pneuli *et al.*, 1994a) is the closest in identity (72% over the M, I and K regions) to TM29.

Analyses of conserved putative secondary structures can distinguish proteins and their biological significance (Pneuli *et al.*, 1991). Alpha helices are capable of promoting molecular interactions within and between proteins and long stretches are present in MADS-box proteins (Pneuli *et al.*, 1991). The secondary structure of TM29 was predicted using PSIPRED, a discrete state-space probability model (Jones, 1999). The amino acid residues forming the putative coil, ß-strands and α-helices were identified (Figure3.3). The predicted secondary structure of TM29 was similar to that of SEP1 MADS-box protein. The K-domain was characterised by two long stretches of α-helices (residues 92-158) an indication of the coiled coil structure of this domain (Alvarez-Buylla *et al.*, 2000).

To assess TM29 relationship to other MADS-box proteins sequences from the MADS-box, the I, and K regions of selected MADS-box proteins were used to construct an unrooted phylogenetic tree. These analyses assigned TM29 to the SEP1 subfamily, including SEP2 and DEFH49 (Figure 3.4). Taken together, the sequence analyses of TM29 suggested it is a member of the SEP1 subfamily of MADS-box proteins and may furthermore be the tomato homologue of SEP1.

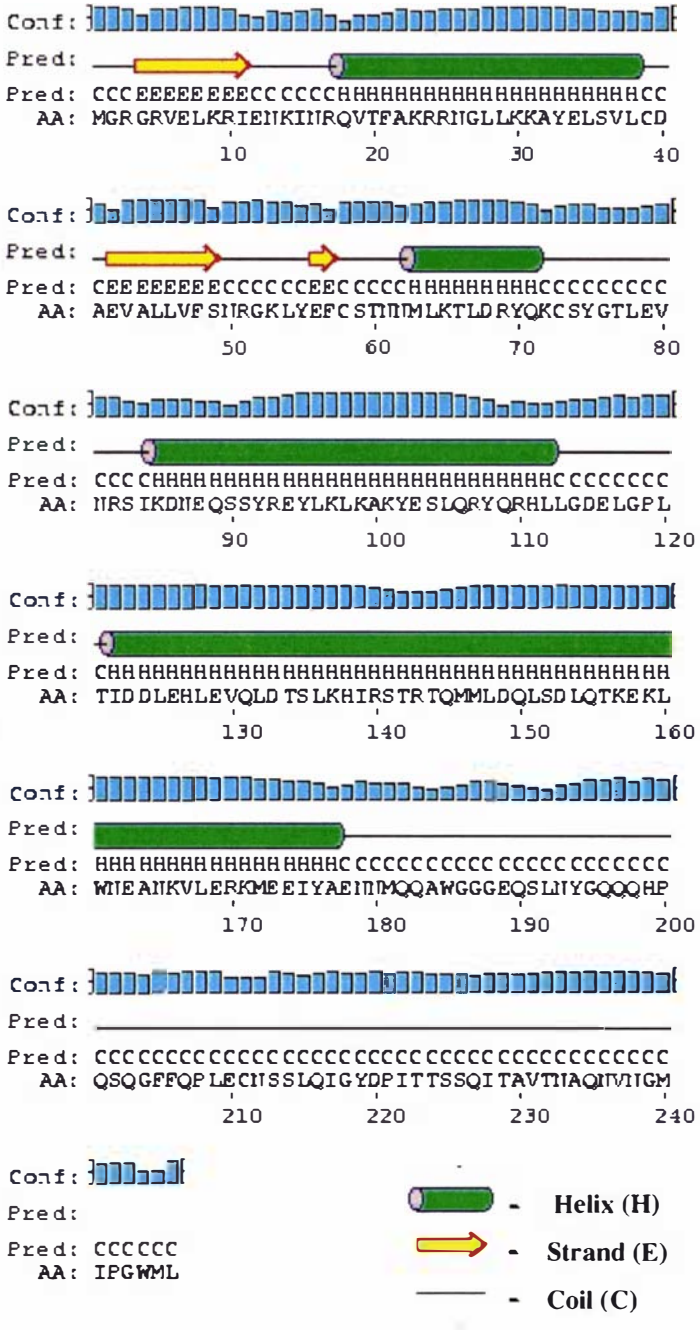

Figure 3.3. Secondary structure of TM29 protein. The structure of TM29 protein was predicted by analyses of the amino acid residues using PSIPRED module (Jones, 1999). The residues in the K-domain (92-158) are predicted by this method to have α-helical structure, an indication of the coiled-coil structure known for this domain (Alvarez-Buylla et al., 2000).

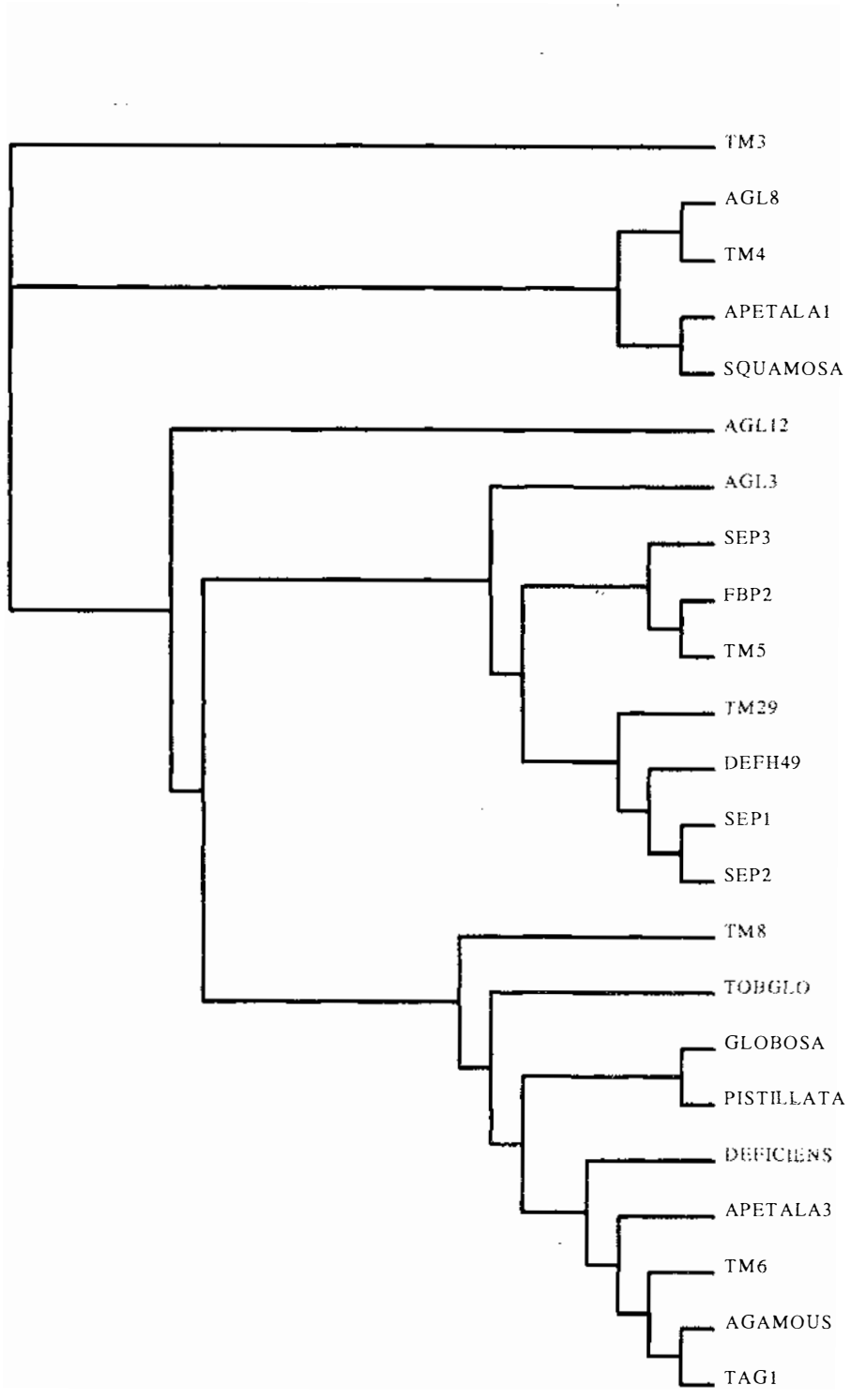

Figure 3.4. An unrooted phylogenetic tree of selected MADS-box proteins. Sequences from the MADS-box, I- and K-regions were used in progressive pairwise distance calculations and corrected with Kimura's distance correction method. The NJ method (Saitou and Nei, 1987) was used to cluster the sequences for reconstruction with Growtree program (GCG). TM29 protein groups with members of the SEP1 subfamily.

3.2.2 *TM29* gene structure

The DNA fragment of *TM29* was amplified from tomato genomic DNA by Polymerase Chain Reaction (PCR) with gene-specific primers TM29-GM1 and TM29-GM2. The PCR was performed in a Techne Progene thermal cycler (John Morris Scientific Ltd, UK) at 94 °C for 2 minutes, 10 cycles of 94 °C for 30 seconds, 55 °C for 30 seconds and 68 °C for 3 minutes. This was followed by 20 cycles of 94 °C for 30 seconds, 55 °C for 30 seconds and 68 °C for 3 minutes (+ 20 seconds after each cycle).

A resultant DNA fragment of 4-kb in size was cloned into pGEM-T Easy Vector (Promega, Madison, WI) in a ligation reaction to give pGTM29. The cloned *TM29* genomic fragment was sequenced in both directions using the M13 forward and reverse primers. Further sequencing carried out with primer pairs (TM29-P1 and TM29-P2, TM29-P3 and TM29-P4, TM29-P5 and TM29-P6, TM29-P7 and TM29-P8) based on reliable internal sequences.

The exons and introns within the genomic DNA sequence of *TM29* were predicted by aligning the genomic sequence with the cDNA sequence using the BLAST program (Altschul *et al.*, 1997). The standard intron donor and acceptor sites, GT and AG respectively, were used as guide to locate intron positions. There were 8 exons forming the open reading frame of the *TM29* gene with seven introns (Figure 3.5; Appendix D). The seven introns were of varying sizes with the first intron (1.46-kb), which is the largest located outside the MADS-box.

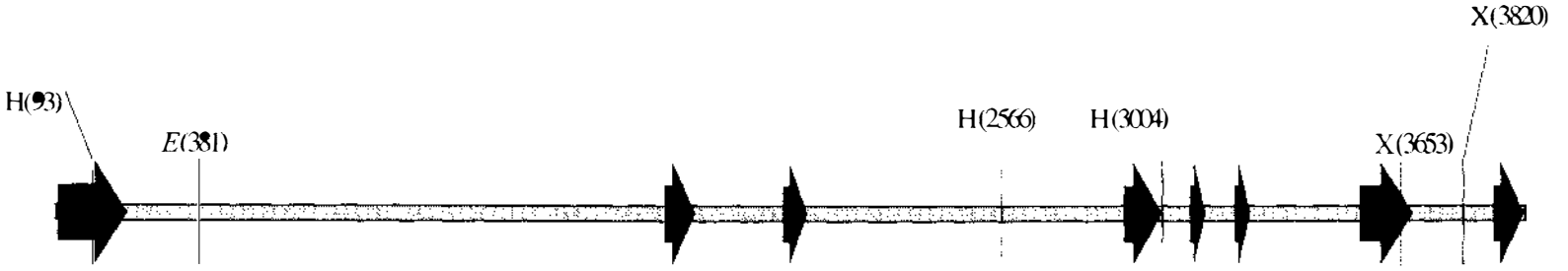

Figure 3.5. Map of *TM29*. Eight exons are indicated by thick black arrows, the hatched line in between exons represent introns. Restriction sites of selected enzymes within the genomic DNA are labelled (E: *Eco*RI; H: *Hin*dIII; X: *Xba*I). Numbers in parentheses indicate nucleotide positions.

There are no introns within the MADS-box, similar to what is observed for most members of this gene family. In comparison, seven exons make up the open reading frame of the *SEP1* and *SEP2* genes (Ma et al., 1991). *TM29* encodes 246 amino acids, while *SEP1* and *SEP2* have 249 and 251 amino acid residues respectively (Ma et al., 1991).

3.2.3 Gene copy number

The gene copy number of *TM29* in tomato was estimated by Southern hybridisation. Restriction digestions of tomato genomic DNA, using three restriction enzymes (*Eco*RI, *Hin*dIII and *Xba*I) were probed with a *TM29*-specific probe. Single major hybridising bands were observed with the *Eco*RI and *Xba*I digests. Two weak hybridising bands were obtained with the *Hin*dIII digestion. *TM29* genomic sequence revealed two *Hin*dIII restriction sites within the region corresponding to the cDNA fragment used as the probe (Figure 3.6). These were expected to give 3 hybridising bands; the smallest expected fragment 0.4-kb containing only 100-bp of cDNA sequence was not detected under the stringent conditions used (refer to methods section 2.6.2). The analysis of the results suggests there is only one copy of *TM29* in tomato.

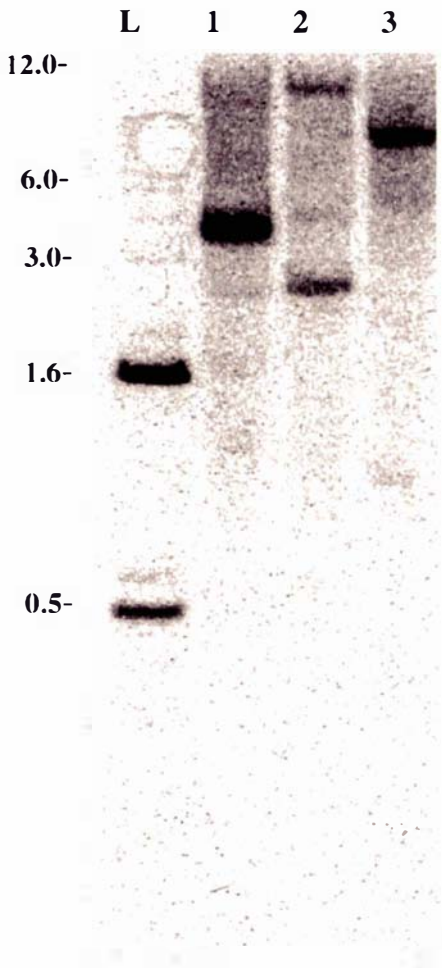

Figure 3.6. Southern hybridisation of tomato genomic DNA digested with three enzymes, using TM29 specific probe. Lanes 1-3 contain tomato genomic DNA digested with *Eco*RI, *Hin*dIII and *Xba*1 restriction enzymes respectively. Single major hybridising band is seen with *Eco*RI and *Xba*I while multiple weak bands are observed with *Hin*dIII digestion. The numbers on the left-hand side represent the fragment sizes in kilobasepairs of the DNA ladder (L).

3.2.4 *TM29* expression detected by northern analyses

Northern blot hybridisation was initially used to detect *TM29* transcripts in various parts of the tomato plant. Total RNA from flowers, fruit, young leaves, shoot tips and roots were probed with *TM29* gene-specific probe. Steady state transcripts were found to accumulate to a high level in flower buds (0.1-3 mm diameter) and in young fruits (1-7 days old) and to a much-reduced level in shoot tips (Figure 3.7A). Transcripts were not detected in leaves or roots. Another experiment to further characterise *TM29* expression in fruit tissues found transcripts in both pre-anthesis and anthesis ovary (fruit initials) as well as 3- to 14- day-old fruits, but not 21-day-old fruit or young leaves (Figure 3.7B). Together, these northern results show that *TM29* is expressed in the shoot meristems, before the switch to reproductive development and then in the flowers through to the cell expansion phase of fruit development.

3.2.5 Spatial and temporal *TM29* expression in tomato

In situ hybridisation was used to further examine the expression pattern of *TM29* in vegetative and floral meristems and in developing floral organs of tomato. Gene-specific RNA (sense and antisense) probes, transcribed and labelled *in vitro*, were used to detect the presence of *TM29* transcripts in tissue sections.

In tomato, the vegetative meristems are responsible for the primary and sympodial shoot growth until their conversion to inflorescence meristems (Schmitz and Theres, 1999). The inflorescence meristem in turn divides into two, to give a floral meristem and an inflorescence meristem (Allen and Sussex, 1996). *TM29* RNA was expressed in vegetative shoot apices and sympodial buds (Figure 3.8A).

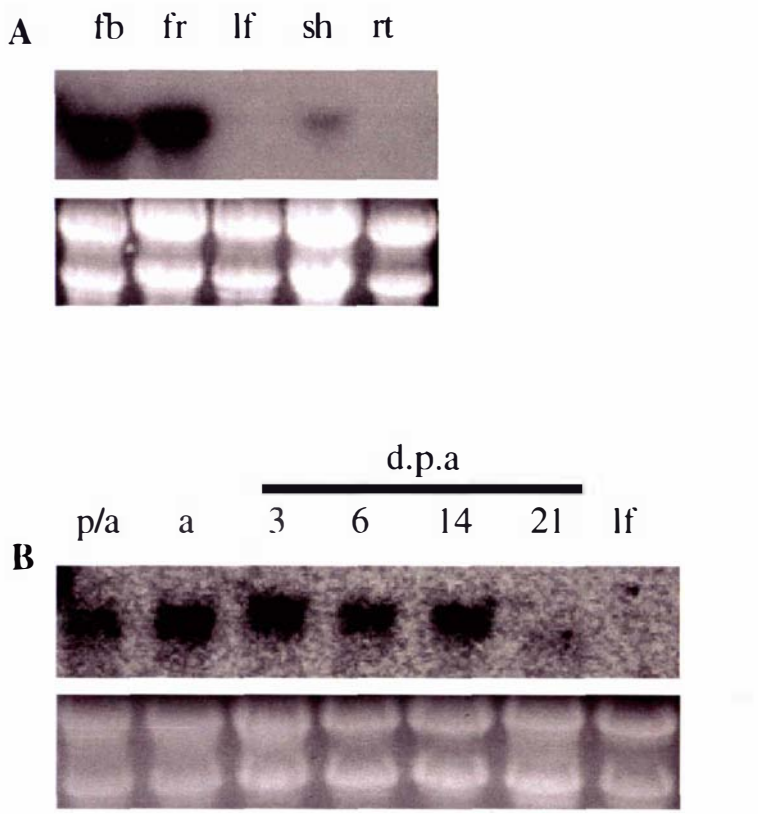

Figure 3.7. Northern analyses of *TM29* gene expression. Northern blots were probed with gene-specific probe prepared from *TM29* cDNA fragment without the MADS-box. Loading levels of RNA samples are shown by gel photographs of stained rRNA bands. **A**. Total RNA was extracted from tomato flower buds (fb), 1-7 day post-anthesis (d.p.a) fruits (fr), young leaves (lf), shoot tips (sh) and roots (rt). **B**. Total RNA was extracted from ovary at pre-anthesis (p/a) and anthesis (a); fruits at 3, 6, 14 and 21 d.p.a and young leaves (lf).

TM29 expression was also detected in inflorescence and in floral meristems. Expression was seen in the bifurcating structure of a floral meristem and an adjacent inflorescence meristem (Figures 3.8B, 3.8C). Thus, T*M29* transcripts were present in vegetative, inflorescence and floral meristems, suggesting that it may have a function in regulating the growth of meristematic cells. It further indicates *TM29* may control development of the different tissues produced by these meristems. The use of the sense RNA probe did not give any signals above background levels (Figures 3.8D, 3.8E and 3.8F).

The floral meristem produces the flower containing four different types of floral organs in concentric whorls. During floral development, the sepal primordia emerge first on the flanks of the floral meristem, followed sequentially by the petals, stamens and carpel (Sekhar and Sawhney, 1984). *TM29* expression was observed in the primordia of all four floral organ types. Expression was detected in the emerging sepal primordia (Figure 3.9A), but not in older sepal primordia or mature sepals (Figure 3.9C). The temporal expression in the petal primordia was found to be similar to that in sepal, i.e. it was detected in emerging petal primordia but not in mature petals (Figures 3.9D, 3.9E). *TM29* expression in stamen primordia was uniform at the earliest stage of emergence (Figure 3.9D). Later in stamen development, expression localises to the anther region of the stamen primordia (Figure 3.9E) and in the tapetal region of the stamen (Figure 3.9G). *TM29* expression was detected in the carpel region of the flower meristem right up to the period of ovary development (Figures 3.9A, 3.9C, 3.9D and 3.9E). There was uniform expression within the ovary primordium at earlier stages, but later when the carpels were well differentiated (with a protruding style) the expression was mainly in the region of the ovary that forms the fruit pericarp (Figure 3.9G). The probing of tissues with sense RNA probe, as controls, did not yield any signals above background level (Figures 3.9B, 3.9H). In tomato fruit (7 d.p.a) *TM29* expression can be detected in the pericarp, placental and in the seeds (Figure 3.10A). A similar section was probed with sense RNA as control (Figure 3.10B).

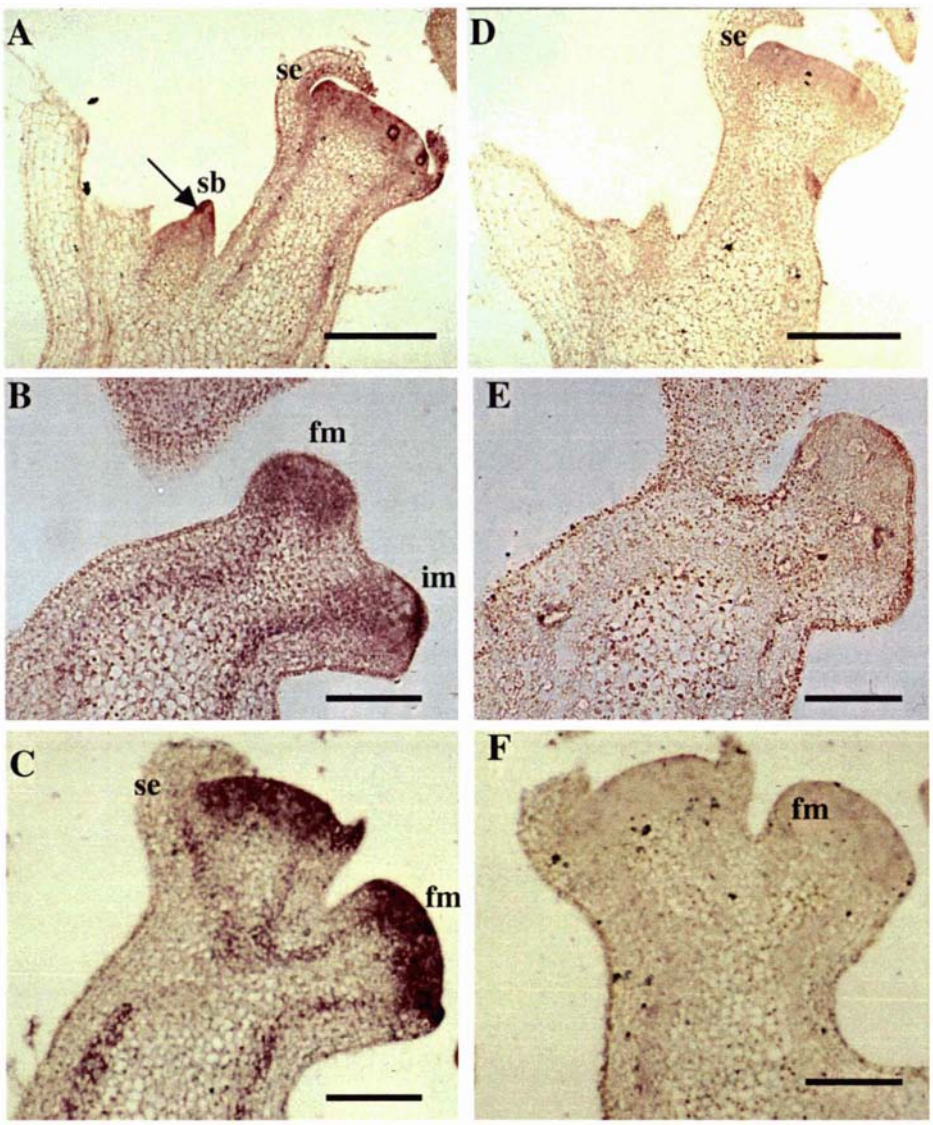

Figure 3.8. *In situ* hybridisation of *TM29* expression in tomato meristems. Sections were viewed under bright-field illumination and signals are indicated by the intensely-stained regions.

(A) A sympodial bud in the axil of a leaf showing *TM29* expression at the tip (arrowed).

(B) A bifurcating structure with a floral meristem and inflorescence meristem. *TM29* is expressed uniformly in the floral meristem and strongly at the tip of the inflorescence meristem. Transcripts are also seen in the vascular bundles.

(C) Floral meristems at different stages showing *TM29* expression is uniform throughout the floral meristem region.

(D), (E) and (F) Tissue sections as in (A), (B) and (C) probed with sense RNA of *TM29* and used as control to indicate background levels.

Bars=150 μm. fm: floral meristem; im: inflorescence meristem; sb: sympodial bud; se:sepal

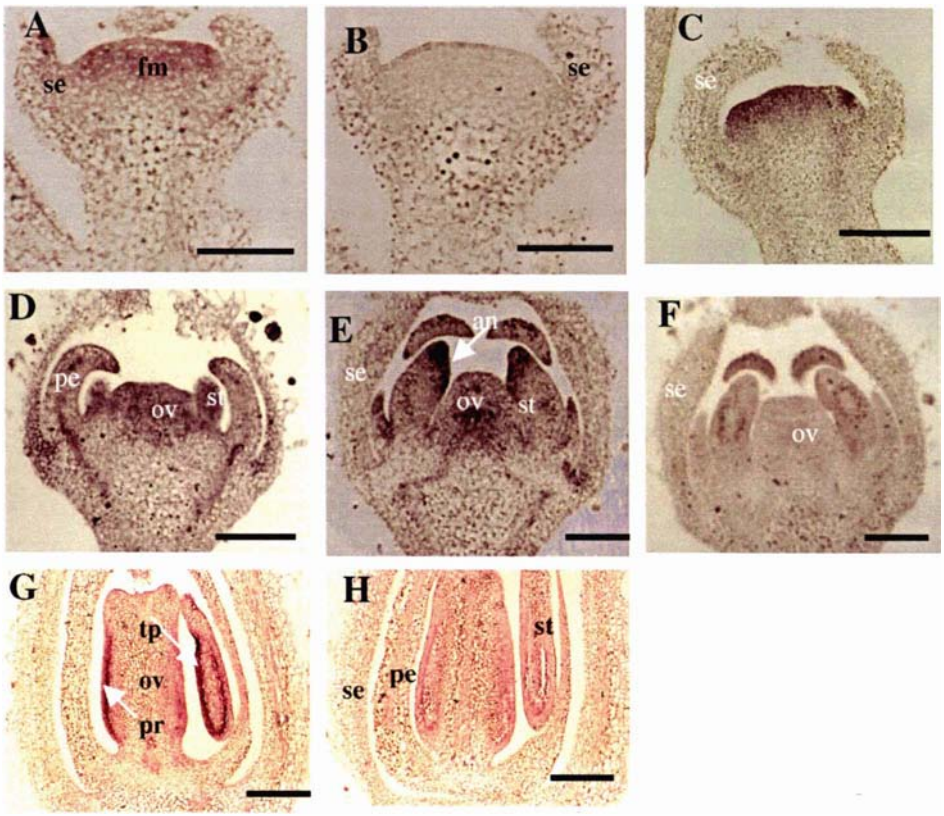

Figure 3.9. *TM29* RNA expression in wild type floral organ primordia.

(A) *TM29* expression decreases in the emerging sepal primordia but still detectable in the floral meristem.

(B) Tissue as in (A) probed with sense RNA as control.

(C) *TM29* expression is reduced in the elongated sepal primordia but detected in the domains of the inner whorls.

(D) A flower tissue showing primordia of all four floral organs. *TM29* transcript level in the petal primordia is low but relatively high expression is observed in the stamen and carpel primordia.

(E) Later, *TM29* expression is localised to the region of the stamen primordia where the anthers will be formed and in the ovary primordium.

(F) Tissue section as in (E) probed with sense RNA to show background levels.

(G) A flower bud at ~4 days before anthesis. *TM29* expression is detected in the pericarp region of the ovary and in the tapetal cells of the stamen.

(H) Tissue section as in (G) probed with sense RNA.

Bars=150 μm. an:anther region; ov: ovary primordium; pe: petal; pr: pericarp; se: sepal; st: stamen; tp: tapetal region

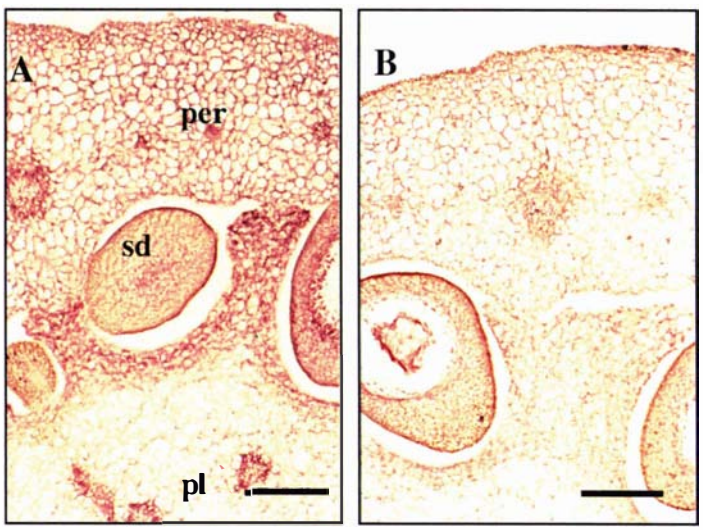

Figure 3.10. *TM29* expression in wild type tomato fruit tissues (6 d.p.a)

(A) *TM29 is* expressed in the pericarp, the placenta and in the seeds.

(B) Tissue as in (A) probed with sense RNA as control.

Bar= 500 µm. per:pericarp; pl: placental tissue; sd: seed

Together these results show that *TM29* is expressed in meristems and in the floral organ primordia. The expression in the floral organs decreases as each organ develops and matures, suggesting that *TM29* may be required early in the development of floral organs. In the mature flower bud, *TM29* transcripts are not detected in the perianth organs (sepals and petals) but its expression localises to specific regions in the stamens and ovary. This pattern suggests *TM29* may have specialised functions in the development of reproductive tissues.

3.2.6 *Agrobacterium* transformation vectors

Three *Agrobacterium* transformation vectors, p69S, p69AS and p69PAS, carrying cDNA fragments of *TM29*, were generated for plant transformation. *TM29* cDNA carrying the full coding region was cloned into the *Bam*HI site of the pART7 cloning vector to give pT729S and pT729AS, with sense and antisense orientation to the CaMV 35S promoter (Figure 3.11A). Restriction digestion of pT729S and pT729AS with *Bam*HI resulted in the expected fragments of 1.3-kb cDNA insert and 5-kb vector backbone (Table 3.3). Subsequent digestion using *Xba*I enzyme gave a diagnostic 0.3-kb DNA fragment for the sense construct and a 0.9-kb fragment for the antisense construct (Table 3.3). The partial-antisense construct (pT729PAS) was obtained by cloning a 0.8-kb *Kpn*I/*Xho*I fragment of the *TM29* cDNA into the *Kpn*I/*Xho*I site of pART7. This resulted in an antisense orientation to the 35S promoter. The 35S-cDNA-OCS cassette of each construct was cloned into the *Not*I site of the pART69 transformation vector, resulting in p69S, p69AS and p69PAS. These vectors were confirmed by digestion with *Not*I and *Xba*I enzymes (Figure 3.11B; Table 3.4). *Not*I digestion resulted in two DNA fragments, the 3-kb 35S-cDNA-OCS cassette and the 15-kb pART69 vector backbone, confirming the presence of the cloned insert. *Xba*I digestion resulted in four different DNA fragments for each vector, which confirmed the correct sizes and orientations of the vectors (Figure 3.11B; Table 3.4).

Table 3.3. Expected fragments from enzyme digestions of vectors

Vector	Enzyme	Expected fragments (kb)
pART70S	*Bam*HI	4.9; 1.3
	*Xba*I	5.9; 0.3
pART70AS	*Bam*HI	4.9; 1.3
	*Xba*I	5.3; 0.9

Table 3.4. Expected fragment sizes from digestion of T-DNA vectors

T-DNA vector	Enzyme	Expected fragments (kb)
P69S	*Not*I	3.0; 12.7
	*Xba*I	0.3; 0.7; 2.6; 12.1
P69AS	*Not*I	3.0; 12.7
	*Xba*I	0.9; 1.7; 2.6; 10.5
P69PAS	*Not*I	2.8; 12.9
	*Xba*I	0.5; 0.7; 2.6; 11.9

A

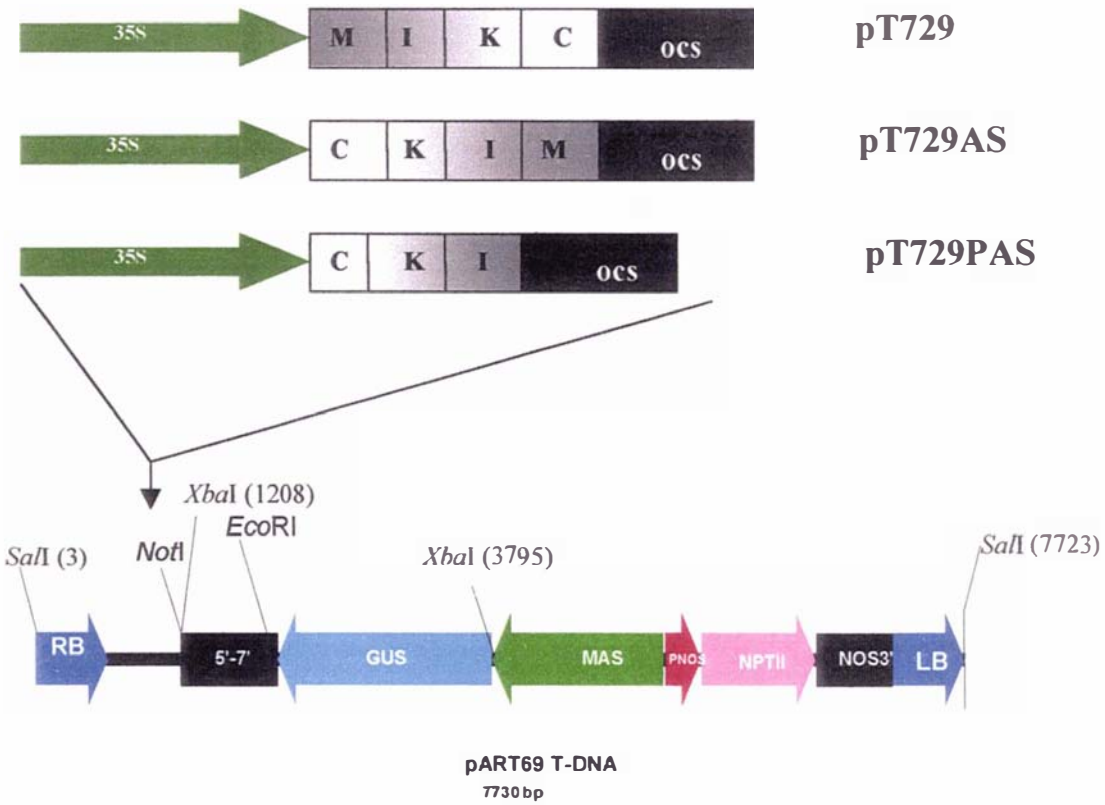
35S
M I K C ocs
pT729
35S
C K I M ocs
pT729AS
35S
C K I ocs
pT729PAS
XbaI (1208)
EcoRI
SalI (3)
NotI
XbaI (3795)
SalI (7723)
RB
5'-7'
GUS
MAS
PNOS
NPTII
NOS3'
LB
pART69 T-DNA
7730 bp

B

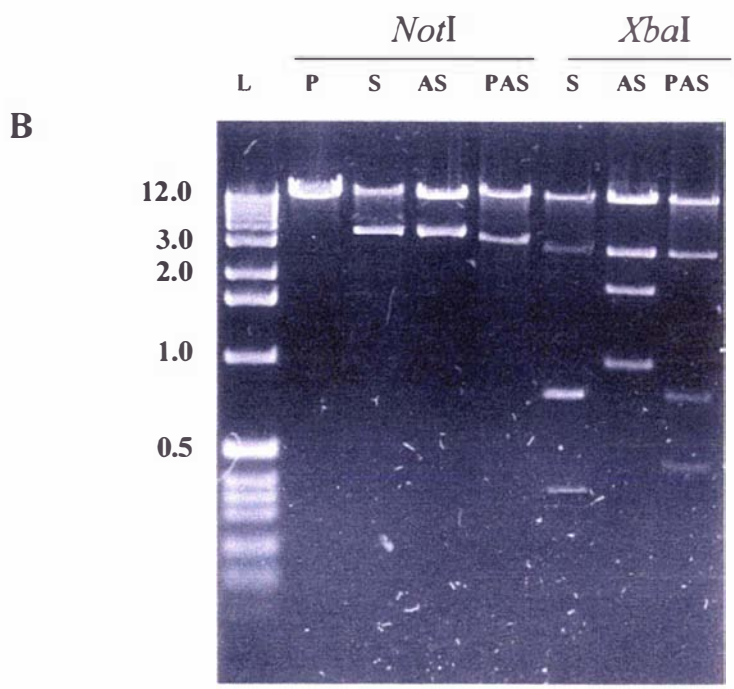
NotI
XbaI
L
P
S
AS
PAS
S
AS
PAS
12.0
3.0
2.0
1.0
0.5

Figure 3.11. Construction of the T-DNA vectors used in transformation.

(A) The 35S-cDNA-OCS fragment of the sense (S), antisense (AS) and partial-antisense (PAS) constructs was cloned into *Not*I site of the pART69 transformation vector.

(B) The *Not*I and *Xba*I enzymes were used to confirm the T-DNA constructs. The *Not*I digestion of the pART69 plasmid (P) and the vectors confirmed the presence of the cloned 35S-cDNA-OCS fragment. *NotI* digestion of the pART69 plasmid resulted in a single linear fragment. The *Xba*I enzyme digestions confirmed the orientations of these vectors.

3.2.7 Tomato transformation

Agrobacterium tumefaciens strain LBA4404 harbouring the transformation vector p69S, p69AS or p69PAS was used to generate independently transformed tomato plants (Table 3.5). Plants were rooted on kanamycin-containing medium in tissue culture and then transferred into soil in a containment glasshouse. Individual transgenic plants were confirmed as transgenic by PCR analysis.

Overall, 22 plants out of a total of 31 regenerated plants were transformed with the sense construct. These were transferred to soil in the containment glasshouse. Of these, only one (S/05) showed variation in phenotype compared to the wild type. Seventy regenerated shoots were obtained from explants inoculated with p69AS. Of these, 10 were successfully rooted on kanamycin selection medium. Six of these primary antisense plants showed morphogenetic alterations (Table 3.5). Another two plants (AS/16, AS/20) showed normal phenotype and produced viable seeds, which were planted to give the T_1 generation of plants. An estimated ten percent (10%) of these plants displayed phenotypes similar to the aberrant primary antisense plants mentioned above. Using p69PAS vector, 121 regenerated plants were initially obtained on selection medium. Upon subsequent transfers to selection medium, 30 plants were successfully rooted and transferred to grow in soil. None of these plants displayed the phenotypes seen in the other two transformed populations. Overall, their characteristics were not different from the wild type tomato plants.

3.2.8 Confirmation of transgenic plants by PCR

These plants were confirmed as transgenic by polymerase chain reaction (PCR). A DNA fragment of 1.4-kb size was amplified from the sense transgenic plants using the p35S-1 and ITM-04 primers (Figures 3.12A, 3.12B). From the antisense and partial antisense plants, a 1-kb DNA was amplified using the p35S-1 and ITM-03 primers (Figure 3.12C-F).

3.2.9 Morphogenetic alterations in tomato transgenic plants

The *TM29* sense and antisense expression caused developmental abnormalities in the primary transgenic flowers but vegetative characteristics of the tomato transgenic plants showed little or no changes compared to the wild type tomato plants.

3.2.9.1 Flower phenotypes of tomato transgenic lines

The wild type tomato flowers consist of four whorls of floral organs: the outer whorl contains five to seven green sepals, which are in the most part separated and characterised by trichomes and stomata on the adaxial and abaxial surfaces. The petals in the second whorl are yellow at anthesis and are less turgid compared to sepals. The number of petals range from five to seven in the wild type. There are six yellow stamens in the third whorl, which are fused to form a cone surrounding the pistil and attached to the base of the petals (Figure 3.13A). The innermost whorl of the flower is occupied by the carpel, consisting of a bilocular or multilocular ovary with a protruded style and a stigma (Lozano *et al.*, 1998). Tomato flowers are usually self-pollinated. After fertilization, the petals and stamens undergo senescence usually 4-5 days after pollination and eventually abscise from the flower.

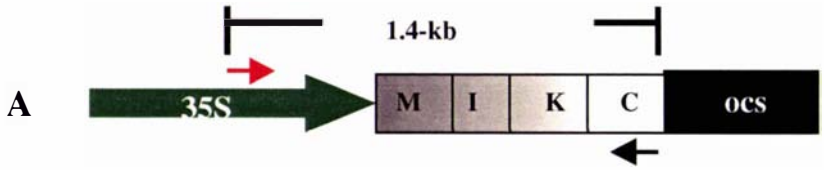
A
1.4-kb
35S
M
I
K
C
ocs

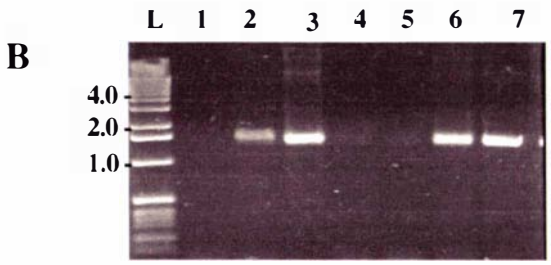
B
L 1 2 3 4 5 6 7
4.0
2.0
1.0

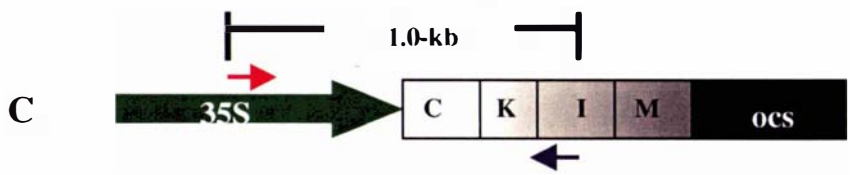
C
1.0-kb
35S
C
K
I
M
ocs

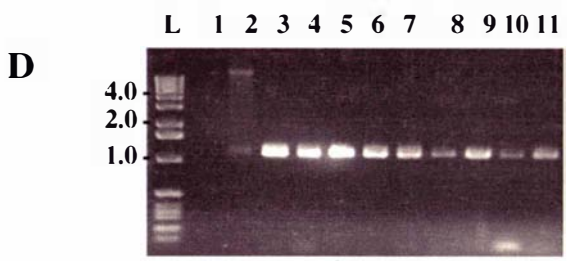
D
L 1 2 3 4 5 6 7 8 9 10 11
4.0
2.0
1.0

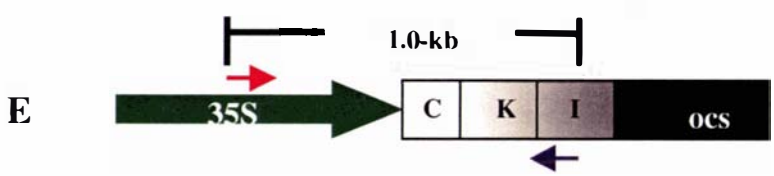
E
1.0-kb
35S
C
K
I
ocs

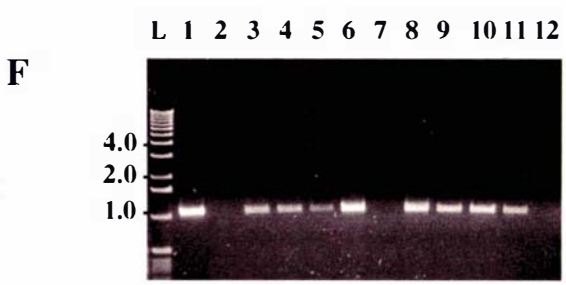
F
L 1 2 3 4 5 6 7 8 9 10 11 12
4.0
2.0
1.0

Figure 3.12. Polymerase chain reaction (PCR) was used to confirm transformed tomato lines.

(A) A schematic drawing showing the primer binding regions of p35S-1 (a 35S promoter-specific primer; red arrow) and ITM-04 (*TM29* reverse primer; black arrow) used to amplify a 1.4-kb DNA fragment from the sense transformed plants.

(B) Gel photograph of PCR products from sense transformed tomato plants. Lane 1 contained PCR product of non-transgenic tomato DNA; lane 2, S/05; lanes 3-7; selected sense transformed lines.

(C) The p35S-1 primer (red arrow) and the ITM-03 primer (blue arrow) were expected to amplify a 1.0 kb DNA fragment from the antisense transformed plants.

(D) Gel photograph of PCR products from antisense tomato plants showing the resultant 1-kb DNA fragment. Lane 1, PCR product from non-transgenic plant; lanes 2-11 contain PCR product from 10 antisense transformed lines.

(E) The p35S-1 primer (red arrow) and the ITM-03 primer (blue arrow) were also expected to amplify a 1.0 kb DNA fragment from the partial-antisense construct.

(F) Gel photograph showing a resultant 1-kb DNA fragment from PCR products of partial-antisense plants. Lanes 1-11 contained PCR products from putative transformed plants; lane 12, product from non-transgenic plant.

The sizes in kilobasepairs of 1-kb DNA ladder (L) fragments is indicated on the left-hand side of figures.

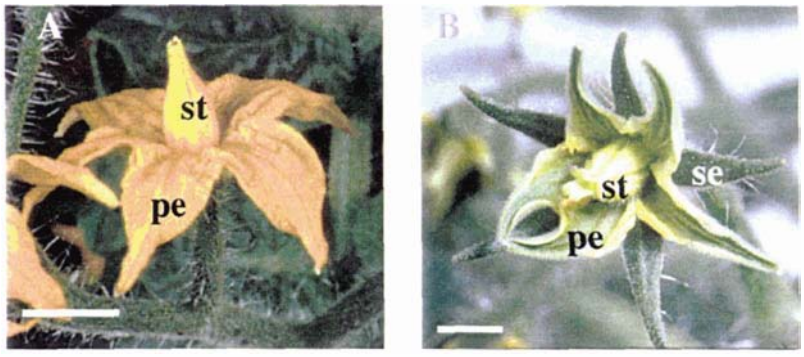

Figure 3.13. *TM29* antisense transgenic flowers display morphogenetic alterations.

(A) A wild-type tomato flower, at ~1 d.p.a. Normal tomato flowers have green sepals (not shown), yellow petals and yellow stamens which form a fused cone around the pistil.

(B) A typical antisense transgenic flower, at a similar stage as in (A) with apparently normal sepals, green petals and green stamens which form a loosely-fused cone around the pistil.

Bars= 2 mm. pe: petal; se: sepal; st: stamen

In contrast to the wild type flower (Figure 3.14A), the antisense transgenic flowers typically showed green petals and green stamens, and an ovary (surrounded by the staminal cone) that developed into parthenocarpic fruit without the need of pollination (Figure 3.13B). This notwithstanding, independent transgenic lines displayed a range of morphogenetic alterations (Table 3.6). Some transgenic plants had yellow petals and stamens with green undertones and were classified as less severe phenotype (Figure 3.14B). The moderately severe plants had green petals with yellowish margins and green stamens (Figure 3.14C). In some transgenic plants such as the sense transformed plant S/05 and the antisense transformed lines AS/38 and AS/45, the petals and stamens displayed severe phenotypes and were green with no streaks of yellow, at anthesis (Figure 3.14D).

Sepal characteristics

The colour and shape of sepals on transgenic plants resembled the wild type (Figure 3.15A). The transgenic sepals appeared fused to each other along most part of their length and delayed in opening (Figures 3.15B, 3.15C). In the wild type flower, the sepals do not display this fusion (Figure 3.14A). In some transgenic flowers, the petals are observed to open before the sepals (Figure 3.15D). The transgenic sepals were significantly larger (7.99 ± 0.3 mm long and 1.81 ± 0.03 mm wide) than wild type sepals (6.01 ± 0.22 mm long and 1.44 ± 0.10 mm wide) (Table 3.7). Examination of the epidermal cell layers with scanning electron microscopy (SEM) revealed stomata and hairs on the abaxial and adaxial surfaces similar to the wild type tomato flower (Figures 3.16A, 3.16B).

Table 3.5. Transformation results

T-DNA constructs	Number of regenerated plants	Number of transgenic plants	Number showing altered phenotypes
Full sense	31	22	1
Full antisense	70	10	6
Partial antisense	121	30	0

Table 3.6. Characteristics of transgenic lines showing altered phenotypes

Transgenic plant [a]	Severity of flower phenotype [b]	% fruit set	Percentage of fruit types on transgenic plants[c]				Produced seeded fruit?	Days from anthesis to ripening
			N	I	II	III		
S/05	+++	38.1	19	21.0	10.5	68.5	No	120
AS/01	++	42.5	11	0	22.2	77.8	No	111
AS/16	-	45.0	35	0	0	100	Yes	66
AS/20	-	51.2	33	0	0	100	Yes	68
AS/38	+++	50.8	31	3.2	6.5	90.3	No	110
AS/45	+++	47.8	27	28.3	9.4	62.3	No	125
AS/69	++	51.1	23	0	8.7	91.3	No	118
AS/70	-	50.0	15	0	6.7	93.3	No	105
AS/83	++	48.8	35	0	5.7	94.3	No	127
WT	-	50.5	33	0	0	100	Yes	47

[a] S: sense, AS: antisense

[b] Severity of flower phenotype was measured as follows:

- normal flower phenotype: yellow petals and stamens
+ petals and stamens are yellow with green streaks.
++ petals have yellowish margins but green midrib; stamen has yellowish green colour.
+++ both petals and stamens are completely green

[c] Fruit types:

N Total number of fruits observed on each plant
I fruit with ectopic flowers emerging
II fruits were swollen or had undefined ectopic organs
III fruits did not show any sign of abnormal growth

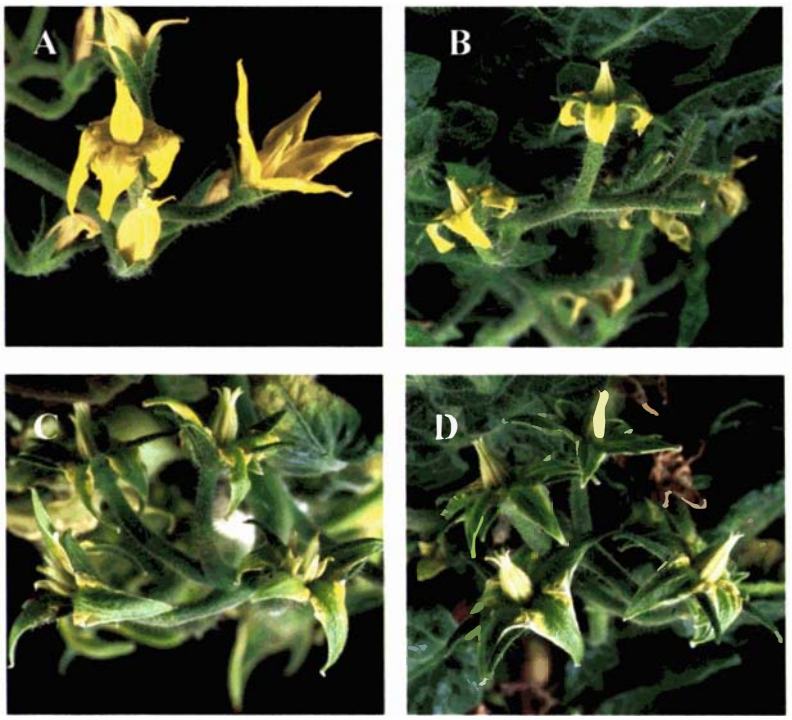

Figure 3.14. Independent transgenic lines displayed a range of phenotypes.

(A) Non-transgenic tomato plant displaying the usual yellow petals and yellow stamens

(B) A transgenic plant (AS/70) with less severe phenotype. Flowers have yellow petals with green streaks in the middle section.

(C) A transgenic plant (AS/83) displaying moderately severe phenotype. Flowers of such plants had green petals with yellow margins and yellowish-green stamens.

(D) Transgenic plant (AS/45) displaying severe phenotype. Petals and stamens of such plants were almost entirely green with little or no yellow streaks.

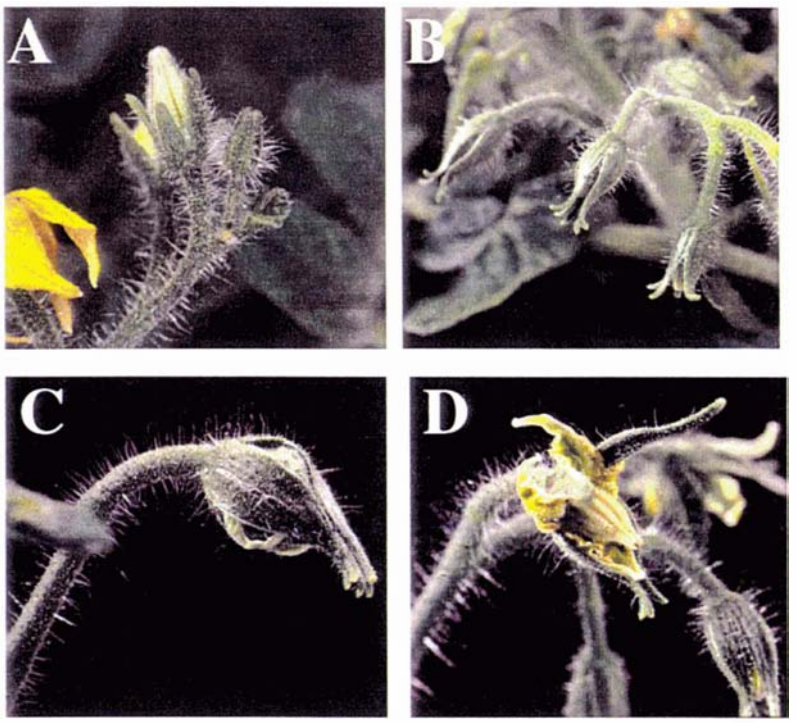

Figure 3.15. The sepals of transgenic flowers are partially fused and delay flower opening.

(A) Tomato flowers at various stages before anthesis. The sepals are for most part separated from each other.

(B) Transgenic flower buds with sepals partially fused together.

(C) A transgenic flower showing partially fused sepals with pressure exerted by the petals within.

(D) At flower opening, sepals are often upright and with some of them still joined together.

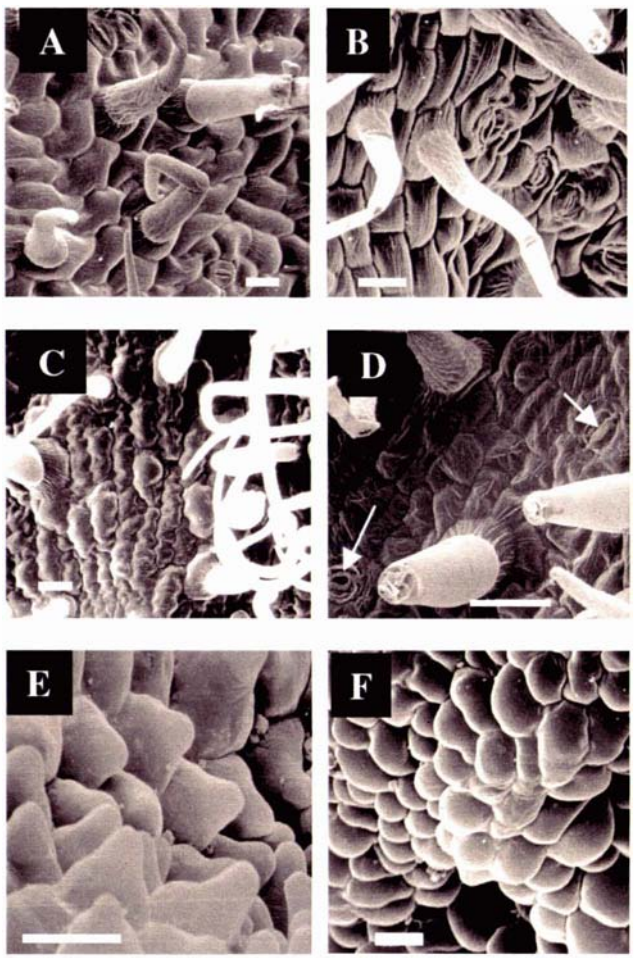

Figure 3.16. Scanning electron micrographs of the epidermal layer of floral organs.

(A) Abaxial surface of wild type sepal

(B) Abaxial surface of transgenic sepal

(C) Abaxial surface of wild type petal

(D) Abaxial surface of transgenic petal with stomata indicated by arrows

(E) Adaxial surface of wild type petal

(F) Adaxial surface of transgenic petal

Bars= 20 μm.

Changes in petal morphology

The transgenic petals were green with a thick cauline texture and tapered sharply towards the apex unlike the yellow thin-textured petals of the wild type flower with the gradual tapering towards the apex (Figure 3.13B). A striking feature of transgenic petals is their anti-senescence characteristic. The petals remain green and turgid on the flower for at least 25 days after anthesis. Senescing of the petal was observed only after this point. In the non-transgenic tomato flower, senescing of petals and stamens are observed 4-5 days after anthesis and these organs are abscised after 7-8 days post-anthesis (Lanahan *et al.*, 1994). The size of the transgenic petal measured under stereo microscope was greater than the non-transgenic counterpart (Table 3.7). At the anthesis stage, the average length and width of the transgenic petals were 7.37 ± 0.41 mm and 2.29 ± 0.34 mm respectively; in comparison the average length and width of the non-transgenic control were 6.01 ± 0.18 mm and 1.88 ± 0.11mm respectively. Detailed examination of the epidermal cell layer by SEM found little change in structural morphology from the wild type cells (Figures 3.16C, 3.16D, 3.16E, 3.16F). However, unlike the wild type petals in which stomata are rare, stomata were present on the abaxial face of the transgenic petal (Figure 3.16D).

Stamen characteristics

The wild type tomato stamens are always joined together until abscised from the flower (Figure 3.17A). The green transgenic stamens were joined to each other to form a cone at anthesis (Figure 3.13B). However, unlike in the wild type, the stamens became dialytic and separated from each other at 2-3 days post anthesis (Figure 3.17B). The individual stamens after separation remained attached to the peduncle and did not abscise as the case is in the wild type tomato flower. The transgenic stamens at anthesis appeared dry and shrunken and did not produce pollen. The average length of the stamens at anthesis, 4.75 ± 0.17 mm was not significantly different from that of the wild type, 4.68 ± 0.10 (Table 3.7).

Table 3.7. Effects of *TM29* downregulation on size of transgenic floral organs[a]

	Sepal		Petal		Stamen		Ovary	
Genotype	**Length (mm)**	**Width (mm)**	**Length (mm)**	**Width (mm)**	**Length (mm)**	**Width (mm)**	**Length (mm)**	**Width (mm)**
Control	6.01 ± 0.22	1.44 ± 0.10	6.01 ± 0.18	1.88 ± 0.11	4.68 ± 0.10	1.18 ± 0.12	5.06 ± 0.10	0.89 ± 0.09
S/05	8.33 ± 0.27	1.75 ± 0.19	7.58 ± 0.1	1.91 ± 0.08	4.70 ± 0.21	1.08 ± 0.12	5.49 ± 0.20	1.58 ± 0.13
AS/01	7.66 ± 0.04	1.83 ± 0.10	7.83 ± 0.30	2.49 ± 0.15	4.74 ±0.15	0.91 ± 0.11	5.41 ± 0.14	1.49 ± 0.05
AS/38	7.83 ± 0.16	1.81 ± 0.11	6.91 ± 0.19	2.33 ± 0.21	4.58 ± 0.16	0.99 ± 0.08	5.52 ± 0.22	1.61 ± 0.10
AS/45	8.16 ± 0.20	1.83 ± 0.13	7.16 ± 0.22	2.44 ± 0.17	4.99 ± 0.05	1.08 ± 0.12	5.61 ± 0.13	1.59 ± 0.10

[a] Values are expressed as mean ± standard deviation. Number of flowers (sample size) used = 5

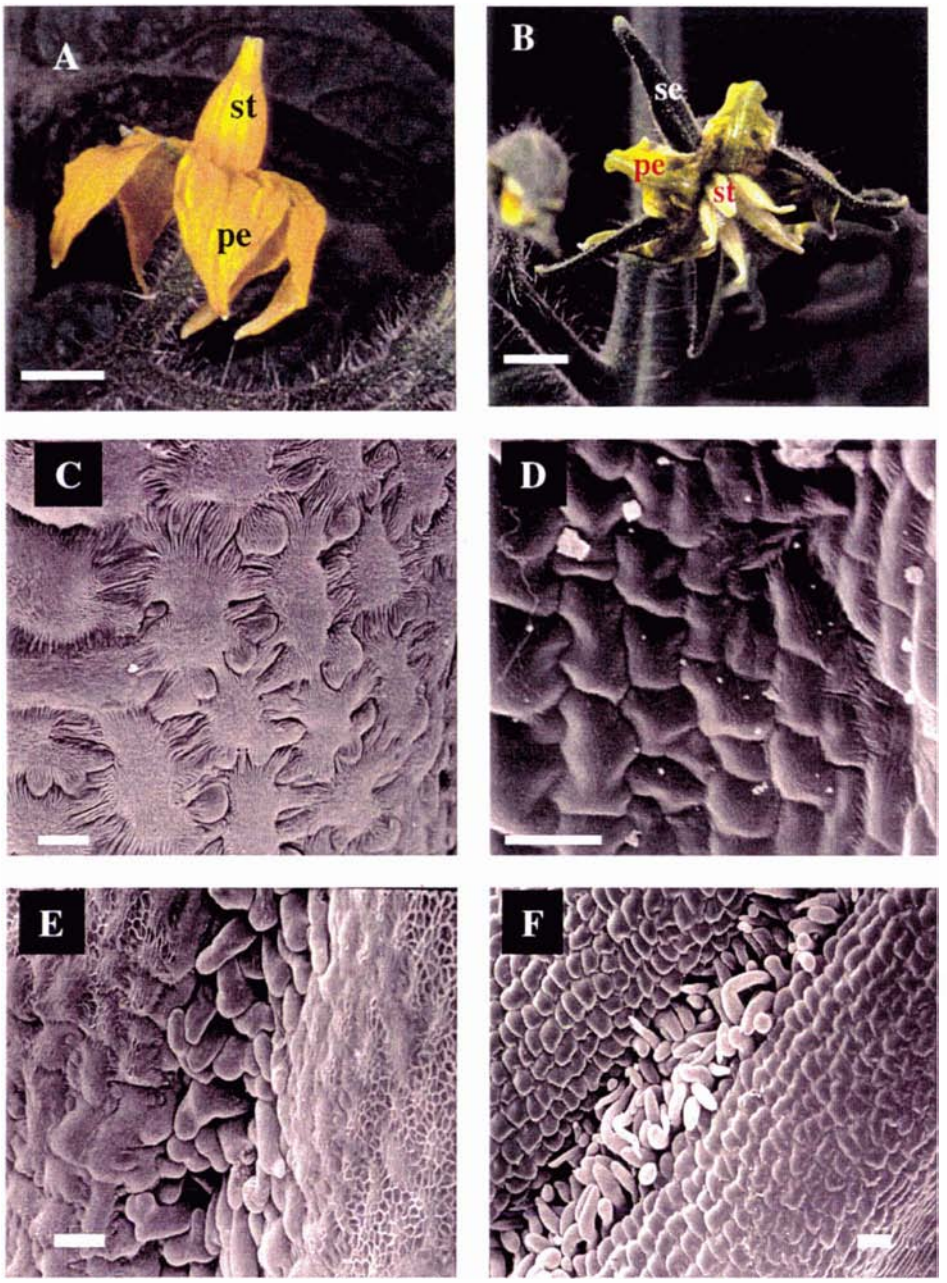
A
st
pe
B
se
pe
st
C
D
E
F

Figure 3.17. Characteristics of transgenic stamens.

(A) A wild type flower 3 d.p.a showing joined stamens

(B) A transgenic flower at 3 d.p.a with separated stamens

(C) SEM of abaxial surface of WT stamen

(D) SEM of abaxial surface of transgenic stamen

(E) SEM showing lateral hairs between WT stamens.

(F) SEM showing poor interweaving between adjacent transgenic stamens.

Bars for (A) and (B)= 2 mm. Bars for (C)-(F)= 20 μm. pe: petal; se: sepal; st: stamen

Electron micrographs revealed some changes in the morphology of the epidermal cells. The cells in the wild type stamen had an interlocking arrangement suggesting they were tightly joined to each other, however, cells in the transgenic stamens did not have this arrangement (Figures 3.17C, 3.17D). In wild type stamens, rows of lateral and adaxial hairs on adjacent stamens interweave to form the staminal cone (Figure 3.17E; Sekhar and Sawhney, 1984). Similar hairs were present on transgenic stamens but these were thinner and did not interweave strongly between stamens (Figure 3.17F). This could explain the loose cone formed by these aberrant stamens.

Carpel characteristics

The morphology of the transgenic ovary displayed some different features from the wild type ovary. The size of the transgenic ovary at anthesis was significantly bigger than that of the wild type (Figure 3.18; Table 3.7). The length of the pistil 5.48 ± 0.10 mm, measured from the stigma to the base of the ovary is slightly more than that of the non-transgenic ovary, 4.98 ± 0.22 mm. The diameter across the widest portion of the ovary at anthesis is 1.57 ± 0.05 mm for the transgenic ovaries compared to 0.89 ± 0.09 mm for the wild type ovary. The width of the ovary measured at 3 days post-anthesis was 2.97 ± 0.26 mm for the transgenic plants and 1.55 ± 0.03 mm for the wild type ovary. This may be because parthenocarpic fruit development in the transgenic plants initiated well before anthesis (Mazzucato *et al.*, 1998). The transgenic ovary was sterile. Several repeated attempts to cross-pollinate with normal pollen failed to produce seed.

Scanning electron microscopy was used to examine the epidermal layers of the wild type and transgenic ovary. There were no trichomes present on the wild type carpel (Figure 3.19A). However, in the transgenic carpel, glandular and non-glandular trichomes covered the surface of the style and ovary (Figure 3.19B). In addition, detailed electron micrographs did not detect stomata on the wild type carpel (Figures 3.19C, 3.19E); however, stomata were present on the transgenic style and the ovary (Figures 3.19D, 3.19F).

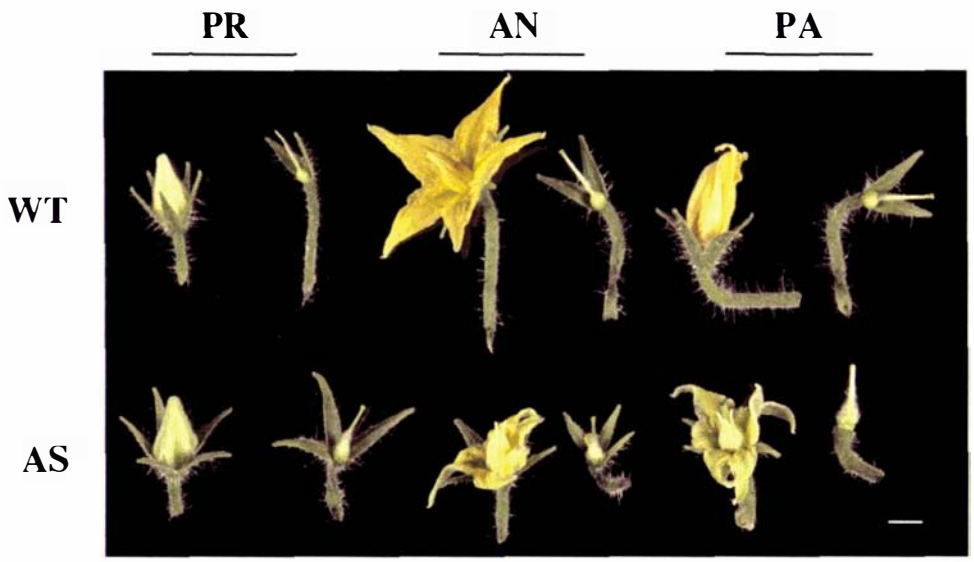

Figure 3.18. Tomato flower and ovary of wild type (WT) and antisense transgenic (AS) plants at 3 developmental stages: pre-anthesis (PR), anthesis (AN) and 4 days-post-anthesis (PA). The transgenic ovary at each stage was significantly bigger than the wild type. Bar= 5 mm

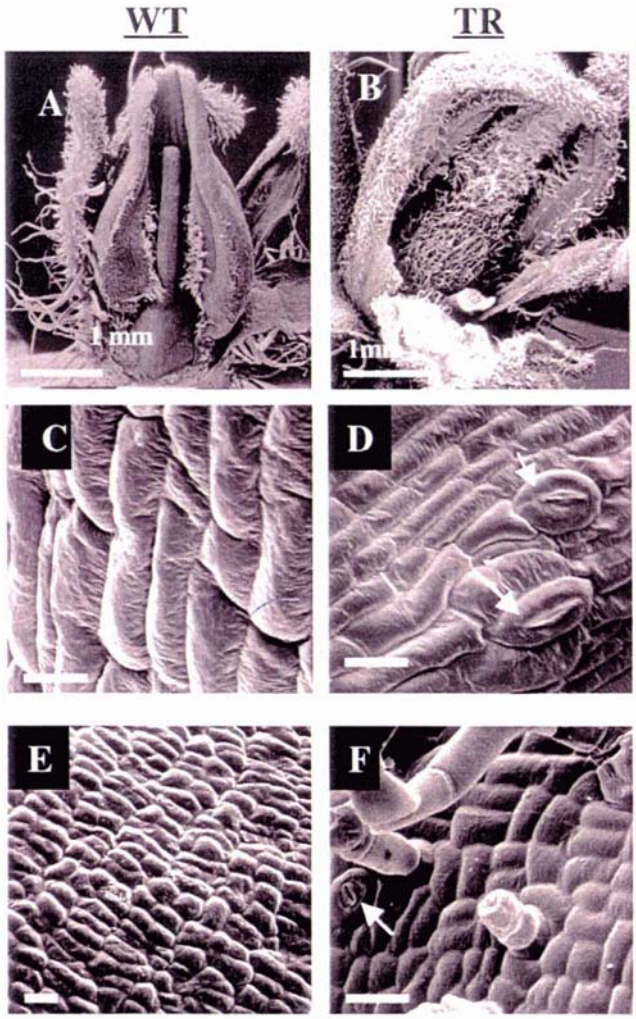

Figure 3.19. SEM of ovary tissues.

(A) Ovary of wild type flower at 2 days before anthesis with no trichomes on surface.

(B) Transgenic flower as in (A) showing ovary and style covered with trichomes.

(C) SEM showing epidermal surface of WT style.

(D) SEM of epidermal surface of transgenic style showing stomata (arrowed).

(E) Epidermal surface of wild type ovary

(F) Epidermal surface of transgenic ovary displaying stomata (arrowed).

TR: transgenic; WT: wild type; Bars in (A) and (B)= 1 mm; Bars in (C)-(F)= 20 µm

3.2.9.2 Fruit development

The ovary on the transgenic plants initiated fruit development without pollination. The percentage fruit set, measured as the proportion of flowers that formed fruit, in most transgenic plants did not differ significantly from that observed in the wild type tomato plant (Table 3.6). Fruits produced by primary transgenic plants were characterised into three types (Figure 3.20A; Table 3.6). Type I fruit had ectopic shoots emerging from inside with flowers. Type II fruits were swollen and misshapen or had poorly formed ectopic organs. Type III fruits showed no sign of ectopic structures and could be compared to the fruits on the control plants (Figure 3.20A). The proportion of different fruit types varied among transgenic plants. However, transgenic plants with the most severe flower phenotype had greater percentage of type I fruits (Table 3.6). The transgenic fruits were parthenocarpic and seeds were not produced in any of the different fruit types (Figure 3.20B) except for two transgenic plants (AS/16, AS/20) which displayed normal flower phenotype and produced seeded fruit like the wild type (Table 3.6).

The size of type III fruits in both transgenic and non-transgenic plants showed great variation among fruits of the same plant. Therefore, maximum fruit size measured as the average equatorial diameter of the 5 largest fruits (at breaker stage) was used as indication of fruit growth. The maximum fruit size was much greater in the transgenic plants than in the control plants. The fruit size measured for the wild type control (cultivar Microtom) was 1.5 ± 0.3 cm in diameter. The average diameter of transgenic fruits sampled from transgenic plant AS/45 was 2.8 ± 0.42 cm in diameter.

Transgenic fruits showed a delayed ripening process. The time from anthesis to fruit colour change was significantly longer for transgenic fruits than the wild type (Table 3.6). In some cases, transgenic fruits remained green for 6-8 weeks after reaching final fruit size. This phenotype implicated *TM29* in fruit ripening and suggested it may be involved in the normal ripening process.

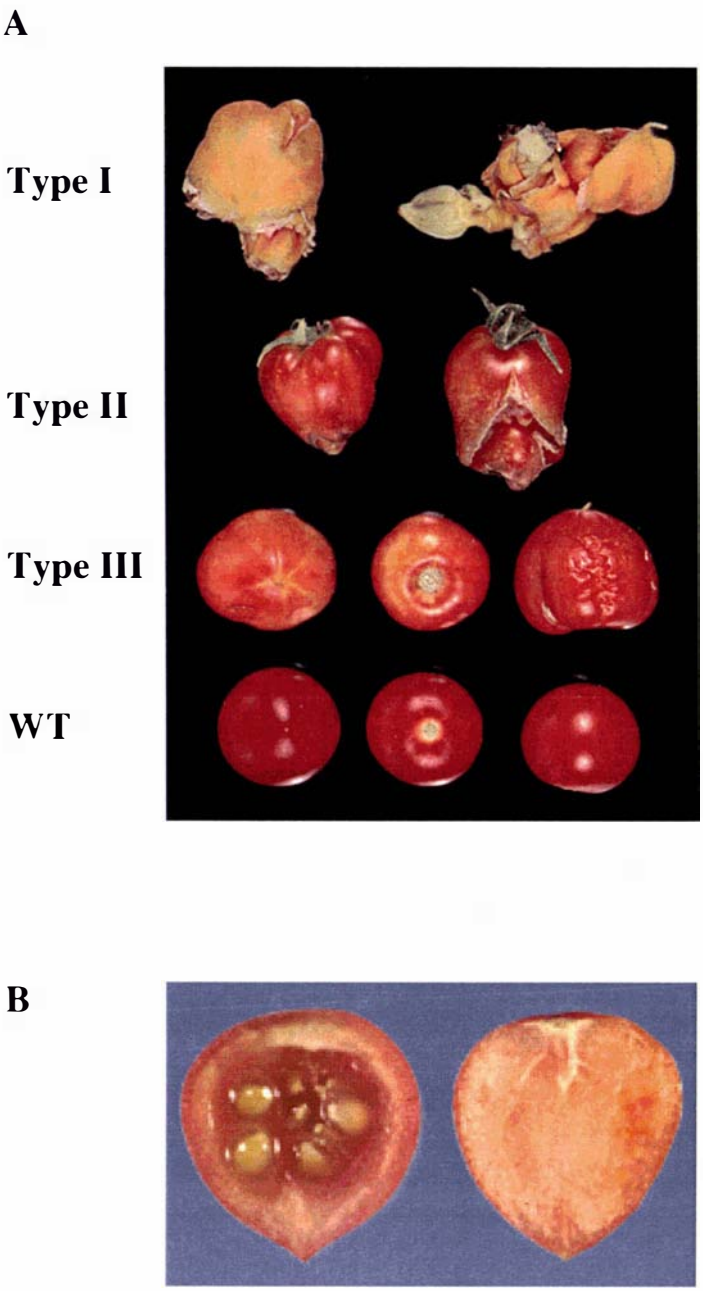

Figure 3.20. The types of fruit produced by tomato transgenic plants. (A) Type I fruits produced ectopic flowers. Type II fruits had ectopic organ not well formed and type III fruits did not display any ectopic organs. Fruits from wild type plant are shown (WT).

(B) Wild type tomato fruit (left) with seeds and transgenic fruit (right) without seeds.

3.2.9.3 Emergence of ectopic structures

Unlike the wild type fruit (Figure 3.21A) transgenic fruit development was abnormal. Fruits became swollen and misshapen with ectopic organs emerging from within these fruits (Figure 3.21B). The pressure exerted by these organs caused breakage of the fruit pericarp allowing the emergence of the ectopic organs (Figure 3.21C). These ectopic structures were of various shapes and forms (Figures 3.21D, 3.21E, 3.21F).

In the type I fruit, the structures resemble shoots with leaves and flowers (Figures 3.21E, 3.21F, 3.21G). The ectopic flowers displayed all four whorls of floral organs, which were identical to those of the aberrant primary flowers. The ovary of the ectopic flower also begins to swell, reiterating the characteristics of the primary flowers. None of the flowers and fruits on the non-transgenic control plants growing under the same conditions showed these characteristics. The type II ectopic organs were of different shapes and forms, some inflorescence-like characteristics while others had fruit-like organs.

The wild type tomato leaf has a unipinnate compound structure (Figure 3.22A; Janssen *et al.*, 1998). The leaf-organs produced by the ectopic shoots were morphologically different: they were smaller in size and were present as simple leaf structures with short petioles arising directly from the ectopic shoot (Figure 3.22B). Nonetheless, these ectopic leaf-organs possessed features similar to the wild type leaflet, i.e. stomata on both abaxial and adaxial surfaces, midrib, glandular and non-glandular trichomes (Figures 3.22C, 3.22D, 3.22E, 3.22F, 3.22G, 3.22H).

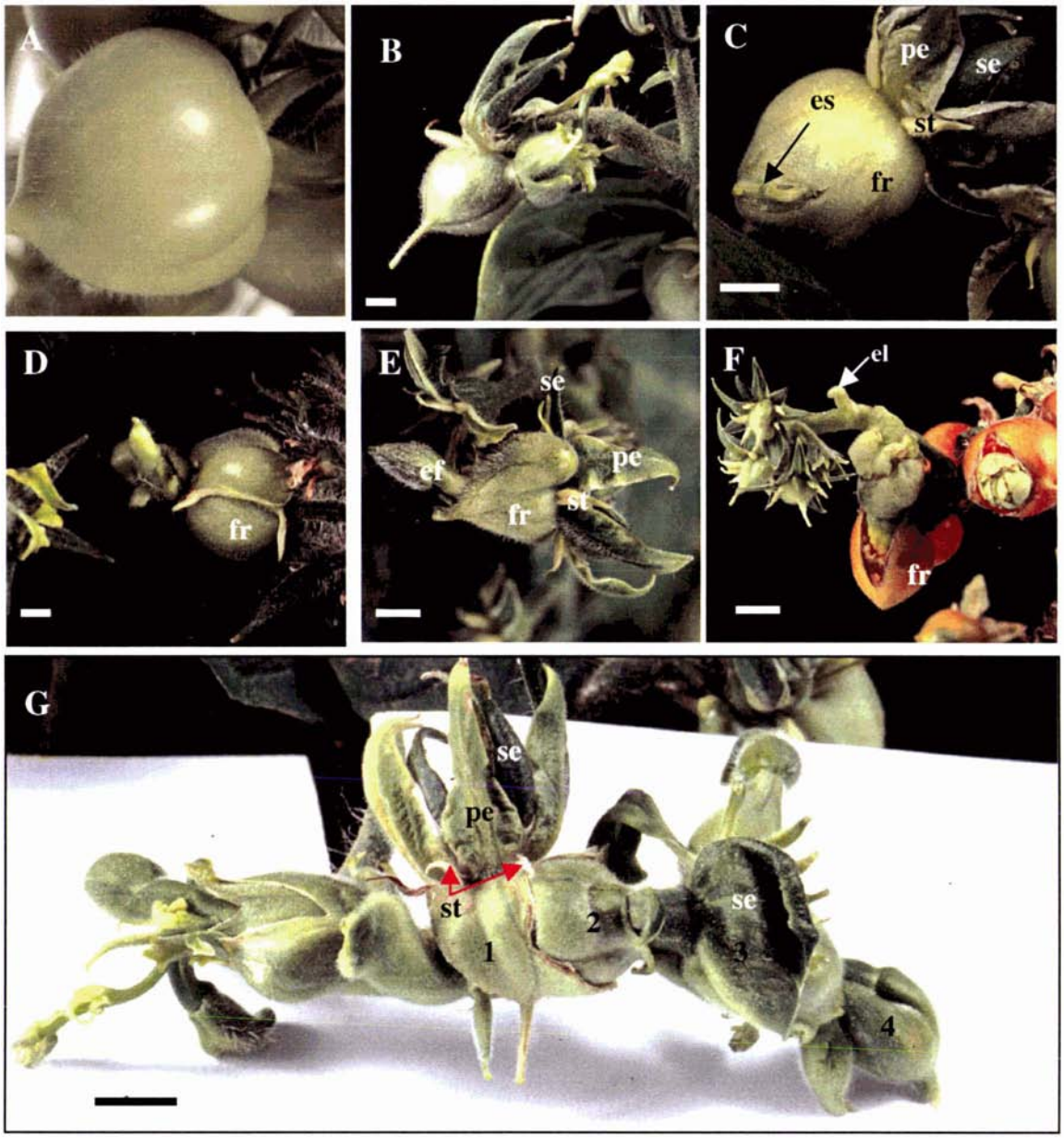
A
B
C
pe
se
es
st
fr
D
fr
E
se
ef
pe
fr
st
F
el
fr
G
se
pe
st
1
2
se
3
4

Figure 3.21. Characteristics of transgenic fruit.

(A) Wild type tomato fruit at mature green stage.

(B) Transgenic flower produced parthenocarpic fruit with ectopic organs emerging from inside.

(C) Pressure exerted within the fruit by the growing ectopic organs cause breakage of fruit pericarp.

(D) A poorly developed shoot structure emerging from inside the fruit.

(E) In some fruits, well-formed ectopic flowers are observed emerging.

(F) An ectopic inflorescence shoot showing a leaf-like organ (arrowed) and flowers. Ovary on ectopic flowers developed reiterating the aberrant phenotype of primary flower.

(G) Ectopic shoot showing different generations (1, 2, 3 and 4) of ectopic inflorescences emerging from one another.

Bars= 2 mm. el: ectopic leaf; es: ectopic shoot; fr: fruit; pe: petal; se: sepal; st: stamen

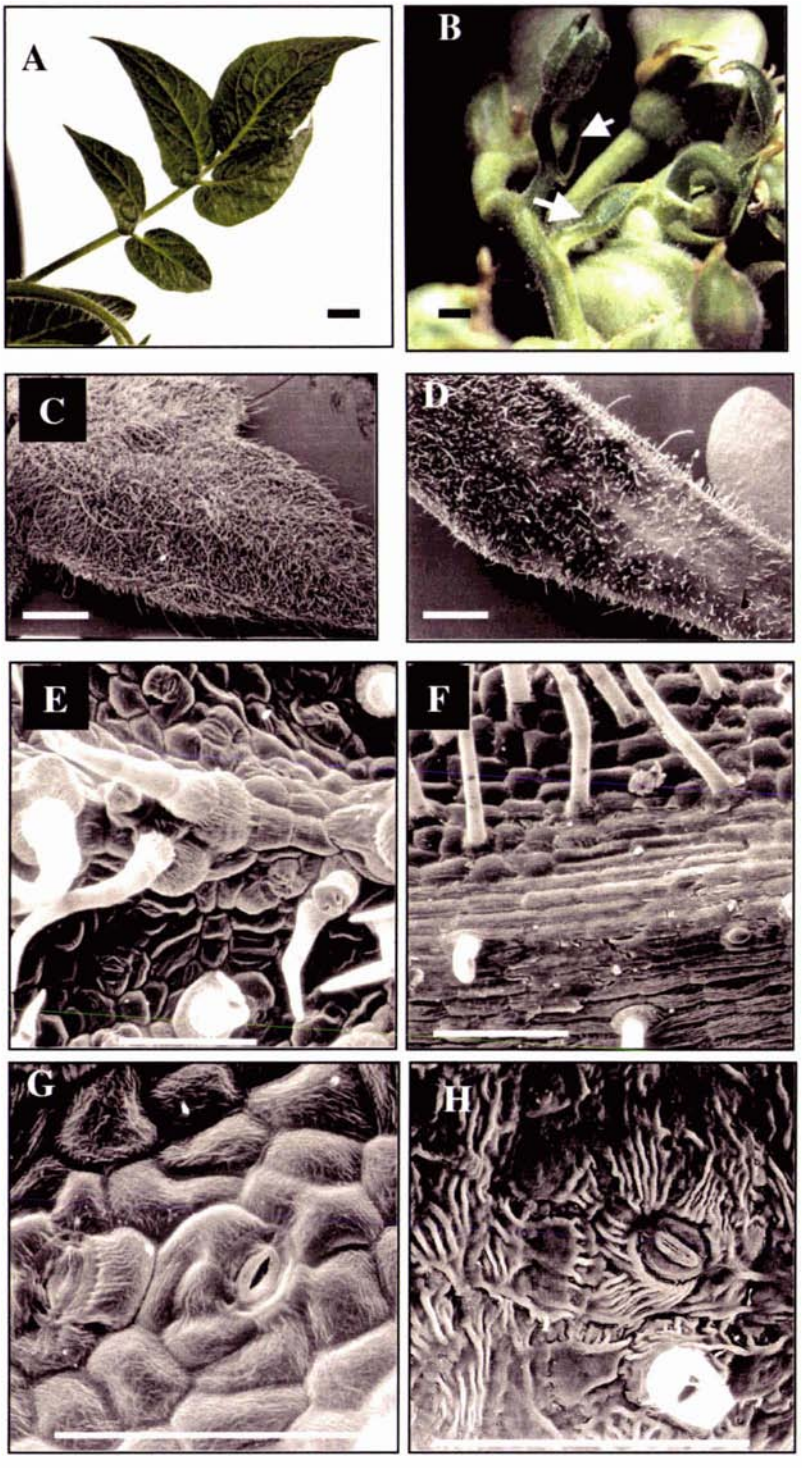
A
B
C
D
E
F
G
H

Figure 3.22. The ectopic shoots produced leaves as well as flowers.

(A) Compound leaf of wild type (WT) tomato

(B) Photographs of ectopic inflorescence with leaves (arrowed).

(C) SEM of the leaflet of wild type compound leaf.

(D) SEM of ectopic leaf.

(E) SEM of abaxial surface of WT leaflet

(F) SEM of abaxial surface of ectopic leaf

(G) SEM of adaxial surface of WT leaflet

(H) SEM of adaxial surface of ectopic leaf.

Bars in (A) and (B)= 2 mm; (C) and (D)= 1 mm; (E)-(H)=100 μm

To observe the early developmental stages of the ectopic shoot, thin ovary sections from the AS/45 transgenic line were stained with toluidine blue. In normal tomato fruit development, the placenta and ovules occupy the entire locular cavity (Figures 3.23A, 3.23C). Inside the transgenic ovary at two days post-anthesis (d.p.a), the ectopic shoot is seen developing from a region closer to the base of the ovary (Figure 3.23B). As the shoot develops (6 d.p.a), it displaces the placenta and ovules to occupy the ovary (Figure 3.23D).

3.2.10 Levels of *TM29* mRNA in tomato transgenic plants

To determine the correlation between *TM29* expression and the phenotypes exhibited in the transgenic lines, *TM29*-specific sense and antisense RNA probes were used to assess the level of transcripts present in selected lines of each construct. For the sense-transformed plants, six lines were examined using an antisense probe, to detect both endogenous and transgenic copies of the *TM29* transcripts. Relatively high levels of the transcript were found in 5 lines that showed normal phenotype. However, *TM29* transcripts were virtually absent in the S/05 line that showed an altered phenotype (Figure 3.24A). This is an indication of co-suppression of the *TM29* transcript in the S/05 line. Co-suppression is the inhibition of gene expression when an introduced transgene is homologous to an endogenous gene, which usually occurs at low frequency (van der Krol *et al.*, 1990; Meyer, 1996).

The levels of the endogenous *TM29* transcripts in the six antisense lines that showed the range of phenotypes were examined with a gene-specific antisense probe. There was significant reduction in the *TM29* transcripts in all the lines compared to the non-transgenic control. The sense probe also detected very low levels of antisense transcripts in these lines suggesting the downregulation of both sense and antisense RNA. The sense

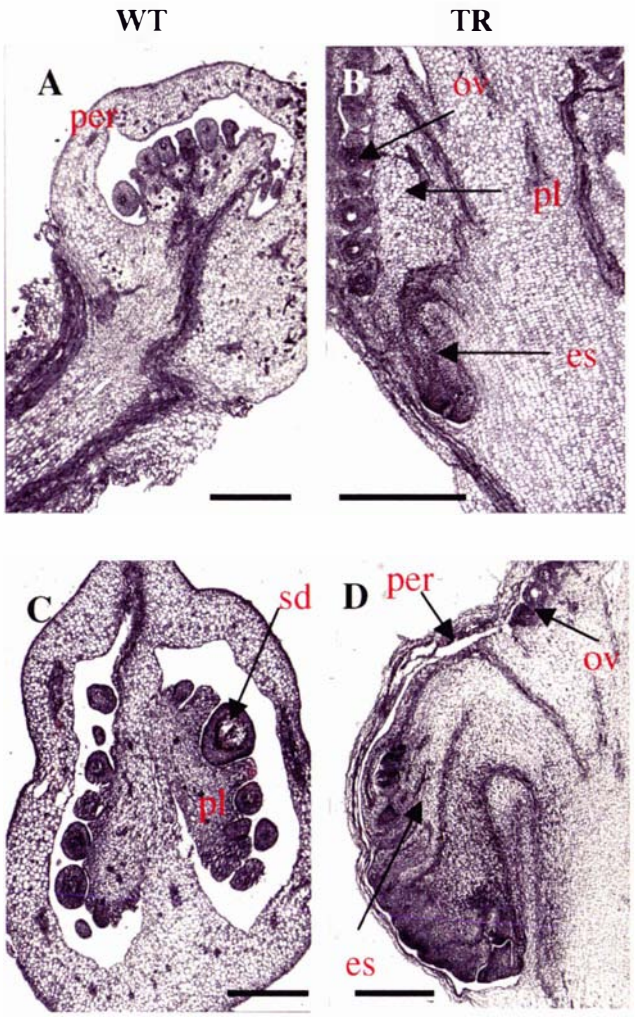

Figure 3.23. Histological staining showing early stages of ectopic shoot.

(A) Longitudinal section of wild type tomato fruit at 4 days post-anthesis (d.p.a)

(B) Transgenic fruit from AS/45 plant at 2 d.p.a showing ectopic shoot.

(C) Wild type fruit at 10 d.p.a

(D) Transgenic fruit at 6 d.p.a. The ectopic shoot displaces the placenta and ovules within the fruit.

es: ectopic shoot; ov: ovule; per:pericarp; pl: placenta; sd: seed; TR: transgenic; WT: wild type

probe did not hybridise to RNA from the wild type control plant (Figure 3.24B). The gene specific sense and antisense probes were also used to detect the levels of endogenous *TM29* and the expressed antisense transcripts in five partial antisense lines. The antisense probe detected high levels of *TM29* transcripts in these lines, an indication that *TM29* expression was not down regulated in these lines. The sense probe also detected the presence of high levels of the expressed antisense transcripts in four of the five lines examined (Figure 3.24C).

Overall, there was strong correlation between the reduced levels of *TM29* expression in the transgenic lines and the altered phenotypes. In partial-antisense plants, down-regulation of *TM29* expression was not successful; here the phenotype of the transgenic lines was not different from the wild type tomato. These suggest that *TM29* expression is involved in the characteristics affected in the transgenic plants.

3.2.11 Expression of other MADS-box genes in tomato transgenic plants

To gain insights into the molecular mechanisms responsible for the phenotypes and to examine whether other MADS-box genes have also been down-regulated in the transgenic lines, the expression of two other tomato MADS-box genes, *TM5* and *TAG1*, in the antisense lines was assessed by northern hybridisation. Further, the spatial expression of *TM5* was examined in transgenic flowers by *in situ* hybridisation. These two genes were selected because *TM5* has the highest sequence identity to *TM29*, among the known tomato MADS-box genes and secondly, the antisense phenotypes of *TM5* and *TAG1* have already been described (Pneuli *et al.*, 1994ab). RNA transcripts of these two genes were detected in the antisense lines, unlike the transcripts of *TM29*, and suggested the antisense *TM29* RNA (Figure 3.25A) has not affected the transcripts of *TM5* and *TAG1*.

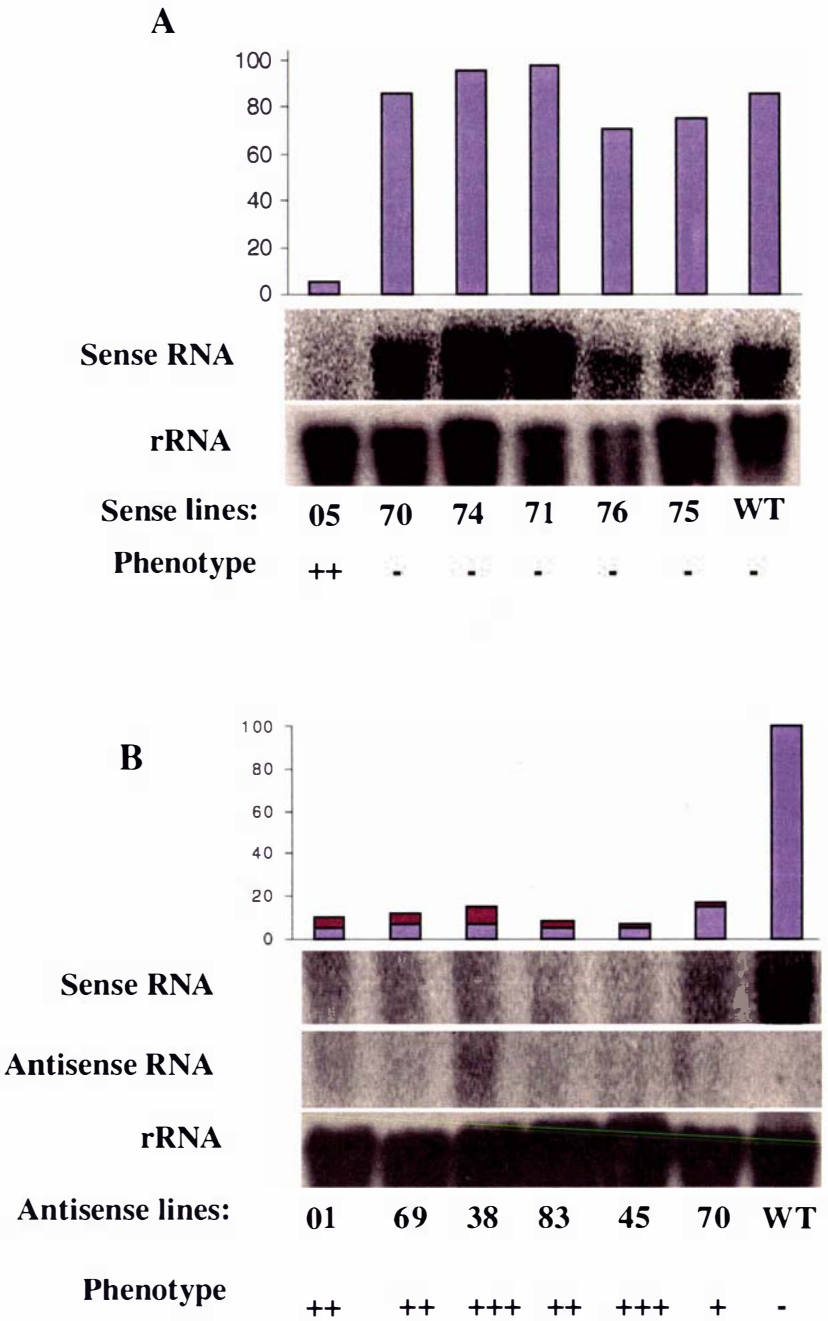
A
100
80
60
40
20
0
Sense RNA
rRNA
Sense lines:
05
70
74
71
76
75
WT
Phenotype
++
-
-
-
-
-
-
B
100
80
60
40
20
0
Sense RNA
Antisense RNA
rRNA
Antisense lines:
01
69
38
83
45
70
WT
Phenotype
++
++
+++
++
+++
+
-

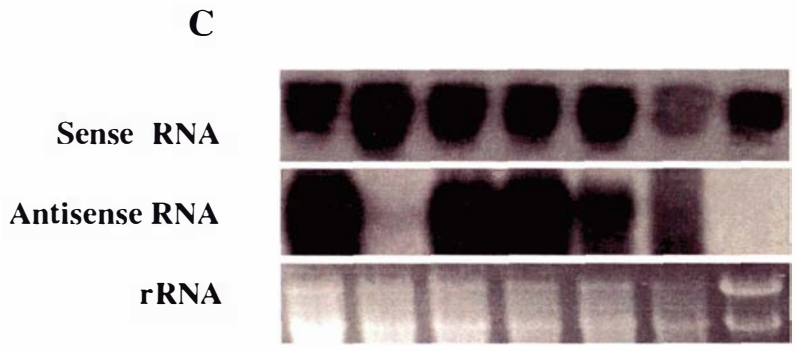

Figure 3.24. The expression of *TM29* sense and antisense transcripts in transgenic plants.

(A) Steady state levels of *TM29* mRNA in sense transgenic plants were measured by RNA gel blot analysis in flower buds. Total RNA was probed with *TM29* antisense probe.

(B) The levels of *TM29* (sense and antisense) RNA in antisense transgenic plants (lanes 1-6) measured by RNA gel blot analysis using total RNA from flower buds. RNA blot was successively probed with gene-specific antisense and sense probes. Stacked graph shows relative levels of sense (blue) and antisense (red) RNA in each line.

(C) *TM29* sense and antisense RNA levels in partial-antisense transgenic lines (lanes 1-5), AS/01 (lane 6) and wild type (lane 7) were analysed by RNA blot analysis.

Loading levels are shown by hybridisation with rRNA gene probe in (A) and (B) and by stained RNA bands in (C). WT: wild type. For symbols of phenotype refer to Table 3.6

Further, *in situ* hybridisation with *TM5*-specific RNA probes on wild type tomato flowers and AS/45 transgenic flowers revealed the expression of *TM5* RNA in the control flowers (Figures 3.25B, 3.25C) was similar to that found in the antisense transgenic flowers (Figures 3.25D, 3.25E). Transgenic tissues probed with sense *TM5* RNA were used as control (Figures 3.25F, 3.25G). The results show that the spatial expression of *TM5* in tomato flowers was not affected by the constitutive expression of antisense *TM29* RNA.

3.2.12 Effects of GA and photoperiod on tomato transgenic phenotypes

GA_3 was applied at 100 μM to individual selected flowers of transgenic lines using a small brush or sprayed on whole plants grown from cuttings. Flowers or plant lines were treated with 0.02% Tween 20 as a control. GA_3 treatment on the flowers of the non-transgenic control plants did not cause significant developmental changes compared to those treated with Tween 20 as treatment controls. The senescence of GA-treated wild type petals and stamens (4-5 days after anthesis) was the same as in those treated with Tween 20 alone. Treated control flowers produced seeded fruit, which developed normally. However, one control flower formed an abnormal fruit though this was not consistently observed among the control plants (Figure 3.26A).

In treated transgenic plants, GA effects were observed in the petals, stamens and carpel growth. The colour of transgenic petals and stamens treated with GA changed from green to yellowish green. There was an increase in the size of the petals and stamens as a result of GA treatment. Average petal length measured at 8 days post anthesis was 10.0 ± 0.2 mm for the non-treated flowers and 18 ± 0.4 mm for the GA treated flowers. GA promoted the senescence of the second and third floral organs. While senescence of untreated transgenic flowers was slower (25-30 days after anthesis); this process was accelerated in the GA treated transgenic flowers (11-16 days after anthesis).

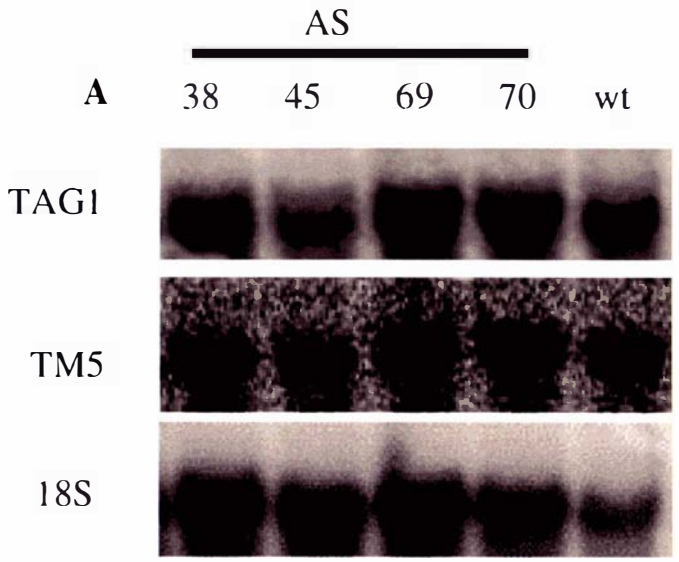
AS
A
38
45
69
70
wt
TAG1
TM5
18S

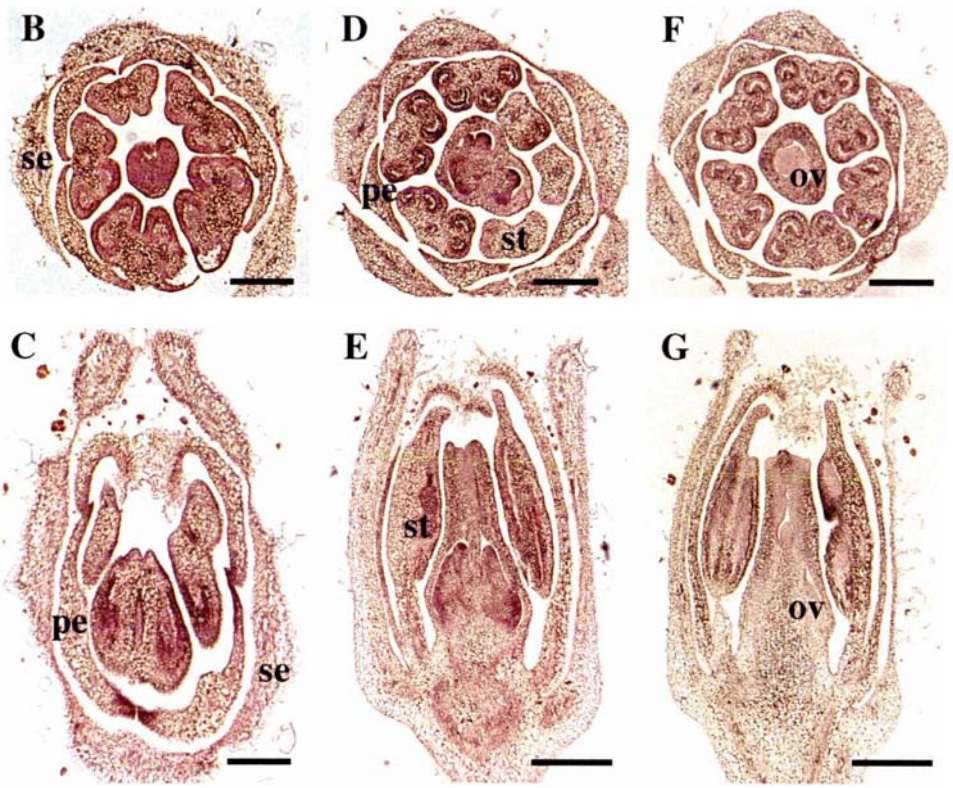
B
se
D
pe
st
F
ov
C
pe
se
E
st
G
ov

Figure 3.25. The expressions of *TM5* and *TAG1* in *TM29* antisense transgenic flowers

(A) Total RNA extracted from flowers of four antisense transgenic plants and the non-transgenic tomato plant was sequentially probed with *TM5*, *TAG1* and 18S rRNA probes.

(B-G) *In situ* hybridisation of *TM5* to wild type and transgenic floral tissues

(B) and (C) sections of wild type tomato floral bud probed with *TM5*

(D) and (E) sections of antisense *TM29* flowers probed with *TM5*

(F)and (G) sections of transgenic flowers probed with sense *TM5* RNA as control.

Bars= 1.5 mm. ov: ovary; pe:petal; se: sepal; st: stamen

GA_3 treatment of the transgenic flowers did not prevent ectopic shoot formation in the fruit. The percentage of fruits formed with type 1 and 2 ectopic structures did not differ from the non-treated transgenic flowers. In one transgenic line AS/38, a few of the aberrant flowers showed further abnormality upon GA_3 application; the fourth whorl was replaced by vestigial structures (Figure 3.26B).

For the photoperiod treatment, there were no observed changes in tomato lines grown under short-day light conditions. The phenotype of flowers and fruit on transgenic plants under short day conditions were similar to those grown under long-day conditions. No morphogenetic changes were observed in the control tomato plants grown under short-day conditions.

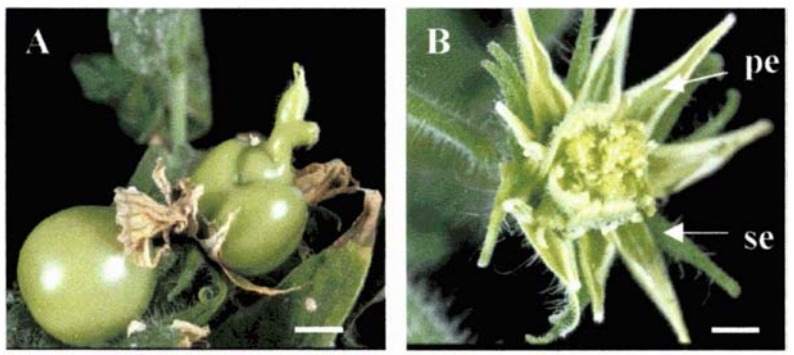

Figure 3.26. GA_3 application caused some phenotypic aberrations in flowers.

(A) A normal tomato flower upon application of 100 µm giberrellin displayed unusual fruit phenotype. This was not a general observation and was seen in only one flower.

(B) An antisense tomato flower displaying further severe phenotype when GA_3 was applied.

Bars= 2 mm. se: sepal; pe: petal.

3.2.13 Tobacco transformation results

The tobacco cultivar *Nicotiana tabacum* (cv Samson) was used as a heterologous host to overexpress *TM29* mRNA. It has been shown previously that heterologous systems enable the functions of MADS-box genes to be examined (Chung *et al.*, 1994; Davies *et al.*, 1996). Transgenic tobacco plants were generated to express the sense RNA of *TM29*. Twenty-four transformed tobacco plants were regenerated from tissue culture, rooted on kanamycin containing medium and transferred to soil to grow in a containment glasshouse. The transgenic nature of these plants was confirmed by PCR analysis. As controls, 10 non-transformed tobacco plants were also regenerated in tissue culture and grown under same growth conditions.

3.2.14 Morphogenetic alterations in tobacco transgenic plants

Tobacco plants, which overexpressed the *TM29* gene, showed reduced apical dominance resulting in a significant increase in the growth of lateral buds from leaf axils, early flowering occurred among transgenic plants and abnormal flowers were formed. The height of plants and the number of nodes to flowering were used as indication of flowering time (Table 3.8). Overall, transgenic tobacco plants flowered sooner than the wild type (Figure 3.27; Table 3.8).

Malformed flowers were observed in some lines. In the wild type tobacco flowers, the anthers are positioned over and above the stigma (Figure 3.28A). However, in the early flowering line, TBS-23, the stamens were shorter in length and did not extend beyond the pistil (Figure 3.28B). The average length of the stamens in control plants, measured

Figure 3.27. Early flowering of transgenic tobacco plants. Shown is non-transgenic tobacco plant (left) and transgenic plant TBS-23 (right) showing early flowering.

from their point of attachment to the petals, was 2.8 ± 0.1 cm while that of the pistil was 3.0 ± 0.2 cm; in contrast the average stamen length for TBS-23 was 1.9 ± 0.2 cm and pistil length 2.8 ± 0.2 cm. For the flowers on TBS-30, the stamen length was 2.6 ± 0.2 cm and the pistil length, 3.0 ± 0.2 cm. In TBS-14 and TBS-30, some flowers did not have proper floral organs in the inner three whorls. These organs were converted into sepals or green leaf-like structures (Figure 3.28C). However, flowers that formed later on these plants had the full complement of floral organs, with only subtle changes in petal shape. Seed formation was completely absent in TBS-23; attempts at cross-pollination did not result in seed formation suggesting the ovary is infertile.

There was active growth of the axillary buds in the transgenic plants. The lateral buds in wild type tobacco plants were generally dormant (Figure 3.29A). In transgenic lines, TBS-14, TBS-22, TBS-23 and TBS-30, an average of 10 lateral buds were active and producing leaves and flowers. In these lines a bud just below the cymose inflorescence extended higher above the terminal inflorescence, resembling sympodial growth of tomato (Figure 3.29B, Table 3.8). No such growth pattern is seen in the control non-transgenic plants. The expression of *TM29* RNA in the tobacco transgenic lines was detected by northern hybridisation. There was correlation between the levels of *TM29* transcript and plant height and number of nodes to flowering in some of the transgenic tobacco lines (Figures 3.30A, 3.30B).

Table 3.8. Characteristics of tobacco transgenic plants expressing *TM29*

Transgenic plant	Height at flowering (cm)	Number of nodes to flowering	Phenotype
Control	90 ± 2.6	31 ± 2.1	Wild type
4	84	32	Normal
6	65	25	Normal
10	90	26	Normal
13	65	32	Normal
14	87	26	Poor flower development; sympodial shoot growth
15	71	31	Poor flower development
19	75	20	normal
23	45	22	Short stamens; no pollen; sterile ovary. Axillary growth promoted
30	78	29	Flowers have vegetative characteristics. Promoted axillary growth. Sympodial shoot growth
31	59	29	normal
40	60	25	Normal

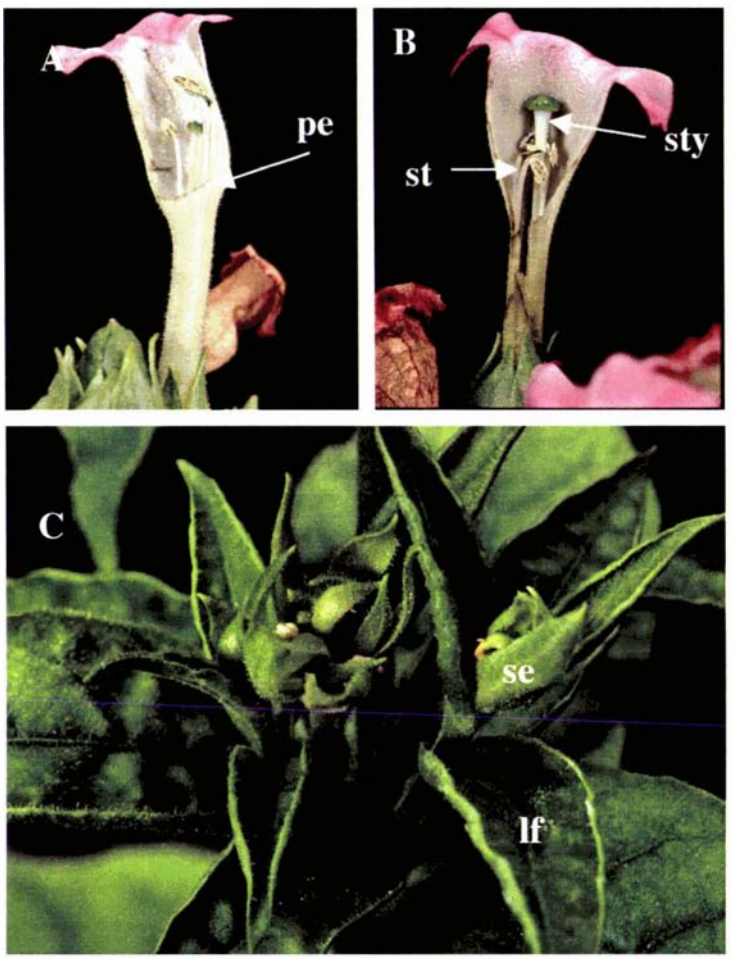

Figure 3.28. Abnormal flowers produced in *TM29* transgenic tobacco plants.

(A) A normal tobacco flower with a section of the petals removed to show the stamen and pistil. Stamens have their anthers placed over and above the stigma

(B) An abnormal flower from TBS-23 transgenic plant with section of petal removed. The stamens were shorter in length and positioned well below the stigma.

(C) Transgenic tobacco flowers with floral organs replaced by sepals.

lf:leaf; pe: petal; se: sepal; st: stamen; sty: style

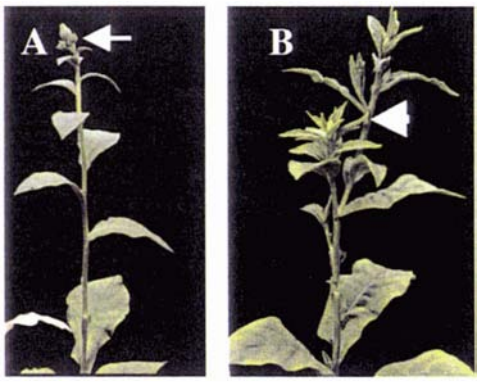

Figure 3.29. Tobacco transgenic plants displayed sympodial-like shoot growth

(A) Wild type tobacco plant showing terminal inflorescence (arrowed).

(B) A transgenic tobacco plant with 'sympodial' shoot (arrowed) growing from the axil of a leaf below the terminal inflorescence.

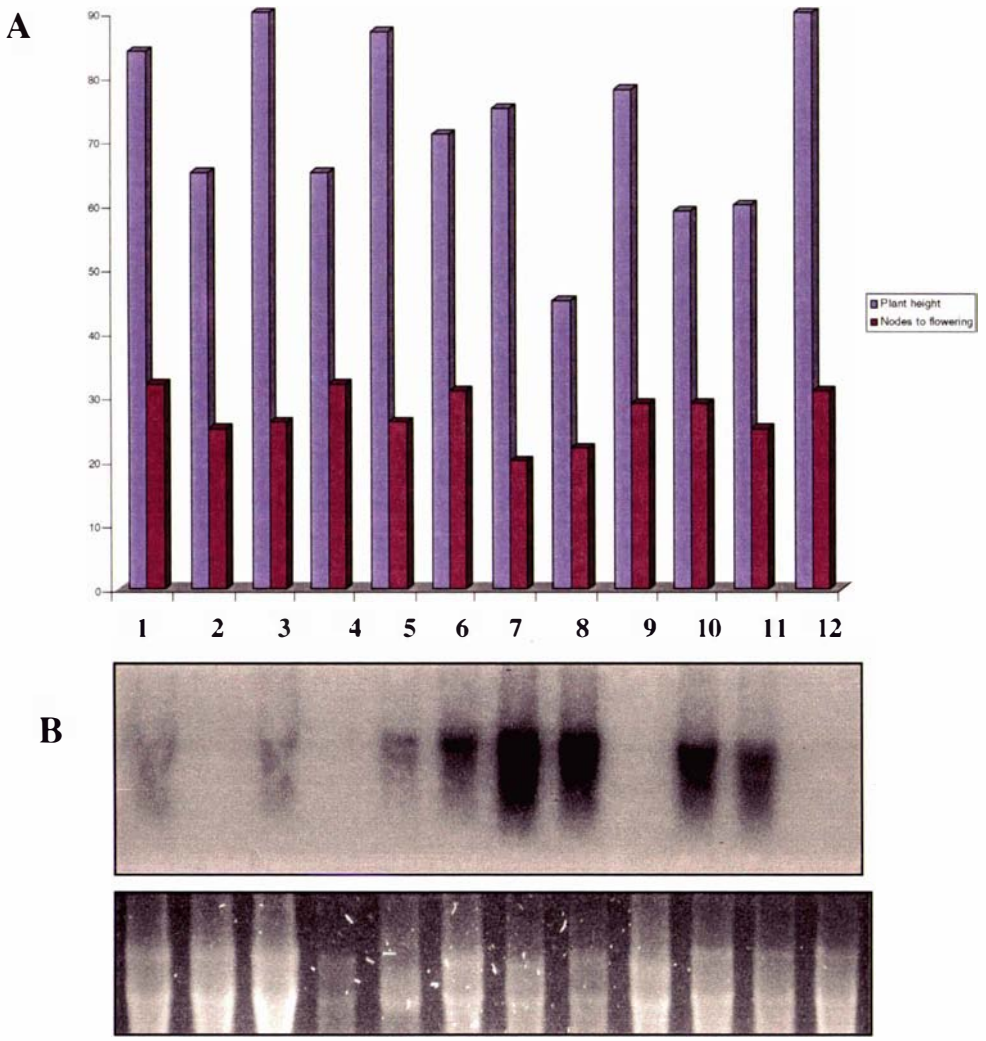

Figure 3.30. *TM29* RNA levels in transgenic tobacco plants showing early flowering.

(A) Graph of plant height (cm) and number of nodes at flowering for transgenic tobacco plants (1-11) and wild type (12).

(B) Levels of *TM29* RNA expressed in transgenic tobacco plants (1-11) and wild type (12) measured by RNA blot analysis. Stained RNA bands are shown to depict loading levels.

3.3 Discussion

A new tomato MADS-box gene (*TM29*) was characterised using sequence and expression analyses. The results of these analyses point to *TM29* as a member of the *SEP1* subfamily of MADS-box genes. The reported number of MADS-box genes belonging to this group is on the increase. The functions of *TM29* were examined by genetic transformation experiments using co-suppression and antisense RNA techniques. The phenotypes of transgenic tomato and tobacco plants expressing *TM29* RNA suggest that *TM29*:

- promotes sympodial growth
- promotes early flowering and mediates events in floral organ development
- plays an important role in maintenance of floral meristem identity
- is required for the fruit development process

3.3.1 *TM29* belongs to the *SEP1*-group of MADS-box genes

TM29 showed significant nucleotide and amino acid sequence similarity to *Arabidopsis SEP1* and members of the *SEP1* sub-family of MADS-box genes. This was inferred from sequence analyses, the amino acid compositions in these proteins and putative secondary structures in TM29, which were similar to members of this group. TM29 showed 78% identity to DEFH49 and 68% to SEP1. Despite these similarities, there are

subtle differences between *TM29* and *SEP1*. *TM29* has an open reading frame (ORF) of 738 basepairs (bp) which encodes 246 amino acids while *SEP1* has a longer ORF of 747-bp encoding 249 amino acids. Analyses of the exon-intron positions within the ORF revealed eight exons in *TM29* while the *SEP1* ORF consists of seven exons (Ma *et al.*, 1991). Overall, the characteristics of *TM29* suggest it is a cognate homologue of *SEP1* or *SEP2*.

Phylogenetic analyses groups *TM29* to the *SEP1* subfamily of MADS-box genes. Prominent members of this family are the *SEP1*, *SEP2* and *SEP3* of *Arabidopsis*, *FBP2* of petunia (Angenent *et al.*, 1992) and the tomato *TM5* (Mandel and Yanofsky, 1998). Other recently identified members of this family include Asparagus *AOM1* (Caporali *et al.*, 2000), apple *MdMADS3* and *MdMADS4* (Sung *et al.*, 2000), *MdMADS7* and *MdMADS8* (Yao *et al.*, 1999), *Gerbera GRCD1* (Kotilainen *et al.*, 2000) and rice *OsMADS7*, *OsMADS8* (Kang *et al.*, 1997).

TM29 expression shows some similarities as well as differences to MADS-box genes of *SEP1* subfamily. *TM29* transcripts are expressed in vegetative shoot meristems, inflorescence meristems and floral meristems but not in roots or leaves. *TM29* RNA transcripts were detected in both the juvenile- and adult-phase shoot meristems of tomato. This is in contrast to the *SEP1* and *SEP2* genes, which are expressed exclusively in the flower (Flanagan and Ma, 1994; Savidge *et al.*, 1995). Other members such as the Asparagus *AOM1* and apple *MdMADS4* are expressed in inflorescence meristems as well as floral meristems but not in vegetative meristems. *TM29* is so far the only member of this group expressed in vegetative meristems. This suggests *TM29*, in addition to flower-specific roles may control vegetative characteristics in tomato.

TM29 expression in the flower, however, is similar to the general pattern observed among the *SEP1* group of MADS-box genes. *TM29* RNA is detected in the primordia of all four floral organ types, a characteristic feature of members of this group and a variation from the ABC pattern of gene expression (Theißen, 2001a). These analyses, therefore, suggest that *TM29* is a member of the *SEP1* group of MADS-box genes; however, certain differences in expression suggest *TM29* may have additional functions to that known for members of this group.

3.3.2 *TM29* may be involved in sympodial development

Tomato shoot architecture differs from that of tobacco or *Arabidopsis* in that vegetative and reproductive phases alternate during its sympodial pattern of growth. There is an initial juvenile vegetative phase of shoot growth where 7-12 leaves are produced after which the shoot meristem is converted into an inflorescence meristem to bear flowers. A second phase of adult shoot growth initiates from the bud in the axil of the youngest leaf. This shoot generates three leaves and is terminated by an inflorescence. This pattern of growth is repeated to give a main axis composed of reiterated sympodial units consisting of three nodes and a terminal inflorescence (Hareven *et al.*, 1994; Allen and Sussex, 1996; Pneuli *et al.* 1998; Schmitz and Theres, 1999). In tobacco by contrast, a flower terminates growth of the main shoot, with lateral meristems directly below the terminal flower giving rise to additional flowers and resulting in a cymose pattern (Amaya *et al.* 1999). The vegetative buds in the lower leaf axils of tobacco are usually suppressed and remain dormant. However, further down the main shoot, a new shoot may arise from a lateral meristem.

The evidence for *TM29* involvement in sympodial growth was weakly indicated by poor sympodial growth pattern in the tomato transgenic plants in which *TM29* expression was downregulated. Growth was terminated usually after the first sympodial shoots compared to 3-4 sympodial growth cycles seen in the wild type Microtom tomato plants under the growth conditions. However, *TM29* involvement in sympodial growth was clearly illustrated in the sympodial growth characteristics observed in the tobacco transgenic plants ectopically expressing the RNA of *TM29*. In the tobacco transgenic plants, the termination of shoot growth by the terminal flower caused another shoot growth from the axil of a leaf below the cymose inflorescence, producing leaves and flowers. This sympodial-like growth seen in the tobacco transgenic plants is therefore a direct response to the *TM29* RNA expressed in these plants and is an indication of reduced apical dominance. A proposed activity of *SEP1* class genes in reducing apical dominance is consistent with the reduced apical dominance of tobacco plants overexpressing *OsMADS1*, a *SEP1*-like MADS-box gene from rice (Chung *et al.*, 1994).

3.3.3 The transition to flowering in tobacco is responsive to *TM29* expression

The over-expression of *TM29* RNA also leads to early flowering in tobacco plants as seen in a reduced number of nodes and plant height at flowering. The average number of nodes produced by the non-transgenic tobacco was 31 ± 2.1 compared to 22 nodes in TBS-23 transgenic line (Table 3.8). This suggests that the phase change from vegetative to reproductive growth in tobacco is responsive to *TM29* RNA. This is consistent with the ectopic expression of rice MADS-box genes *OsMADS7* and *OsMADS8* (two *SEP1*-like genes) in tobacco which resulted in dwarfism and early flowering (Kang *et al.*, 1997). *OsMADS1* also caused early flowering in tobacco plants (Chung *et al.*, 1994).

There was no observation in the tomato transgenic plants that implicated *TM29* in the control of flowering time. Such a function for *TM29* in tomato should have resulted in the lengthening of the vegetative phase or an increase in the number of nodes produced by sympodial shoot in the plants with reduced *TM29* expression. The lack of such phenotype could be due to functional redundancy in the control of flowering time in tomato. The tomato *FALSIFLORA* gene, a homologue of *Arabidopsis LFY* is identified to control flowering time in tomato (Molinero-Rosales *et al.*, 1999). *TM29* may function redundantly to control flowering time in tomato. Likewise, overexpression of *TM29* in the sense transformed tomato plants did not result in early flowering. The Microtom tomato cultivar used in this study is an early flowering type that flowers, after producing 9-10 leaves at a height of about 8-10 cm above soil level compared to the tomato cultivar UC82B, which flowers at about 50-60 cm under the same growth conditions (Meissner *et al.*, 1997). This early flowering characteristic of Microtom cultivar may override the early flowering effect of *TM29* overexpression in transgenic plants.

3.3.4 *TM29* is required for proper floral organ development

The phenotypes of the aberrant tomato transgenic flowers put together with the RNA expression pattern clearly implicate *TM29* in the development of the floral organs. *TM29* expression in the floral meristem occurs before the emergence of any of the floral organs and most likely, before expression of the floral organ identity genes. This

suggests *TM29* may be required to regulate the temporal and spatial expression of the organ identity genes. The expression pattern observed in the floral organ primordia indicated that it may be required in the early stages of floral organ development.

The level of *TM29* RNA transcripts in the floral organs was high during the early stages of the primordia development but decreased as the organ matured. This suggests *TM29* function may be required for activities of the floral organ identity genes as well as the proper development of the organs. At later stages of flower development, *TM29* transcripts localise to specific tissues within the organs suggesting *TM29* may have specialised functions in those tissues. The above hypotheses on *TM29* functions were tested when its RNA was reduced by antisense and co-suppression techniques. The most conspicuous effect of the absence of *TM29* RNA was the morphogenetic changes in the inner three whorls of the tomato flower even though the first whorl organ also displayed certain aberrant characteristics. The sepals in the transgenic flowers were temporarily joined to each other along their entire length and this delayed the opening of the flowers. This contrasted with the sepals in wild type tomato flower, which are separate from each other for most part of their length before the petals open. This observation may be an indication of *TM29* function in sepals. So far no effects on sepal development have been described for the *SEP1* group of MADS-box genes.

Tomato flowers are characterised by their intense yellowish petals and stamens. The greenish petals and stamens in the transgenic flowers point to an alteration in the development of these floral organs. The green petals and stamens are similar to the phenotypes of transgenic flowers caused by the expression of antisense *TM5* RNA in tomato (Pneuli *et al.*, 1994a) and cosuppression of *FBP2* in petunia (Angenent *et al.*, 1994). Together, these characteristics of *FBP2*, *TM5* and *TM29* transgenic flowers bear a striking resemblance to the flowers of the recently described *SEPALLATA* mutant (Pelaz *et al.* 2000).

The sepallata flower is a result of mutations in three *Arabidopsis* genes *SEP1*, *SEP2* and *SEP3*. The triple mutant of these genes bears flowers with sepals in the first three whorls, with the fourth whorl replaced by a new sepallata flower. These three genes are redundant in their function of mediating the activities of the B and C floral organ identity genes. Sequence analyses suggest *TM5* is the designated homologue of *SEP3* (Mandel and Yanofsky, 1998) while *TM29* also share some similarities with the *SEP1*

and *SEP2* genes. The putative orthologue of *SEP3* in petunia, *FBP2* also affects similar morphogenetic features. *FBP2* is highly homologous to *TM5* and *SEP3*. Inhibition of *FBP2* RNA by co-suppression resulted in green petals and green petaloid stamens (Angenent *et al.*, 1994).

The phenotypes of the inner floral organs of *TM29* tomato transgenic flowers suggest a partial transformation into sepals in several respects, including cellular morphology. Examination of the epidermal layer of the transgenic floral organs showed some variation in cell morphology. Stomata were present on the surface of transgenic petals and ovary. The carpel was also covered with trichomes, unlike in the wild type. Stomata and trichomes are characteristic of tomato sepals but are typically absent from inner whorls. In the sepallata flower, presence of stomata on inner whorls was associated with their complete conversion to a sepal identity (Pelaz *et al.*, 2000). Unlike the sepallata flower, the downregulation of *TM29* resulted in a partial transformation of the floral organs. This may be a result of the redundancy that may exists among similar sets of *SEP*-like genes in tomato (Smyth, 2000). *TM29* shares functional similarity to *TM5* and may both be involved in the B and C organ identity functions in tomato.

The mode of function of *TM29* and *TM5* can be inferred from those proposed for the *SEP* genes. The resemblance of the sepallata flower to the double mutant of B and C organ identity functions indicates the *SEP* genes are required for the proper functions of the B and C genes (Bowman *et al.*, 1991; Pelaz *et al.*, 2000; Honma and Goto, 2001; Pelaz *et al.*, 2001b). This *SEP* function has been designated as E-function, extending the ABC model of floral organ identity, which already has a D-function responsible for ovule identity (Angenent *et al.*, 1995; Jack, 2001ab; Theißen, 2001ab).

3.3.4.1 Reproductive defects in *TM29* transgenic flowers

In wild-type tomato, interwoven rows of lateral and adaxial hairs on stamens join them together to form a cone around the pistil (Sekhar and Sawhney, 1987). Pollination and fertilisation in wild type flowers then promotes the senescence and abscission of both petals and stamens during the early growth of the ovary. Separation of stamens is not seen in wild type flowers. In contrast, tomato mutants such as dialytic (dl) (Llop-Tous *et al.*, 2000) and parthenocarpic fruit (pat) mutant (Mazzucato *et al.*, 1998) display

stamens that are not united. These mutants are characterised by suppressed hair growth on the stamens.

The stamens from transgenic plants in which *TM29* is suppressed are loosely fused and separated from each other as the ovary developed. They remain on the flower in lateral positions for a long period and do not abscise. The lack of fusion among the stamens can be attributed to a number of factors. These include (a) absence or poor growth of lateral and adaxial hairs on these stamens, (b) lack of interweaving between the hairs of adjacent stamens, or (c) pressure exerted by growth of the ovary combined with failure to abscise. Scanning electron microscopy was used to closely examine these possibilities.

Electron micrographs revealed that lateral and adaxial hairs are present on the *TM29* transgenic stamens. Significantly however, these hairs did not interweave among themselves and thus could be responsible for the failure of stamens to be joined. Further, the delayed senescence and abscission of the stamens subjected them to the pressure exerted by the developing ovary. On the whole, the transgenic stamens were weakly held together due to poor interweaving of adaxial and lateral hairs. The delay in stamen senescence and abscission, together with the rapid growth of the ovary contributed to the dialytic phenotype of the transgenic stamens.

Pollen was not detected in the transgenic stamens suggesting *TM29* function affects male gametogenesis in tomato. Lack of pollen could be due to poor pollen formation or a more indirect result of anther defects, which would block dehiscence. The pollen mother cells formed during gametogenesis comprise of an outer endothecium, a middle layer and tapetum, which are crucial to gametogenesis (Sanders *et al* 1999; Sanders *et al*., 2000; Yang and Sundaresan, 2000). *TM29* transcript accumulation in the wild type stamens localises to the endothecial and tapetal cells and may be required for the proper development of these tissues.

3.3.5 Reduced levels of *TM29* RNA induces fruit development without fertilization

The ovary of the transgenic flowers formed parthenocarpic fruits. The proportion of flowers that formed fruits in transgenic plants did not differ significantly from wild type plants suggesting that the reduction in *TM29* RNA or the lack of pollination and fertilisation did not affect fruit set. In wild type tomato, unpollinated ovaries grow very little and abscise shortly after anthesis (Fos *et al.*, 2001).

Unlike in the wild type tomato fruits, no seeds were found in fruits of transgenic plants showing phenotype. This could be attributed to the lack of pollen produced by the transgenic stamens; however, attempts at pollination with viable pollen did not produce seeds in these transgenic fruits, suggesting that the transgenic ovary is sterile. Several natural parthenocarpic tomato lines are facultative and are able to produce seeds in fruit (Mazzucato *et al.*, 1998). Similarly, engineered parthenocarpic plants of tobacco and eggplant produce viable seeds when flowers are pollinated (Rotino *et al.*, 1997). The failure of the *TM29* transgenic plants to produce seeded fruit when pollinated with viable pollen could be a consequence of malformed embryo sacs in ovules or unfavourable conditions for pollen tube growth in the stigma. Given that *TM29* RNA accumulates in the ovary throughout its development and later in seeds, *TM29* may be required for proper development of the ovules and seeds.

The parthenocarpic fruit development of the transgenic flowers is a suggestion that *TM29* has a role in fruit development and may function as a negative regulator which represses parthenocarpic fruit development in wild type tomato. Consistent with such repressor activity is the *Arabidopsis* mutant, *fruit without fertilisation* (*fwf*), which initiates seedless fruit in the absence of pollination and also the tomato *pat* mutants (Mazzucato *et al.*, 1998; Fos and Garcia-Martinez, 2000; Fos *et al.*, 2001; Vivian-Smith *et al.*, 2001). Parthenocarpy is recessive in these mutants suggesting that the corresponding wild type genes repress fruit development in the absence of fertilisation.

3.3.6 *TM29* may be involved in fruit ripening

In transgenic plants with reduced *TM29* RNA, there was delay in the onset of fruit ripening. After reaching the final fruit size, transgenic fruits remained green for a longer period before showing signs of colour change. The fruit ripening process is associated with changes in gene expression and given that *TM29* is a potential transcription factor, it may be involved in regulating the transcription of ripening related genes (Schuch *et al.*, 1989; Gray *et al.*, 1992; Gillaspy *et al.*, 1993; Manning, 1998; Brummell *et al.*, 1999).

In addition to delayed ripening, transgenic fruits did not ripen fully; they turned orange colour and did not soften like wild type fruit. The fruit ripening process is associated with biochemical and physiological changes, which include chlorophyll pigment degradation and synthesis of new carotenoid pigments such as ß-carotene and lycopene. There is also starch breakdown into glucose and fructose and softening of cell wall by enzymes (Grierson and Kader, 1986; Gray *et al.*, 1992). The orange colour of the transgenic fruit may be due to accumulation of ß-carotene instead of lycopene, suggesting that *TM29* may be required for normal synthesis of carotenoids during fruit ripening in tomato. (Grierson and Kader, 1986).

3.3.7 *TM29* is involved in determinate growth of the flower

The flowers of the *TM29* transgenic plants displayed indeterminate characteristics in the fourth whorl. In addition to carpel development into fruit, other ectopic structures were formed within the carpel, as a result of indeterminate growth. This suggests a role for *TM29* in the control of determinate growth in the flower. The structure of the flower in most angiosperms is determinate and characterised by defined number of floral organs whose position and identity are determined by genetic interactions that precede their formation and development. Normally, the development of carpel into fruit terminates growth of the flower.

Indeterminate growth of tomato flower is not commonly observed. Recently however, a tomato pleiotropic mutant, *clausa* was described with formation of ectopic organs within the fruit. The *CLAUSA* gene was found to regulate this perturbation, partly by regulating the tomato *LeT6* homeobox gene (Avivi *et al.* 2000). Antisense expression of the *TAG1* and *TM5* genes also resulted in indeterminate characteristics of the fourth whorl of tomato flowers (Pneuli *et al.* 1994ab). The indeterminate function of *TM29* is consistent with the *SEP* gene functions. The *SEP* genes mediate the determinate function of *AG*, in addition to its B and C organ identity functions. In the sepallata flower phenotype, the fourth whorl is replaced by a new flower (Pelaz *et al.*, 2000). Similar phenotypes are observed in antisense *TM5* tomato flowers and co-suppressed *FBP2* petunia flowers (Pneuli *et al.*, 1994a; Angenent *et al.*, 1994). *TM29* may be required to mediate the determinate function of the *TAG1* gene in tomato.

The indeterminate growth in *TM29* transgenic flowers is not simply the result of replacement of the carpel by another flower or the emergence of structures within the fourth whorl organ. Instead, a new shoot grows out of the carpel producing leaves and flowers. This differentiates the *TM29* plants from the *Arabidopsis agamous* and sepallata flower mutants, as well as the antisense *TM5* tomato flower. By contrast, this *TM29* phenotype shows similarity to the co-suppressed *FBP2* flowers and the double mutant flower of *agamous* and *constans*, in which new inflorescence emerged from the swollen carpel (Angenent *et al.*, 1994; Okamuro *et al.*, 1996; Mizukami and Ma, 1997).

3.3.8 *TM29* may act to maintain floral meristem identity

The eventual emergence of ectopic shoot from inside the fruit was an interesting aspect of the *TM29* transgenic phenotype. This shoot produced leaves and multiple flowers. The leaves were small in size but had the same epidermal cell-type and features of the normal leaf. The ectopic flowers were a reiteration of the aberrant flowers on the transgenic plants. The growth of the ectopic shoot is an indication that floral meristems present in the carpel have undergone reversion to shoot meristem identity (Okamuro *et al.*, 1996; Mizukami and Ma, 1997). Plants normally produce a predictable sequence of meristems: vegetative, inflorescence and floral meristems. These meristem types are

landmarks of transitional phases of shoot growth; for instance the inflorescence meristem marks a switch from vegetative growth to reproductive growth (Levy and Dean, 1998). The emergence of flower-bearing shoot within a flower is a suggestion that the identity of the floral meristems have switched to inflorescence meristem. An alternative view is that, there are remnants of shoot meristems present in the flower that can generate this ectopic inflorescence (Okamuro *et al.*, 1996). However, in *Arabidopsis ag-1 co-2* double mutant, it has been established that pre-existing indeterminate floral meristem produce the ectopic inflorescence shoot (Mizukami and Ma, 1997).

In tomato, the sympodial shoot meristem is converted into an inflorescence meristem after producing three leaves; the inflorescence meristem then produces flowers. The presence of leaves on the ectopic shoot of *TM29* flower indicates that the floral meristem reverted to a vegetative meristem identity. This reversion of a floral meristem to a vegetative meristem in *TM29* transgenic flowers is a step beyond what was reported for *FBP2* in petunia and the double mutant of *AG* and *CO* in *Arabidopsis*. Rather, this *TM29*-induced reversion is similar to floral reversion observed in purple-flowered *Impatiens balsamina* (Pouteau *et al.*, 1997). In *Impatiens*, environmental conditions have a strong influence on reversion. In non-inductive conditions, there is complete shift from flower development to production of leaves, which continues until favourable inductive conditions are imposed (Pouteau *et al.*, 1997; Pouteau *et al.*, 1998ab). This phenotype of *TM29* transgenic flowers is consistent with the hypothesis *TM29* may control floral reversion in wild-type tomato by the maintenance of floral meristem identity.

3.3.9 Mechanisms controlling floral reversion

Floral reversion is controlled by both environmental and internal factors that influence flowering as well as meristem development in plants. For example, in *Arabidopsis*, flowering is promoted by long-day photoperiod while floral reversion occurs under short-day conditions, in the absence of *LFY* or *AG* (Okamuro *et al.*, 1996; Mizukami and Ma, 1997). In *Impatiens balsamina*, flowering is promoted under short-day light

conditions. Growth under long-day conditions favours reversion to vegetative growth (Poteau *et al.*, 1997; Pouteau *et al.*, 1998ab).

In *Impatiens*, a floral signal induced in the leaves must reach the floral meristem continuously throughout flower development to avoid reversion. Leaf removal experiments with *Impatiens balsamina* have provided evidence to support this hypothesis (Poteau *et al.*, 1997; Pouteau *et al.*, 1998b; Tooke and Battey, 2000). The nature of this floral signal however, remains elusive and similar experiments have not been reported in *Arabidopsis* or any other plant species (Hempel *et al.*, 2000). In *Arabidopsis*, *AG* and *LFY* control the short-day mediated floral reversion (Okamuro *et al.*, 1996; Mizukami and Ma, 1997). *LFY* is a floral meristem identity gene and the differentiation of the floral meristems are associated with increase in its expression. *AG* controls identity of stamen and carpel as well as determinate growth of floral meristem.

Floral reversion has not been reported in tomato, a photoperiod insensitive plant, hence the control of this characteristic is not known. The results presented here show that *TM29* may control this phenomenon in tomato. Unlike in *Arabidopsis*, *TAG1* (the tomato *AG* homologue) gene and *FALSIFLORA* (*FA*; the tomato *LEAFY* orthologue) may not be involved in controlling floral reversion in tomato. *TAG1* regulates determinate growth of the floral meristem and performs the C-organ identity function in tomato (Pneuli *et al.*, 1994b) while *FA* controls floral meristem identity and flowering time (Allen and Sussex, 1996; Molinero-Rosales, 1999). It is possible the mechanisms controlling floral reversion in tomato is different from *Arabidopsis*.

Photoperiod or GA may not control floral reversion in tomato. To further examine how floral reversion may be controlled in tomato, the effects of photoperiod and gibberellin on the tomato transgenic phenotypes were studied. Short-day treatment or exogenous application of GA_3 did not prevent floral reversion in *TM29* transgenic plants nor did they induce this trait in wild type flowers. In contrast to these results in tomato, exogenous application of GA inhibits floral reversion in *Arabidopsis ag* mutant growing under short-day conditions suggesting that maintenance of *Arabidopsis* floral meristem identity is positively regulated by GA and mediated by short-day light conditions (Okamuro *et al.*, 1996). These results further suggest floral reversion is controlled differently in tomato and that *TM29* may be a key regulator of this trait.

3.3.10 Downregulation of *TM29* RNA by cosuppression and antisense techniques

The phenotypes analysed in this study were generated using genetic transformation to obtain plants with downregulated *TM29* expression through cosuppression and antisense RNA methods. In this study a cosuppressed tomato line (S/05) showed similar aberrant phenotypes as the antisense generated plants. The similarity between the phenotypes of cosuppressed and the antisense transgenic lines is consistent with the hypothesis that downregulation of *TM29* gene is responsible for the phenotypes observed. The amount of *TM29* transcripts (both transgene and endogenous) detected in the transgenic plants was reduced. This suggested a post-transcriptional gene silencing mechanism. The low level of both sense and antisense transcripts in the antisense transgenic plants, as detected by the gene-specific RNA probes, may be due to a silencing mechanism mediated by a co-ordinated degradation of antisense RNA and corresponding sense RNA (Baulcombe, 1996; Wassenegger and Pelissier, 1998; Stam *et al.*, 2000).

Co-suppression and antisense gene techniques have been used to reduce the expression of endogenous genes so that the resultant phenotype mimics that of a knock-out mutant (Mizukami and Ma, 1992; ; Pneuli *et al.*, 1994ab; Angenent *et al.*, 1995; Stam *et al.*, 2000). These methods have been used to study functions of *FLORAL BINDING PROTEIN 7 (FPBP7)* and *FBP11* MADS-box genes of *Petunia* (Angenent *et al.*, 1995). Recently, the same technique was employed in determining the function of *PETUNIA FLOWERING GENE* (*PFG*), a MADS-box gene involved in the transition from vegetative to reproductive development (Immink *et al.*, 1999). Antisense plants of *Arabidopsis AG* and tomato *TAG1* display similar phenotypes to known *agamous* mutants (Pneuli *et al.*, 1994b; Mizukami and Ma, 1995). These studies have therefore shown that the phenotypes of transgenic plants may accurately reflect loss of gene function.

3.3.10.1 Partial antisense transformed tomato did not display aberrant phenotypes

In previous studies, full-length cDNA sequence of MADS-box genes were used to produce antisense transgenic plants (Pneuli *et al.*, 1994ab; Mizukami and Ma, 1995; Kotilainen *et al.*, 2000). In an effort to determine if a targeted degradation of *TM29* transcripts could be achieved using a partial antisense cDNA construct and whether the

resulting plant phenotypes will be comparable to that produced with the full-antisense cDNA construct, transgenic plants were generated with partial antisense construct. The transgenic plants transformed with the partial antisense construct did not show aberrant phenotype. These plants mostly resembled the wild type phenotype. The difference between the partial construct and the full-antisense construct was the removal of the conserved MADS-box region and a portion of the I-region from the former. The normal phenotype of the partial-antisense plants could be explained in two ways: (1) that the expressed partial antisense RNA failed to trigger downregulation of *TM29* RNA in the transgenic lines or (2) there is redundancy with another gene, which requires the full length construct to suppress. These possibilities were examined using *TM29* gene-specific RNA probes to detect steady state transcripts of both the endogenous and partial antisense genes in the transgenic plants.

The analyses of *TM29* transcript levels using a gene-specific probe showed high levels of both the endogenous *TM29* RNA and the transgene-expressed partial antisense RNA in the transgenic lines, suggesting that *TM29* was not downregulated in these plants. This is in contrast to the full-antisense plants in which both the endogenous and antisense RNA were downregulated. The presence of both the sense and antisense *TM29* RNA in the partial-antisense plants suggests the failure to trigger the RNA degradation mechanism seen in the other transgenic plants and is consistent with the normal phenotype observed.

The reasons for the inability of the partial construct to downregulate *TM29* RNA are not clear. Also, the effect of the *TM29* transgene on other MADS-box genes cannot be fully proven. Overall, however, the normal phenotype of the partial-antisense transgenic lines put together with the failure to downregulate *TM29* RNA is further evidence supporting *TM29* role in the unusual phenotypes seen in the aberrant transgenic lines.

CHAPTER 4 Characterisation of a new tomato MADS-box gene, *TM10*

4.1 Introduction

The MADS-box gene family in tomato has not been extensively characterised with only about a dozen members described to date (Pneuli *et al.* 1991; Pneuli et al., 1994ab; Kramer et al., 1998; Mao et al., 2000). There are at least 80 MADS-box genes in *Arabidopsis thaliana*, (Alvarez-Buylla et al, 2000a; Jack 2001a) and given conservation of functions controlling growth and development, a similar number of MADS-box genes would be expected in tomato.

To further understand the role of this gene family in flower and fruit development, an attempt was made to identify more genes expressed in tomato flowers and fruit. The conserved sequence in the MADS domain offers the opportunity to design degenerate primers for amplification of MADS-box gene fragments. Sequence analyses identified tomato MADS-box genes that were previously uncharacterised. Subsequently, a longer fragment of one, *TM10* was obtained and characterised. This chapter describes the method used to identify new MADS-box genes and the subsequent characterisation of *TM10*, amplified from a fruit cDNA. This general method should be applicable for the isolation and characterisation of additional members of the MADS-box family.

4.2 Results

4.2.1 Identification of tomato MADS-box genes

Total RNA was isolated from flower buds and fruit using the Trizol method. This was followed by poly (A) mRNA purification using the mRNA MessageMaker Reagent Assembly (Gibco BRL). cDNA was synthesized from the mRNA using SuperScript II reverse transcriptase system (Gibco BRL) and used as templates to amplify short DNA fragments of 145 bp from MADS-box region. Degenerate primers DEG-1 and DEG-2, corresponding to conserved residues MGRGKV/I, LCDAEV in the MADS-box respectively were used in PCR. Because several bands from the PCR were detected on agarose gel, the DNA in a band of the expected size was excised from the gel and purified using Highpure PCR purification kit (Roche). The DNA fragment was cloned into the pGEM-T vector, transformed into *Escherichia coli* and selected on plates containing ampicillin. 60 transformed colonies were picked at random into culture and grown overnight; plasmid DNA purified and sequenced.

MADS-box sequences representing individual genes in tomato were identified from the sequencing of the 145-bp fragments. Sequences were aligned using the Pileup program (GCG software) and the alignment submitted to the BOXSHADE server (www.ch.embnet.org/software/BOX_form.html) to highlight similarities and differences (Appendix E). Differences in nucleotide sequence in the region outside of the primer binding sites were used to determine whether clones represent similar or different genes. The analyses of 52 short sequences identified 18 different clones representing MADS-box genes in tomato. Each of the 18 different sequences was analysed for similarity to known MADS-box sequences using the BLAST program (Atschul et al., 1997). These analyses identified two fragments, *TM10* (*Tomato MADS-box 10*) and *TM18* as representing tomato MADS-box genes previously uncharacterised.

The longer fragment of *TM10* was subsequently amplified with overlapping gene specific primers, TM10-P1 and TM10-P2 and a 3' anchor primer using the rapid amplification of cDNA ends (3' RACE) technique (Ohara et al., 1989). The sequence of the 3' anchor primer was part of the *NotI* primer-adapter used for cDNA synthesis. TM10-P1 and TM10-P2 were used in primary and secondary reactions respectively, in combination with the anchor primer. The amplification conditions were as follows: initial denaturation at 94°C for 2 minutes, 30 cycles of 94°C for 30 seconds, 50°C for 30 seconds, 72°C for 1 minute and a final elongation step at 72°C for 5 minutes. A 1:100 fold dilution of the primary PCR product was used as template in the secondary PCR. These reactions produced a 0.9-kb DNA fragment of *TM10*.

4.2.2 *TM10* characterisation

The longer DNA fragment of *TM10* was cloned into the pGEM-T vector utilising the single deoxyadenosine (A) added to PCR fragments by the Taq DNA polymerase. The DNA fragment was sequenced in both directions by M13 forward and reverse primers using the ABI prism sequencer (Waikato DNA Sequencing Facility, Hamilton, New Zealand). The length of the *TM10* cDNA fragment was 864 nucleotides starting from the **ATG** translation start site to the polyadenylation region. *TM10* has an open reading frame of 603 bp encoding 201 amino acids and a 3' untranslated region of 261 nucleotides (Figure 4.1). It carries sequences corresponding to the 4 regions (MADS-box, I-region, K-box and C-terminal) typical of plant MADS-box genes (Krizek and Meyerowitz, 1996). The derived protein has a computed molecular weight of 23 kDa and isoelectric pH of 6.5, which is comparable to those of other MADS-box proteins (Mandel et al., 1998).

ATGGGGCGGGGGAAGGTTCAAATGAAGAGGATAGAGAATCCAGTTCATCGACAAGTCACT
M G R G K V Q M K R I E N P V H R Q V T

TTCTGCAAACGTCGAGCAGGCCTTCTTAAGAAGGCCAAAGAGCTCTCCGTTTTGTGCGAT
F C K R R A G L L K K A K E L S V L C D

GCTGAAATTGGTCTTTTCATTTTCTCCGCTCACGGAAAGCTCTATGAACTTGCTACTAAA
A E I G L F I F S A H G K L Y E L A T K

GGAAGCATGCAAGGGCTGATTGAGAGGTACATCAAGTCAACCAAGGGAGTTGAGGTGGCT
G S M Q G L I E R Y I K S T K G V E V A

GAGGAAGCCAAAGATACACAACCTCTGGACCCAAAAGAGGAGATCAACATGCTGAGGAAT
E E A K D T Q P L D P K E E I N M L R N

GAGATTGACGTACTCCAGAAAGGCTTAAGCTACATGTATGGGGGAGGCGCAGGAACAATG
E I D V L Q K G L S Y M Y G G G A G T M

ACACTAGATGAACTTCATTCACTTGAAAAGTACCTTGAAATTTGGATGTATCATATTCGT
T L D E L H S L E K Y L E I W M Y H I R

TCAGCAAAGATGGATATCATGTTTCAAGAGATCCAACTGTTGAAGAATAAGGAAGGGATA
S A K M D I M F Q E I Q L L K N K E G I

CTGGAAGCTGCAAACAAATATTTACAGGATAAGATAGATGAGCAATACACTGTGACTAAC
L E A A N K Y L Q D K I D E Q Y T V T N

ATGACCCAGAATTTGACTGACTTTCAATGCCCACTAACTGTACAAAATGAGATATTTCAG
M T Q N L T D F Q C P L T V Q N E I F Q

TTTTAACATATGCTCACTATGTAAGTTATTCTTGTTGTGAAGCATCTATGTAATTTGGTA
F *
AGGAGATGTAATAATGATGATTGAGTAATTTCACTTTGGAGAGATGAACATATAAGTATG
TTATTATGTTCAATTTAGGTAATATGTTTAGTGTGTGAGCCTTTTTAGTGTATCTTCTCT
AGTATGGTGCTACTTATTATATATGTCATCTTATAATTTCTGAGTCAACTTCTTGTTTTG
TTATTCAAAAAAAAAAAAAAAAAA

Figure 4.1. Sequence map of *TM10* cDNA and derived amino acid residues. The nucleotide sequence of the positive strand of TM10 fragment. The 3' untranslated region has been *italicised.* The boxed sequences indicate degenerate primer regions. The * marks the translational stop signal.

4.2.3 TM10 shows homology to AGL12

For comparison with other MADS-box sequences, the amino acid composition of TM10 was calculated and compared with related MADS-box proteins; it was found to be closest to that of *Arabidopsis* AGL12 (Table 4.1; Rounsley et al., 1995). Further, the amino acid sequence of TM10 aligned with other MADS-box protein sequences showed high similarity to AGL12, across the entire sequence (Figure 4.2). The amino acid sequence of TM10 has an overall identity of 64% to AGL12 protein of *Arabidopsis thaliana*. Within the conserved MADS-box (56 amino acids), TM10 showed 84% identity to AGL12 and 73% to Tomato MADS-box 4 (TM4). To further explore TM10 relationship with other MADS-box sequences, an unrooted phylogenetic tree was constructed using amino acid sequence from the conserved MADS-box, the intervening region and the K-box, avoiding the variable C-terminal region. TM10 and 19 other MADS-box protein sequences, obtained from the public database, were analysed using PILEUP (GCG software) with Kimura's distance correction method. Sequences were clustered using the neighbor-joining analyses of Saitou and Nei (1987) and plotted using Treeview software (Page, 1996). Phylogenetic analyses assigned TM10 to the orphaned group of *Arabidopsis* AGL12 (Figure 4.3).

For further characterisation of the TM10 sequence, the secondary structure of its conceptual protein was predicted using the PSIPRED model (Jones, 1999). The predicted structure revealed a pattern of α-helices, ß-strands and coils typical of plant MADS-box proteins and most similar to the AGL12 protein (Figure 4.4). Overall, the sequence analyses suggested TM10 is the tomato homologue of AGL12.

Table 4.1. Amino acid composition (%) of TM10 and selected MADS-box proteins

	TM10	AGL12	AGL3	TM4
Alanine	5.5	4.7	7.0	4.0
Arginine	4.0	3.8	6.6	7.0
Asparagine	4.0	5.7	5.8	4.8
Aspartic acid	4.5	3.3	5.0	3.5
Cysteine	1.5	1.4	0.8	0.9
Glutamic acid	6.5	5.7	9.3	7.0
Glutamine	9.5	9.5	7.0	8.4
Glycine	7.0	7.5	4.6	4.0
Histidine	2.0	1.0	2.7	4.0
Isoleucine	7.0	6.6	2.7	5.3
Leucine	11.0	11.5	10.8	12.0
Lysine	9.0	9.0	7.0	10.1
Methionine	5.0	5.2	3.5	1.7
Phenylalanine	3.5	3.8	3.1	2.6
Proline	2.0	3.3	2.7	0.9
Serine	3.5	5.7	9.7	10.1
Threonine	5.5	4.7	3.9	3.5
Tryptophan	0.5	0.5	0.8	0.9
Tyrosine	4.0	2.8	3.1	2.6
Valine	4.5	4.3	3.8	6.6

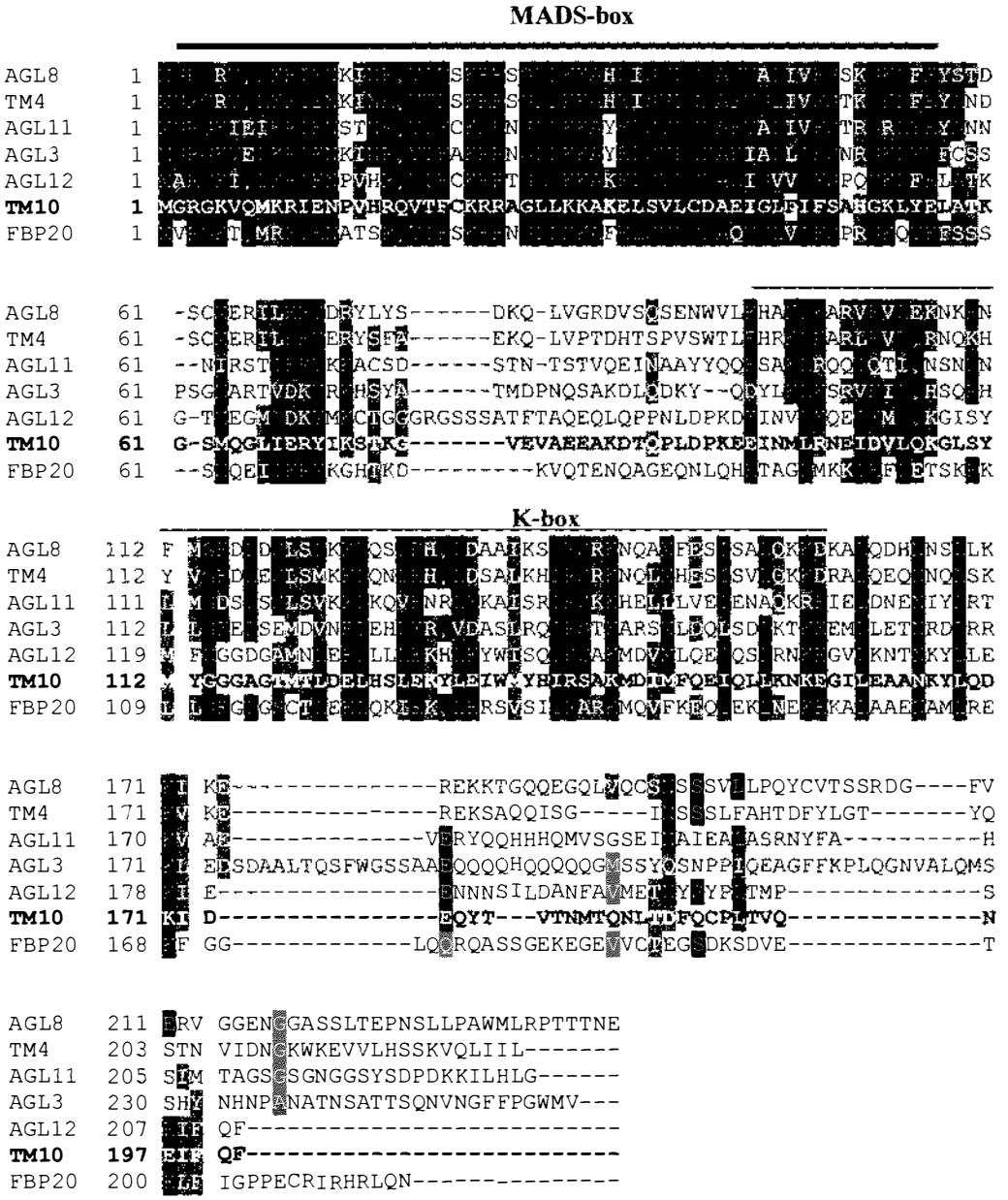

Figure 4.2. Alignment of selected MADS-box proteins using clustal W analyses. The TM10 sequence is in bold letters. Gaps were introduced to achieve maximum alignment. Conserved residues are shaded black and moderately conserved residues in grey. The conserved MADS-box and K-box are labelled with thick and thin lines respectively.

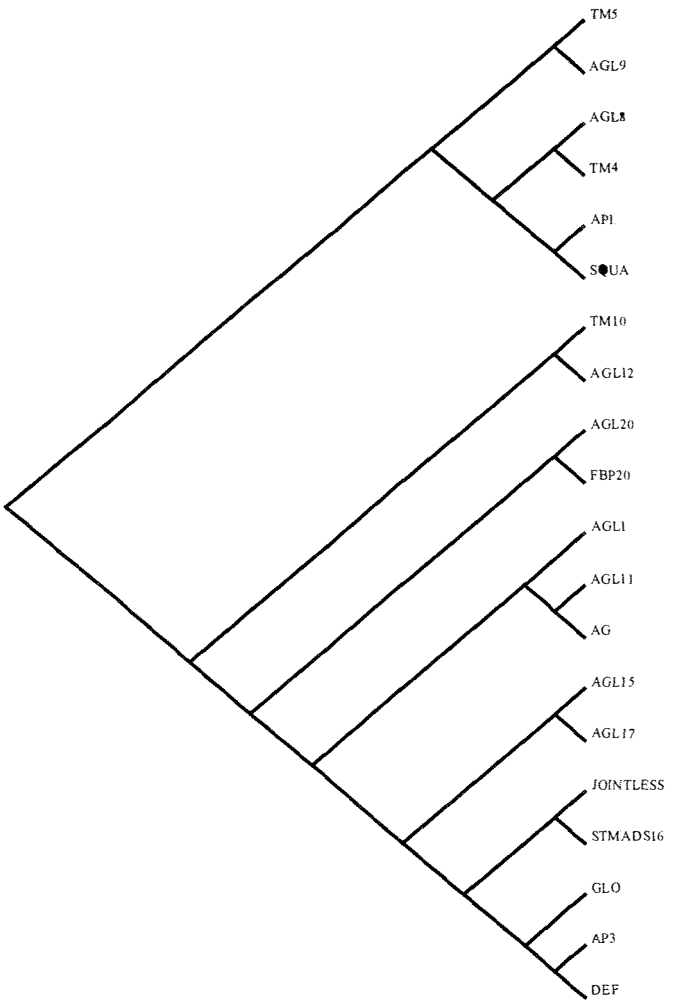

Figure 4.3. A cladogram of selected MADS-box proteins. The tree was obtained from neighbour-joining analyses of pairwise distances. Sequences from the MADS-box, the I region and the K-box only were used in these analyses. TM10 protein grouped with AGL12 of Arabidopsis.

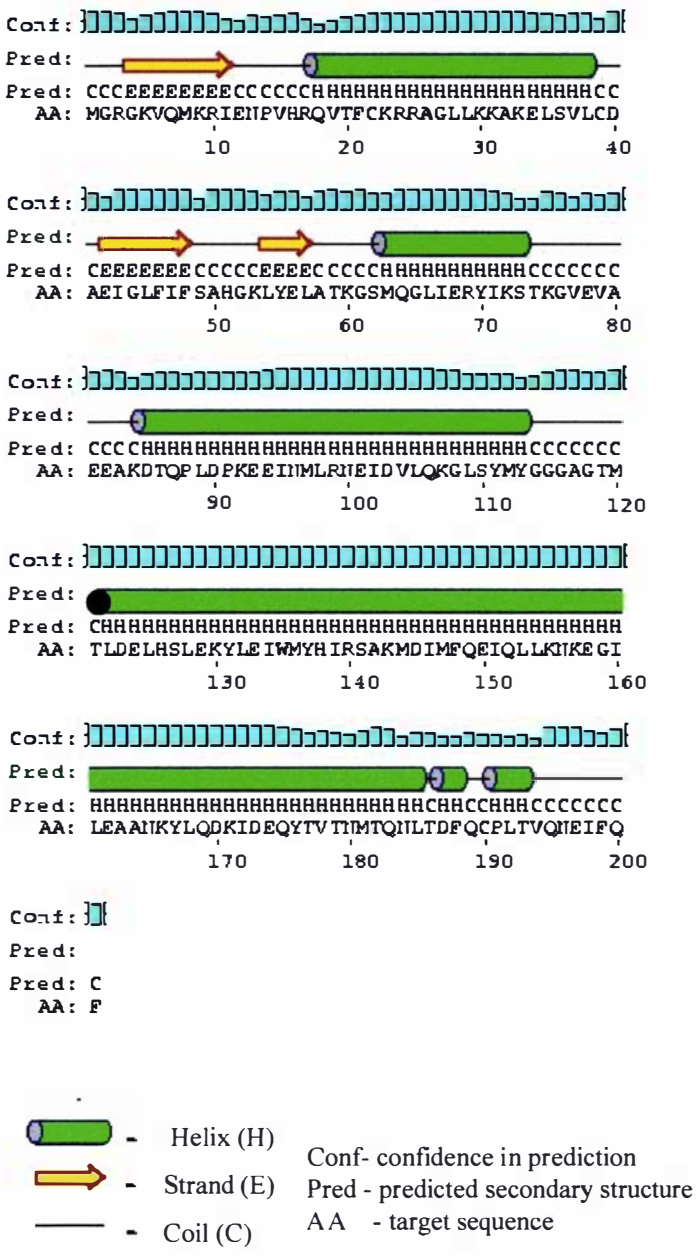

Figure 4.4. Secondary structure of TM10 protein. The amino acid residues were predicted as α-helix, ß-strand or coil using PSIPRED (Jones, 1999). The MADS-box and K-box are represented by amino residues 1-58 and 93-158, respectively.

4.2.4 Gene copy number

To estimate the gene copy number of *TM10*, Southern hybridisation was performed using a gene-specific probe to hybridise to tomato genomic DNA digested with *Eco*RI, *Hin*dIII and *Xho*I enzymes. The probe hybridised to multiple fragments in the *Eco*RI digest but to single bands in *Hin*dIII and *Xho*I digests (Figure 4.5). The *Eco*RI recognition sequence (GAATTC) may be present at several sites within the genomic DNA sequence of *TM10*. The results suggest there is one copy of *TM10* in tomato.

4.2.5 *TM10* is expressed in above-ground tissues at very low levels

To characterise the expression pattern of *TM10*, total RNA from flower buds, early fruit (7-10 days post-anthesis (d.p.a)), young leaves, shoot tips and roots were analysed by northern hybridisation. However, *TM10* transcript could not be detected in these tissues using this technique, even at reduced stringency. Further experiments using total RNA from different fruit samples also did not detect any *TM10* transcripts. These results suggested *TM10* may be expressed at very low levels in these tissues or there may be a post-transcriptional regulatory pathway affecting mRNA accumulation (Kuhn et al., 2001). The more sensitive reverse transcriptase polymerase chain reaction (RT-PCR) was therefore used to further examine *TM10* expression in tomato tissues. In RT-PCR, a reverse transcriptase synthesises DNA copies of mRNA transcript, which is then amplified by a DNA polymerase (Hadidi and Yang, 1990).

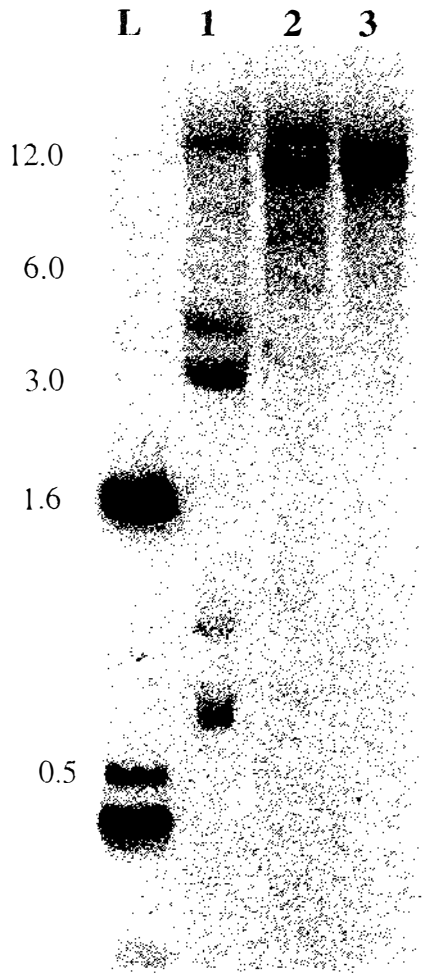

Figure 4.5. Southern hybridisation of tomato genomic DNA digested with *Eco*RI (Lane 1), *Hin*dIII (Lane 2) and *Xba*I (Lane 3), using labelled *TM10*-specific probe. Four to five fragments in the *Eco*RI digestion hybridised to the probe. The *Hin*dIII and *Xba*I digestions resulted in single major hybridised bands. Lane L contained the 1-kb DNA ladder and the numbers on the left-hand side represent the fragment sizes in kilobasepairs.

Gene-specific primers ITM-01 and ITM-02 were used in a one-step RT-PCR (as described in Chapter 2) to amplify a 0.6-kb DNA fragment using 1 μg total RNA as template in a 50 μl reaction. The RT-PCR products were electrophoresed on agarose gel, transferred to Hybond N^+ membrane (Amersham) and probed with a labelled *TM10*-specific probe (Hadidi and Yang, 1990). The hybridisation was analysed with Storm phosphorimager and Imagequant software (Molecular Dynamics). Total RNA from young leaves (0.5-1.0 cm long), large leaves (2-5 cm long), growing shoot tips, roots, flower buds, fruit of 7-10 d.p.a and 14-21 d.p.a were analysed. The results showed that *TM10* is expressed in both small and immature big leaves, shoot tips, flower buds, early and late fruit tissues but, not in roots (Figure 4.6A). This pattern suggests that *TM10* expression is specific to shoot tissues.

4.2.6 *TM10* is expressed in fruits

To further characterise *TM10* expression in detail, total RNA from sepals, petals, stamens, ovary of flower buds and ovary at anthesis were analysed. *TM10* expression in the different floral organs was barely detected but expression is relatively higher in anthesis ovary (Figure 4.6B), indicating a possible increase in *TM10* expression at anthesis. To analyse *TM10* expression during fruit development, total RNA from fruits at 2, 4, 6, 9, 14 and 21 d.p.a were also analysed for levels of transcript. *TM10* expression was detected at comparable levels in all fruit samples examined (Figure 4.6C). The expression of *TM10* in all the fruit tissues examined suggests it may be involved in the multiple stages of tomato fruit development.

Taken together, *TM10* expression is at very low levels specific to shoot tissues of tomato with relatively high level of expression in leaves. In the flower, *TM10* expression was relatively higher in the ovary at anthesis and this continued through fruit development to at least 21 days post-anthesis.

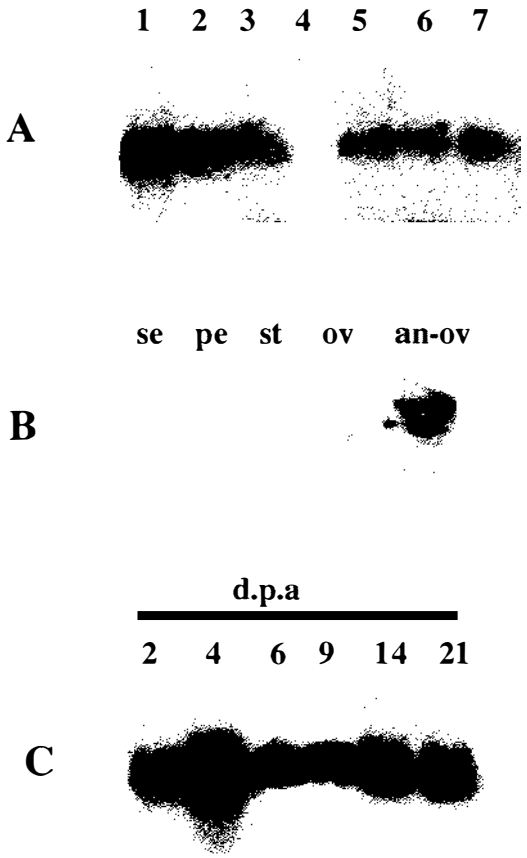

Figure 4.6. RT-PCR expression analyses of *TM10* in tomato tissues. RT-PCR products (after 25 cycles) were subjected to electrophoresis in 1% agarose gel, transferred to a membrane and hybridised with TM10-specific probe. Total RNA used as templates were isolated from: **A**. Small leaves (1), large leaves (2), shoot tips (3), roots (4), flower buds (5), early fruit (6) and late fruit. **B.** Pre-anthesis sepals (se), petals (pe), stamens (st), ovary (ov) and anthesis ovary. **C**. Fruits of 2, 4, 6, 9, 14 and 21 days post-anthesis (d.p.a).

4.2.7 *In situ* hybridisation

In situ hybridisation technique was used to examine *TM10* expression in early floral tissues. Digoxigenin-labelled *TM10*-specific RNA probes were prepared from *TM10* DNA fragment amplified using ITM-01 and ITM-02 primers. The primers ITM-01 and ITM-02 carried promoter sites for the T3 and T7 RNA polymerases, which were used for *in vitro* transcription. The antisense RNA probe was used to detect *TM10* transcript while the sense probe was used for background levels. Here also, the level of *TM10* transcript was very low. However, in vegetative tissues, *TM10* transcript was detected at the tip of the sympodial bud, in the leaf axil and in leaf blade (Figures 4.7A, 4.7C). Hybridisation with sense probe was used as indication of background level (Figure 4.7B). *TM10* transcripts were also detected in the floral meristem and in the stamen and ovary of mature flower bud (Figures 4.7C, 4.7D).

4.2.8 Tomato transformation

Agrobacterium transformation vectors, pART270S and pART270AS, carrying the *TM10* cDNA in sense and antisense orientations to the CaMV 35S promoter, were constructed as described in Chapter 2. Transgenic tomato plants were generated with *Agrobacterium tumefaciens* harbouring pART270S, the *TM10* sense vector. A total of 496 tomato cotyledon explants were inoculated with this vector and selected on kanamycin containing medium. Overall, 117 explants (23.5% of explants inoculated) produced putative transgenic shoots at an average of 1.2 shoots per explant. After repeated transfers to selection medium, 32 putative transgenic plants were selected and rooted on kanamycin-containing medium.

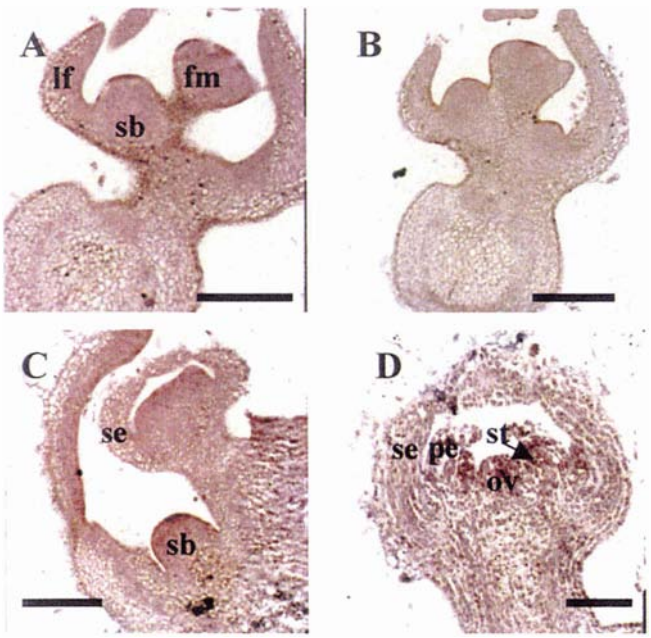

Figure 4.7. RNA in situ hybridisation analysis of *TM10* expression in tomato tissues. **A.** *TM10* transcript was detected in leaf blades, sympodial buds and in floral meristems. **B**. Similar section in A probed with sense RNA as control. **C**. *TM10* expression was not expressed in emerged sepal primordia but was detected in the floral meristem at this stage. **D**. In mature floral bud, *TM10* transcripts were detected at low levels in the petals, stamen and ovary.

Bars= 150 μm. ov:ovary; pe: petal; sb: sympodial bud; se: sepal; st: stamen.

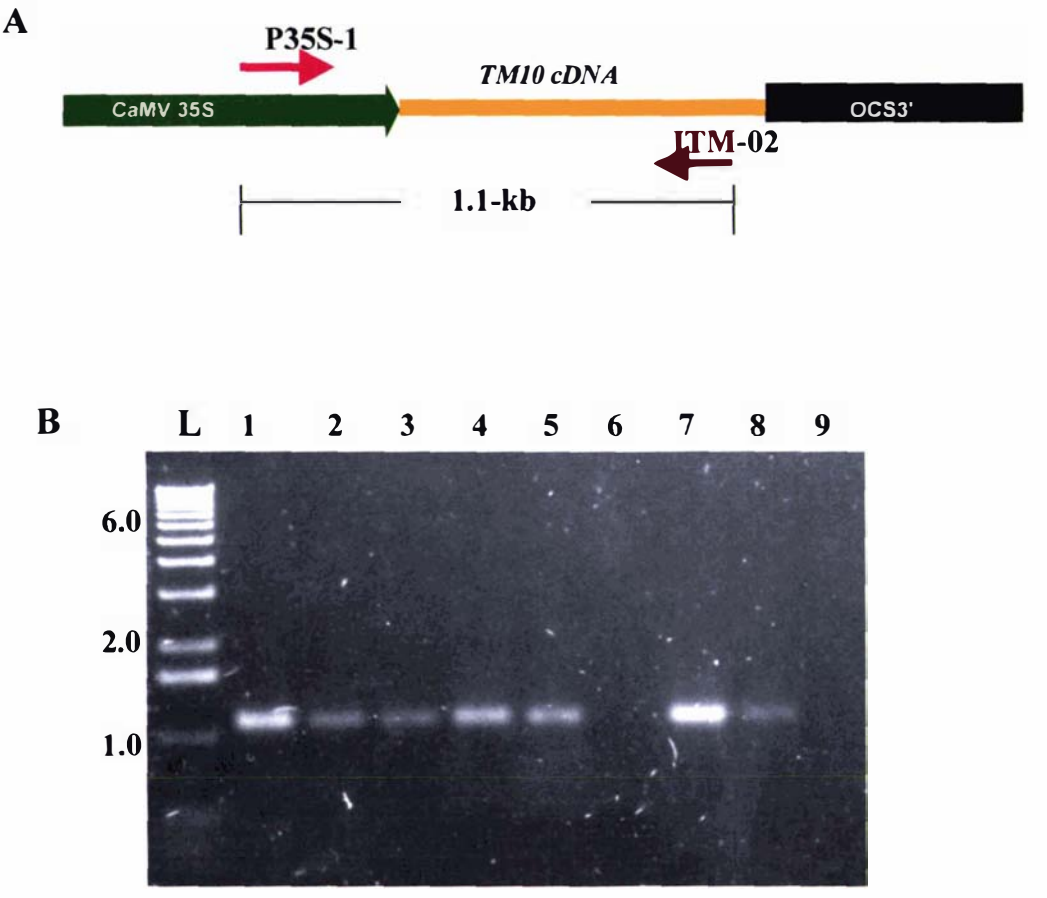

Figure 4.8. PCR of *TM10* transgenic tobacco plants. **A**. A schematic diagram showing the binding sites of the primers p35S-1 and ITM-02, used to amplify a 1.1-kb fragment. **B**. Gel photograph of PCR products from some tobacco transgenic lines. Lanes 1-8 contain PCR products of putative transformed plants,; lane 9, product of non-transgenic control plant. The lane marked L contains the 1-kb DNA ladder (GIBCO-BRL). The size of the ladder fragments in kilobasepairs is indicated on the left-hand side.

These were transferred to soil together with 10 non-transgenic tomato plants regenerated through tissue culture. Transgenic plants were confirmed by PCR using P35S-1 primer, specific to the 35S promoter and ITM-02 (Figure 4.8).

4.2.9 Phenotypes of transgenic plants

The majority of the transgenic tomato plants carrying the *TM10* DNA under the 35S promoter did not show any abnormal phenotype. Vegetative growth characteristics, flower phenotype and fruit development in these transgenic lines was same as in the non-transgenic tomato plants. However, one transgenic plant in this population, T270S-15 displayed aberrant characteristics in flower and fruit morphology (Figure 4.9).

In wild type tomato flower, the petals and stamens are yellow at anthesis and senesce 4-5 days after anthesis (Figure 4.9A) but in flowers of the T270S-15 line, there was a homeotic transformation of the sepals of flowers to leaf-like organs (Figure 4.9B). These leaf-like sepals were bigger (12.4 ± 0.5 mm long) than the wild type tomato sepal (6.18 ± 0.27 mm long). In addition, the petals and stamens of T270S-15 did not develop normally. These second and third whorl organs were reduced in size and they senesced before emerging from the calyx tube. The petals of T270S-15 were smaller (1.1 ± 0.1 mm long) than the wild type petal (6.0 ± 0.2 mm long). Similarly, the T270S-15 stamens were smaller (1.0 ± 0.11 mm) than the wild type stamen (4.6 ± 0.2 mm). Although, the petals and stamens senesced 4-5 days after anthesis these organs remained on the flower and did not abscise (Figure 4.9D). The transgenic ovary looked normal and was similar in size (0.8 ± 0.05 mm wide) to the wild type ovary (0.9 ± 0.08 mm wide). However, whereas in the wild type, the development of ovary into a fruit depends on pollination and fertilisation (Figure 4.9C) the transgenic ovary was able to develop in the absence of pollination, to produce parthenocarpic fruit (Figure 4.9D). The size of transgenic fruits (2.2 ± 0.5 cm diameter) at the breaker stage was significantly bigger than the wild type fruit (1.5 ± 0.3 mm diameter).

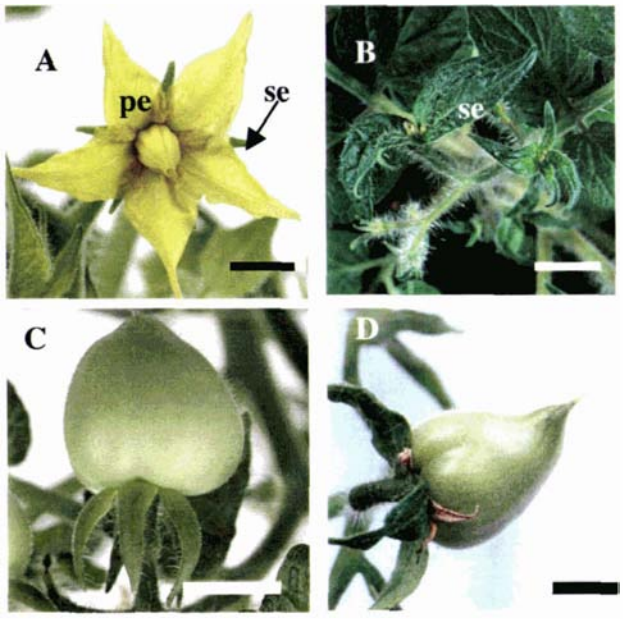

Figure 4.9. Phenotype of the aberrant T270S-15 tomato transgenic plant. **A**. Tomato wild type flower at anthesis. **B**. Transgenic flower at anthesis with sepals replaced with leaves in the first whorl. The petals and stamens were green and reduced in size. **C**. A wild type tomato fruit. **D**. Transgenic ovary developed into parthenocarpic fruit.

Bars= 2 mm. pe: petal; se: sepal

To confirm the change in identity of the transgenic sepal to leaf, scanning electron microscope (SEM) was used to examine the abaxial and adaxial surfaces of these first-whorl organs, in detail (Figures 10A, 10B). The arrangement of epidermal cells in these sepals was different from those of wild type sepals (Figures 10C, 10D). SEM revealed features such as midrib, trichomes, stomata and epidermal cell shape, normally found in tomato leaves (Figures 10E, 10F). The level of *TM10* RNA in the tomato transgenic lines was assessed by northern analysis, by probing total RNA isolated from these lines with *TM10*-specific probe. The results suggested that, unlike the other transgenic lines *TM10* RNA did not accumulate in the T270S-15 aberrant line (Figure 4.11).

4.2.10 Tobacco transformation

To further examine the functional role of *TM10*, tobacco plants were used as heterologous hosts to express the *TM10* RNA. Sixty leaf disks were inoculated with *Agrobacterium* harbouring pART270S vector. From this experiment, 18 regenerated tobacco plants were selected and rooted on kanamycin before transferring to soil in the glasshouse. In addition, seven non-transgenic tobacco plants, regenerated in tissue culture, were transferred to the glasshouse as control. Transgenic tobacco plants displayed early flowering. Flowering time was measured by number of nodes to flowering and plant height at flowering (Table 4.2). The flowers formed on the transgenic tobacco plants showed little or no change in phenotype compared to the wild type flowers.

There was increase in the growth of axillary buds, which suggests reduced apical dominance in transgenic tobacco plants. In the wild type tobacco, axillary buds below the terminal inflorescence are suppressed for most part of shoot growth, although few buds further down the stem may grow into shoots (Amaya et al., 1999). In contrast, there was increased tillering in the transgenic tobacco plants with a significant number of axillary buds actively generating leaves (Figure 4.12; Table 4.2).

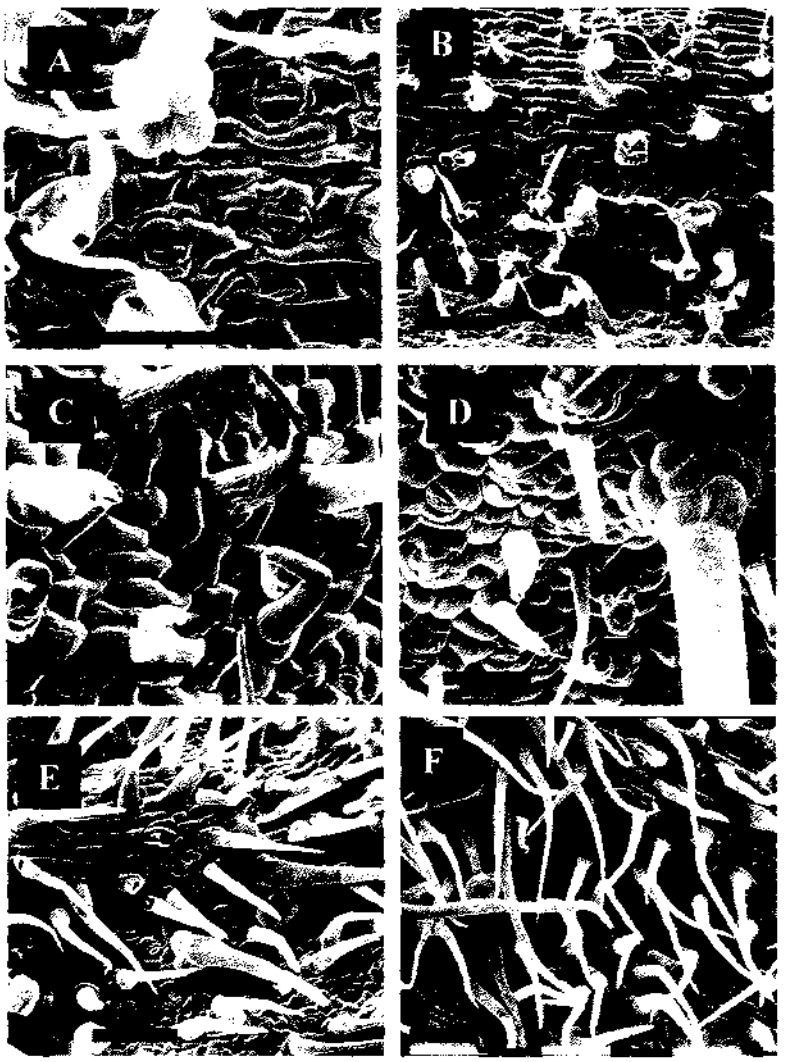

Figure 4.10. Epidermal features of aberrant *TM10* transgenic tomato sepal.

(A) SEM of adaxial surface of transgenic sepal

(B) Abaxial surface of transgenic sepal

(C) Adaxial surface of WT sepal

(D) Abaxial surface of WT sepal

(E) Adaxial surface of WT leaflet

(F) Abaxial surface of WT leaflet

Bars= 100 μm

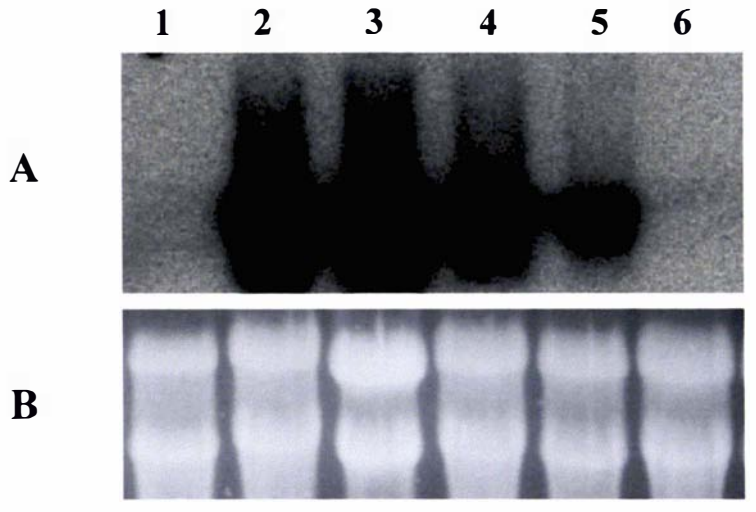

Figure 4.11. Northern analysis of TM10 RNA in tomato transgenic lines. **A**. Total RNA (20 μg) from 270S-15 (lane 1), four other transgenic plants (2-5) and wild type tomato (6) were hybridised with TM10-specific probe. **B**. Photograph of stained rRNA bands showing loading levels.

Table 4.2. Characteristics of transgenic tobacco plants of TM10

Transgenic line	Height at flowering (cm)	Number of nodes to flowering	Number of active axillary buds
Control	90 ± 2.3	31 ± 1.5	0
1	52	25	3
5	61	39	5
7	78	23	4
8	63	30	5
9	78	27	8
10	81	28	6
11	64	28	18
16	72	30	2
17	90	30	0
20	82	24	7
21	67	30	1
23	90	29	3
25	64	44	6
30	70	31	0
31	81	27	0
34	88	22	5
90	75	21	8
91	67	28	7

There was poor seed formation observed in at least two transgenic plants, TB270S-11 and TB270S-17, though, the general morphology of flowers on these transgenic plants resembled the wild type. The stamens on these flowers were normal and produced pollen. However, the carpels failed to produce seeds and later senesced like the petals and stamens. To find out whether the poor seed formation in these lines was a result of infertile pollen, wild type pollen was used to pollinate these flowers but they did not form seeds suggesting ovule sterility.

4.3 Discussion

In this chapter, degenerate PCR was used to identify tomato MADS-box genes expressed in flower and fruit and this showed there were at least 18 tomato MADS-box genes expressed in flowers and fruit. One of these, *TM10* was amplified from cDNA templates and subsequently characterised by expression and transgenic analyses.

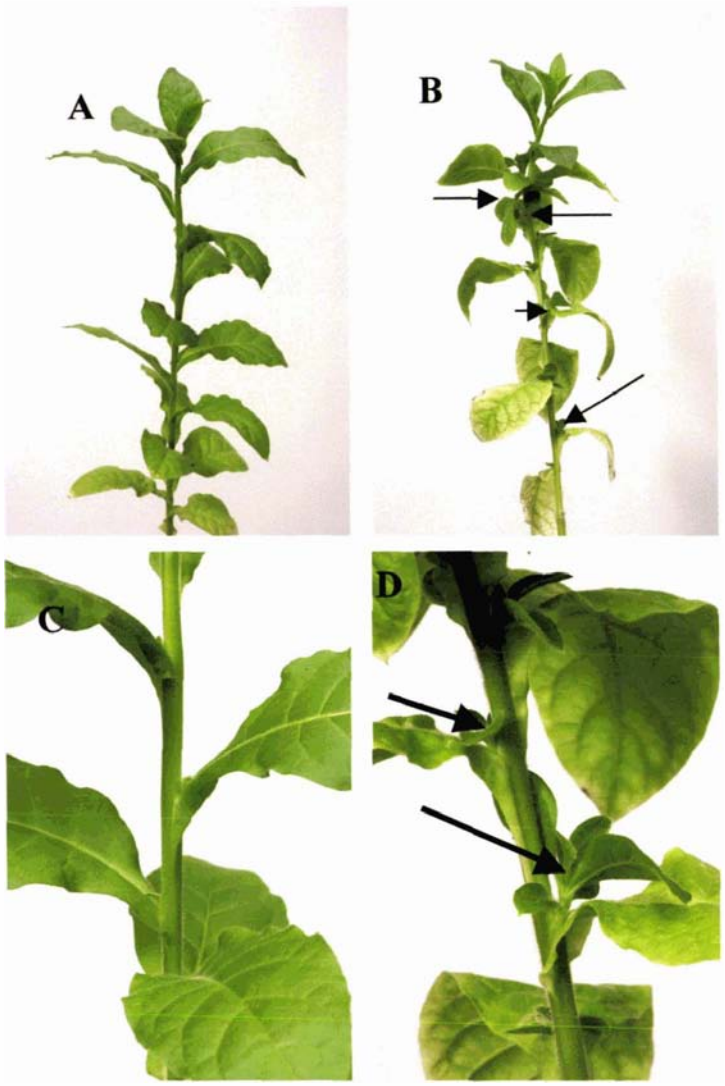

Figure 4.12. Transgenic tobacco plants displayed reduced apical dominance. **A**. In wild type tobacco, axillary buds are dormant. **B**. Transgenic tobacco plant showing actively growing axillary buds (arrowed). **C**. Close up view of plant in **A**. **D**. Close-up view of transgenic plant in **B** showing growing buds (arrowed).

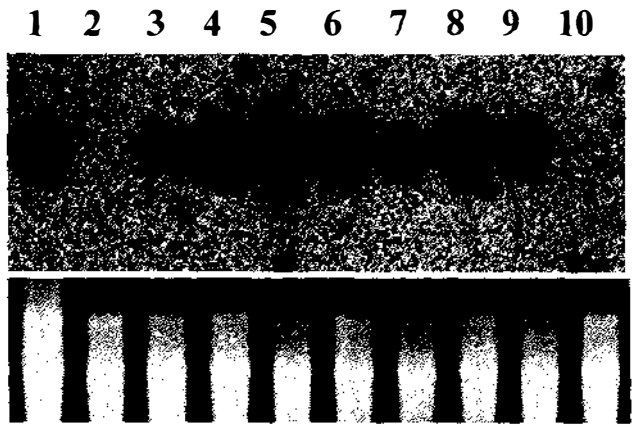

Figure 4.13. Northern analysis of *TM10* RNA in tobacco transgenic plants. Lanes 1-9 contained total RNA from tobacco transgenic plants and lane 10 contained RNA sample from non-transgenic tobacco plant. **B**. Gel photograph of stained rRNA bands showing loading levels.

4.3.1 *TM10* represents a novel tomato MADS-box gene

The analyses of nucleotide and deduced amino acid sequence of *TM10* suggested it is a homologue of the *Arabidopsis AGL12* MADS-box gene; the high sequence homology and also the similarity in amino acid composition support this observation. The amino acid sequence identity of 64% between TM10 and AGL12 is comparable to 72% identity between the tomato TAG1 protein and its *Arabidopsis* orthologue AG. Similarly 67% identity is observed between TM29 and its likely *Arabidopsis* orthologue SEP1. However, the similarity in sequence between TM10 and AGL12 is contrasted by their different expression patterns, which suggest they have different functions.

TM10 is expressed at very low levels in tomato and could not be detected by northern hybridisation. Transcriptional regulatory factors or post-transcriptional control of RNA stability may be responsible for the low level of *TM10* expression in tissues. It is possible *TM10* may require specific stimuli (exogenous or endogenous) to activate expression or that its expression is inhibited by sequence motifs that may be present in untranslated regions (UTR) (Currie and McCormick, 1997). Post-transcriptional mechanisms such as high rate of mRNA decay can also lead to low gene transcript levels (Anderson et al., 1999; Gutierrez et al., 1999; Hua et al., 2001).

To detect *TM10* mRNA, reverse transcriptase-PCR was employed. RT-PCR detected transcripts in vegetative leaves and shoots, in flower buds and fruit tissues but not in roots. In contrast, *AGL12* expression was detected in only roots (Rounsley et al., 1995). If the expression pattern is used as an indication of where the gene functions, then *TM10* functions may be directly opposite that of *AGL12*, such that *TM10* cannot be the orthologue of *AGL12*. The expression of *TM10* in the shoot tissues only is rather similar to the expression of *Arabidopsis AGL3* MADS-box gene (Huang et al., 1995). *TM10* represents a new tomato MADS-box gene whose expression is tightly regulated to yield low transcript level and may perform various functions specific to shoot development.

TM10 expression was present in floral buds when examined as a whole but RT-PCR could not detect transcript in samples from the individual floral organs. This further confirms the low expression of *TM10* in these organs. *TM10* expression was

significantly greater in ovary tissues at anthesis compared to pre-anthesis ovary. The anthesis stage in tomato corresponds with full opening of the flower followed shortly by anther dehiscence and pollination (Picken, 1984). Pollination regulates a syndrome of developmental events, such as growth and development of the ovary and ovules, which collectively prepare the flower for fertilisation (O'Neill, 1997). The significant increase in *TM10* transcript level in anthesis ovary suggests its expression is upregulated in anticipation of ovule fertilisation and subsequent fruit development.

4.3.2 *TM10* may regulate events in fruit development

In tomato, fruit development can be divided into three phases characterised by cell division (phase I), cell expansion (phase II) and fruit ripening (phase III) (Narita and Gruissem, 1989; Gillaspy et al., 1993). Anther dehiscence and pollination occur at about a day after anthesis which leads to fruit set at 2-3 d.p.a (Picken, 1984). Following fruit set, there is a rapid cell division phase of fruit growth, which lasts up to about 14 d.p.a and largely determines the number of cells in the fruit (Ho, 1984). The period of cell division is followed by a cell expansion phase characterised by cell enlargement and mainly accounts for the final fruit size (Gillaspy et al., 1993). Because *TM10* was detected in anthesis ovary and fruits of 2-21 d.p.a, this gene may regulate events prior to fruit set as well as the cell division and cell expansion stages of fruit development. As a putative transcription factor, TM10 could regulate these diverse events through interaction with other factors.

4.3.3 *TM10* causes aberrations in transgenic plants

Out of the population of transgenic tomato plants expressing sense *TM10* RNA, only one, T270S-15 displayed aberrant phenotype. Further, 478 cotyledon explants were infected with *Agrobacterium* harbouring pART270AS vector, following the procedure described above. Explants in this experiment produced callus on selection medium but had poor shoot regeneration. PCR reactions confirmed the calli as transgenic. Transgenic calli were frequently transferred to fresh shoot regeneration medium to

stimulate shoot production; however this resulted in only four (4) putative transgenic shoots, which did not show any abnormal phenotype. This difficulty in regenerating transgenic shoots was unique to the explants inoculated with pART270AS vector.

4.3.4 Cosuppression of *TM10* results in aberrant phenotype

The level of *TM10* RNA in the tomato T270S-15 line was virtually absent, though it was under the control of the constitutive 35S promoter. Other transgenic lines carrying the same construct showed high levels of *TM10* transcript. This observation suggested *TM10* has been co-suppressed in the T270S-15 line. Co-suppression is a rare occurrence and often, only a small percentage of transgenic plants display this phenomenon (Napoli *et al.*, 1990; van der Krol *et al.*, 1990).

The aberrant phenotype of T270S-15 suggests *TM10* controls sepal identity and may be required for proper development of the petals and stamens. The transgenic sepals were completely replaced by a whorl of leaf-like organs. This homeotic conversion was confirmed by scanning electron microscopy. Recently, a new class (E-function) of MADS-box genes has been identified as regulating the identity of petals, stamens and carpels in *Arabidopsis* through interaction with the B and C organ identity genes (Pelaz et al., 2000). The absence of this E-function converts the inner floral organs to sepal identity. However, no such gene has been identified to mediate the A-function of controlling sepal identity. The loss of such function will be expected to convert the sepals into leaves, the ground state of floral organs (Weigel and Meyerowitz, 1994). *TM10* may be a candidate for such function in tomato.

The cosuppression of *TM10* also caused phenotypic aberrations in the inner three whorls of the flower. The petals and stamens were reduced in size and did not abscise from the flower. The ovary developed into parthenocarpic fruit, which grew bigger than the wild type fruit. These phenotypes are consistent with the expression pattern of *TM10* and suggest *TM10* may be required for the proper development of all the floral organs. *TM10* may control fruit size through its expression during the cell division and expansion stages of tomato fruit development.

4.3.5 Ectopic expression of *TM10* caused phenotypic alterations in tobacco

TM10 overexpression in tobacco heterologous system resulted in various alterations in plant morphology. *TM10* expression promoted early flowering, reduced apical dominance and poor seed development in transgenic tobacco lines. Though the mechanisms by which *TM10* affected these traits in tobacco are unknown, these suggest that *TM10* may be involved in similar pathways in tomato (Chung *et al.*, 1994; Kang *et al.*, 1995).

The early flowering of tobacco transgenic lines suggests that *TM10* product could have induced the expression of genes involved in floral induction. In *Arabidopsis*, the transition to flowering is controlled in at least four pathways (Levy and Dean, 1998; Pineiro and Coupland, 1998). Flowering in tobacco may be controlled by similar set of genes as in *Arabidopsis* (Kempin et al., 1993; Kelly et al., 1995). Similarly, *TM10* may have an effect on the pathways controlling apical dominance. Apical dominance in tobacco can be associated with specific levels of endogenous hormones. Elevated levels of cytokinins or reduced auxin levels result in increased axillary bud growth (Romano et al., 1991; Sano et al., 1994; McKenzie et al., 1998; Eklof *et al.*, 2000). Conversely, low levels of cytokinins or high auxin levels promote apical dominance (Harrison and Kaufmann, 1984; Romano et al., 1991). The poor seed development in the transgenic plants as a result of sterile ovules indicates *TM10* effect on ovule development. The *TM10* product may have resulted in the negative regulation of factors required for proper seed development in tobacco. The sterile transgenic ovules may be due to embryo sac degeneration, abnormal ovule integument development or aberrant differentiation of the megagametophyte (Ray *et al.*, 1994; Western and Haughn, 1999). *TM10* RNA or product may have disrupted the genetic pathway for normal ovule development.

TM10 is a tomato MADS-box gene with high homology to the *AGL12* of *Arabidopsis*. *TM10*, however, has a different expression pattern to what is known for *AGL12*, suggesting these two genes have different functions. The expression analysis and the phenotypes of the transgenic plants generated with *TM10* indicate it may regulate events in flower and fruit development.

CHAPTER 5 General Discussion

Over the last decade, plant MADS-box genes have been studied extensively to reveal their control of floral development and by virtue of these roles in flower development, including the carpel and ovule, they are strong candidates for regulating fruit development. This research was aimed at identifying the role of MADS-box genes in flower and fruit development. The approach used in this study was to identify new members of the tomato MADS-box family, which are expressed in flower and fruit, to characterise these genes using molecular techniques and to examine their functions using genetic methods. Tomato was chosen as a model crop, for this project, because it produces a berry fruit and has a good system to study fruit development, unlike the silique produced by *Arabidopsis*, which is a good model of the Brassicaceae.

Two previously uncharacterised tomato MADS-box genes were obtained. *TM29* was isolated from a young fruit cDNA library by screening with homologous MADS-box fragments and degenerate PCR was used to identify *TM10*, which was subsequently isolated using 3'-RACE PCR. For functional annotation of genes, sequences were first analysed. This is based on the general assumption that genes with same sequence structures may have similar functional properties. Sequence homology searches, phylogenetic analysis, protein composition and structure identified homologous genes whose functions were known. In addition, northern hybridisation, reverse transcriptase PCR and *in situ* hybridisation techniques were used to define the temporal and spatial gene expression to give indications of where the genes function.

Despite the valuable information that accrues from analysing gene sequence and expression patterns, it is only through functional analyses that the role of a gene can be established with certainty. The primary strategy for studying gene function has been forward genetics, which begins with a mutant phenotype and screens for the loss-of-function mutations (Martin, 1998; Krysan *et al.*, 1999). However, this strategy rarely

identify genes that act redundantly or whose loss of function do not result in remarkable phenotype. Reverse genetics on the other hand, begins with a gene sequence and determines its loss-of-function phenotype. The recent availability of genome sequences has created opportunities for reverse genetic tools, such as activation tagging which randomly activate the expression of genes (Weigel *et al.*, 2000) and insertional mutagenesis, which disrupt gene expression through inserting T-DNA or transposons (Krysan *et al.*, 1999). Alternatively, transgenic techniques allow plant genes to be overexpressed by using cDNA fragments linked to strong promoters or silenced through antisense and cossupression phenomena (Napoli *et al.*, 1990; van der Krol *et al.*, 1990). Though, the effectiveness of the transgenic techniques are variable and not controllable, they are particularly versatile and have been widely used to study gene functions (Mizukami and Ma, 1992; Pneuli *et al.*, 1994ab; Angenent *et al.*, 1995). In this project, the transgenic methods were used to overexpress or to reduce the level of gene transcripts in tomato. In addition, tobacco was employed as a heterologous host to overexpress the MADS-box genes. The use of heterologous host provides indications of gene functions, which may be silent in the original host due to functional redundancy (Kang *et al.*, 1995).

Overall, the functional implications from the transgenic phenotypes generated from these transformations were consistent with the inferences drawn from their sequence and expression patterns.

Summary of findings

Tomato MADS-box 29

TM29 cDNA is 1.2-kb long and has an open reading frame of 738 nucleotides encoding 246 amino acids. The conceptual TM29 protein has a molecular weight of 28 kilodaltons (kDa) and isoelectric pH (PI) of 8.28. Sequence similarities and phylogenetic relationships suggested *TM29* is a homologue of *Arabidopsis SEP1* gene.

TM29 expression in vegetative, inflorescence and floral meristems suggested its role in the development of the various tissues formed from these cells. This observation was in contrast to *SEP1*, expressed only in floral meristems (Flanagan and Ma, 1994).

The pattern of *TM29* expression in floral organ primordia, which is high during early stages of organ primordium and diminishes as the organ matures, indicates the gene controls events in the early stages of floral organ development. *TM29* expression in the stamens and ovary was suggestive of its role in reproductive development. Unlike in the mature perianth organs (sepals and petals) where *TM29* expression was barely detected, *TM29* transcripts localised to the tapetal region of the stamen and the pericarp region of the ovary. Such expression pattern indicates that *TM29* might be involved in controlling the development of these reproductive tissues. In the fruit, *TM29* is expressed in the pericarp, the placenta and in the seeds.

The temporal and spatial expression of *TM29* in the floral organs was in agreement with the phenotypes caused by reduced *TM29* RNA in tomato transgenic plants. Transgenic plants produced bigger floral organs and the inner three organs developed characteristics typical of sepals: green, presence of stomata, delayed senescence and no abscission. *TM29* function in the reproductive organs was observed in the aberrant stamens and ovary. The transgenic stamens did not produce pollen indicating that *TM29* expression in the tapetum may be required for the proper development of anthers.

Another abnormality observed in the transgenic stamens was poor interweaving among the lateral and adaxial hairs causing the dialytic phenotype, which further pointed to *TM29* role in the morphogenetic development of the floral organs.

The significant number of transgenic flowers that produced parthenocarpic fruits indicated *TM29* role in fruit development, suggesting it might be a genetic repressor of parthenocarpic fruit development in wild type tomato. Fruit ripening was delayed in the transgenic plants indicating that *TM29* may regulate events in fruit ripening.

The transgenic fruit displayed indeterminate growth, characterised by the emergence of ectopic shoots with leaves and flowers. This phenotype suggested that *TM29* controls determinate growth of the tomato flower and may be required to prevent reversion to vegetative shoot growth in the flower. The wild type tomato fruit is a determinate organ, which undergoes ripening after reaching the matured stage (Gillaspy *et al.*, 1993).

In the tobacco heterologous system, *TM29* promoted sympodial growth, early flowering and reduced apical dominance in tobacco. Though, such effects were not obvious in the tomato transgenic plants, it is possible that in tomato *TM29* regulates these traits redundantly with other genes.

Tomato MADS-box 10

The *Tomato MADS-box 10* (*TM10*) has an open reading frame of 603 basepairs encoding 201 amino acids. The predicted protein has a molecular weight of 22.9 kDa and PI of 6.5. Sequence analyses suggested *TM10* might be a homologue of Arabidopsis *AGL12*. Comparatively, AGL12 has a molecular weight of 23.7 kDa and PI of 6.7.

TM10 was expressed at very low levels in tomato tissues and was detected by RT-PCR. Such low transcript level may be due to a tight regulation of its expression. Nonetheless, *TM10* expression was found to be specific to the shoot tissues of tomato contrasting sharply with *AGL12* whose transcripts were detected in roots only (Rounsley et al., 1995). Thus *TM10* may have different functions in tomato from *AGL12* in *Arabidopsis*. The expression of *TM10* suggests it is specific to shoot development. *TM10* transcript

was relatively high in anthesis ovary and in fruits of different stages indicating it may function in fruit development.

The *TM10* cosuppressed line displayed aberrant phenotype in flowers and fruit. There was homeotic conversion of sepals to leaves. The petals and stamens were poorly developed and the ovary formed parthenocarpic fruit suggesting *TM10* might control the proper development of floral organs and fruit. The expression of *TM10* in heterologous tobacco plants also resulted in reduced apical dominance and promoted flowering.

Conclusions

The characteristics of the two tomato MADS-box genes described in this thesis suggested their involvement in important aspects of flower and fruit development, which could be useful in fruit improvement programmes. Floral organ development has significant effect on fruit development. In *Arabidopsis*, the presence of the other floral organs on the flower is believed to inhibit fruit development through inter-organ communication (Vivian-Smith *et al.*, 2001). Secondly, floral organs influence the allocation of nutritive resource to developing fruits. The poor development or senescence of floral organs may contribute to fruit growth through redirection of resources. The effects of *TM29* and *TM10* on floral organs can therefore be utilised to modify the growth of floral organs to enhance fruit development.

Parthenocarpic fruit development is a desirable trait in most fruit types and has great value, for instance in crops such as grapes, banana and pineapple. The effects of *TM29* and *TM10* suggest they could be meaningfully employed to introduce this trait in important crop plants. Their effect on ripening can be utilised to manipulate fruit ripening process so as to enhance shelf life and quality. Taken together, these two genes

and their homologues in other important plant species offer the potential to improve on the useful traits mentioned above.

The findings of thesis can be further investigated. The use of techniques such as yeast-2-hybrid screening of tomato libraries can identify other genes that interact with these MADS-box genes and help explain their mode of functions. The use of cDNA microarray technique would allow gene expression to be assessed at the genome level in transgenic plants to provide a genome-wide picture of other genes that may have contributed to the phenotypes observed. Thirdly, the phenotypes of the transgenic plants, such as organ maturation and fruit ripening, suggest the involvement of hormones such as ethylene and this could be further investigated.

BIBLIOGRAPHY

Acton, T., Mead, J., Steiner, A., Vershon, A. (2000). Scanning mutagenesis of Mcm1: Residues required for DNA binding, DNA bending, and transcriptional activation by a MADS-box protein. *Molecular and Cellular Biology* 20: 1-11

Allen, K.D., Sussex, I.M. (1996). Falsiflora and anantha control early stages of floral meristem development in tomato (Lycopersicon esculentum Mill.). *Planta* 200: 254-264

Alonso, J., Chamarro, J., Granell, A. (1995). Evidence for the involvement of ethylene in the expression of specific RNAs during maturation of the orange, a non-climacteric fruit. *Plant Molecular Biology* 29: 385-390

Altschul, S.F., Madden, T.L., Schäffer, A.A., Zhang, J., Zhang, Z., Miller, W., Lipman, D.J. (1997). Gapped BLAST and PSI-BLAST: a new generation of protein database search programs. *Nucleic Acids Research* 25: 3389-3402

Alvarez-Buylla, E., Liljegren, S.J., Pelaz, S., Gold, S., Burgeff, C., Ditta, G., Vergara-Silva, F., Yanofsky, M.F. (2000a). MADS-box gene evolution beyond flowers: expression in pollen, endosperm, guard cells, roots and trichomes. *Plant Journal* 24: 457-466

Alvarez-Buylla, E., Pelaz, S., Liljegren, S., Gold, S., Burgeff, C., Ditta, G., Pouplana, L., Martinez-Castilla, L., Yanofsky, M. (2000b). An ancestral MADS-box gene duplication occurred before the divergence of plants and animals. *Proceedings of the National Academy of Sciences of the United States of America* 97: 5328-5333

Amaya, I., Ratcliffe, O., Bradley, D. (1999). Expression of CENTRORADIALIS (CEN) and CEN-like genes in tobacco reveals a conserved mechanism controlling phase change in diverse species. *Plant Cell* 11: 1405-1417

Ambrose, B., Lerner, D., Ciceri, P., Padilla, M., Yanfosky, M.F., Schmidt, R. (2000). Molecular and genetic analyses of the *Silky1* gene reveal conservation in floral organ specification between eudicots and monocots. *Molecular Cell* 5: 569-579

Anderson, M., Folta, K., Warpeha, K., Gibbons, J., Gao, J., Kaufman, L. (1999). Blue light-directed destabilization of the pea *Lhcb1*4* transcript depends on sequences within the 5' untranslated region. *Plant Cell* 11: 1579-1589

Angenent, G., Franken, J., Busscher, M., Van Dijken, A., Van Went, J., Dons, H., Van Tunen, A. (1995). A novel class of MADS box genes is involved in ovule development in Petunia. *Plant Cell* 7: 1569-1582

Angenent, G.C., Busscher, M., Franken, J., Mol, J., van Tunen, A.J. (1992). Differential expression of two MADS box genes in wild type and mutant petunia flowers. *Plant Cell* 4: 983-993

Angenent, G.C., Franken, J., Busscher, M., Weiss, D., van Tunen, A.J. (1994). Co-suppression of the petunia homeotic gene fbp2 affects the identity of the generative meristem. *Plant Journal* 5: 33-44

Araki, T. (2001). Transition from vegetative to reproductive phase. *Current Opinion in Plant Biology* 4: 63-68

Atkinson, R., Bieleski, L., Gleave, A., Janssen, B.-J., Morris, B. (1998). Post-transcriptional silencing of chalcone synthase in petunia using a geminivirus-based episomal vector. *Plant Journal* 15: 593-604

Avivi, Y., Lev-Yadun, S., Morozova, N., Libs, L., Williams, L., Zhao, J., Varghese, G., Grafi, G. (2000). *Clausa*, a tomato mutant with a wide range of phenotypic perturbations, displays a cell type-dependent expression of the homeobox gene *LeT6/TKn2*. *Plant Physiology* 124: 541-551

Aznar, M., Almela, V., Juan, M., El-Otmani, M., Agusti, M. (1995). Effect of the synthetic auxin phenothiol on fruit development of 'Fortune' mandarin. *Journal of Horticultural Science* 70: 617-621

Baulcombe, D. (1996). RNA as a target and an initiator of post-transcriptional gene silencing in transgenic plants. *Plant Molecular Biology* 32: 79-88

Baum, D. (1998). The evolution of plant development. *Current Opinion in Plant Biology* 1: 79-86

Becker, A., Winter, K.-U., Meyer, B., Saedler, H., TheiBen, G. (2000). MADS-box gene diversity in seed plants 300 million years ago. *Molecular Biology and Evolution* 17: 1425-1434

Blazquez, M. (2000). Flower development pathways. *Journal of Cell Science* 113: 3547-3548

Blazquez, M., Green, R., Nilsson, O., Sussman, M., Weigel, D. (1998). Gibberellins promote flowering of *Arabidopsis* by activating the *LEAFY* promoter. *Plant Cell* 10: 791-800

Bollard, E. (1970). The physiology and nutrition of developing fruits. In *The biochemistry of fruits and their products*, ed. Hulme, A., pp. 387-425. London, New York: Academic Press

Bonhomme, F., Kurz, B., Melzer, S., Bernier, G., Jacqmard, A. (2000). Cytokinin and gibberellin activate *SaMADS A*, a gene apparently involved in regulation of the floral transition in *Sinapsis alba*. *Plant Journal* 24: 103-111

Borner, R., Kampmann, G., Chandler, J., GleiBner, R., Wisman, E., Apel, K., Melzer, S. (2000). A MADS domain gene involved in the transition to flowering in *Arabidopsis*. *Plant Journal* 24: 591-599

Bowman, J.L., Alvarez, J., Weigel, D., Meyerowitz, E.M., Smyth, D.R. (1993). Control of flower development in Arabidopsis thaliana by APETALA1 and interacting genes. *Development* 119: 721-743

Bowman, J.L., Smyth, D.R., Meyerowitz, E.M. (1991). Genetic interactions among floral homeotic genes of Arabidopsis. *Development* 112: 1-20

Bradley, D., Carpenter, R., Sommer, H., Hartley, N., Coen, E. (1993). Complementary floral homeotic phenotypes result from opposite orientations of a transposon at the *plena* locus of Antirrhinum. *Cell* 72: 85-95

Brady, C., McGlasson, B., Speirs, J. (1987). The Biochemistry of fruit ripening. In *Tomato Biotechnology*, ed. Nevins, D., Jones, R., pp. 279-288. New York: Alan R. Liss, Inc.

Brummell, D., Harpster, M., Dunsmuir, P. (1999). Differential expression of expansin gene family members during growth and ripening of tomato fruit. *Plant Molecular Biology* 39: 161-169

Buchner, P., Boutin, J.-P. (1998). A MADS box transcription factor of the AP1/AGL9 subfamily is also expressed in the seed coat of pea (*Pisum sativum*) during development. *Plant Molecular Biology* 38: 1253-1255

Bunger-Kibler, S., Bangerth, F. (1983). Relationship between cell number, cell size and fruit size of seeded fruits of tomato (*Lycopersicon esculentum* Mill.), and those induced parthenocarpically by the application of plant growth regulators. *Plant Growth Regulation* 1: 143-154

Cano-Medrano, R., Darnell, R. (1997). Cell number and cell size in parthenocarpic *vs* pollinated blueberry (*Vaccinium ashei*) fruits. *Annals of Botany* 80: 419-425

Caporali, E., Spada, A., Losa, A., Marziani, G. (2000). The MADS bos gene *AOM1* is expressed in reproductive meristems and flowers of the dioecious species *Asparagus officinalis*. *Sexual Plant Reproduction* 13: 151-156

Carmona, M., Ortega, N., Garcia-Maroto, F. (1998). Isolation and molecular characterisation of a new vegetative MADS-box gene from *Solanum tuberosum* L. *Planta* 207: 181-188

Chung, Y.-Y., Kim, S.-R., Finkel, D., Yanofsky, M., An, G. (1994). Early flowering and reduced apical dominance result from ectopic expression of a rice MADS box gene. *Plant Molecular Biology* 26: 657-665

Church, G.M., Gilbert, W. (1984). Genomic sequencing. *Proceedings of the National Academy of Sciences of the United States of America* 81: 1991-1995

Clark, S.E., Runnung, M.P., Meyerowitz, E.M. (1993). CLAVATA1, a regulator of meristem and flower development in Arabidopsis. *Development* 119: 397-418

Coen, E., Meyerowitz, E. (1991). The war of the whorls: genetic interactions controlling flower development. *Nature* 353: 31-37

Coen, E.S., Romero, J.M., Doyle, S., Elliot, R., Murphy, G., Carpenter, R. (1990).

floricaula: A homeotic gene required for flower development in Antirrhinum majus. *Cell* 63: 1311-1322

Colombo, L., Franken, J., Koetje, E., van Went, J., Dons, H., Angenent, G.C., van Tunen, A.J. (1995). The petunia MADS box gene *FBP11* determines ovule identity. *Plant Cell* 7: 1859-1868

Colombo, L., Franken, J., Van der Krol, A., Wittich, P., Dons, H., Angenent, G. (1997). Downregulation of ovule-specific MADS box genes from Petunia results in maternally controlled defects in seed development. *Plant Cell* 9: 703-715

Curie, C., McCormick, S. (1997). A strong inhibitor of gene expression in the 5' untranslated region of the pollen-specific *LAT59* gene of tomato. *Plant Cell* 9: 2025-2036

Davies, B., Eagea-Cortines, M., de Andrade, S., Saedler, H., Sommer, H. (1996). Multiple interactions amongst floral homeotic proteins. *EMBO Journal* 15: 4330-4343

Davies, B., Motte, P., Keck, E., Saedler, H., Sommer, H., Schwarz-Sommer, Z. (1999). *PLENA* and *FARINELLI*: redundancy and regulatory interactions between two *Antirrhinum* MADS-box factors controlling flower development. *EMBO Journal* 18: 4023-4034

Dellaporta, S., Calderon-Urrea, A. (1994). The sex determination process in maize. *Science* 266: 1504

Delmas, V., Stokes, D., Perry, R. (1993). A mammalian DNA-binding protein that contains a chromodomain and an SNF2/SWI2-like helicase domain. *Proceedings of the National Academy of Sciences of the United States of America* 90: 2414-2418

Doyle, J.J., Doyle, J.L. (1990). Isolation of plant DNA from fresh tissue. *Focus* 12: 13-15

Doyle, K., ed. 1996. *Promega protocols and application guide*. USA: Promega Corporation

Drews, G.N., Bowman, J.L., Meyerowitz, E.M. (1991). Negative regulation of the Arabidopsis homeotic gene *AGAMOUS* by the *APETALA2* product. *Cell* 65: 991-1002

Eagea-Cortines, M., Saedler, H., Sommer, H. (1999). Ternary complex formation between the MADS-box proteins SQUAMOSA, DEFICIENS and GLOBOSA is involved in the control of floral architecture in *Antirrhinum majus*. *EMBO Journal* 18: 5378-5379

Eklof, S., Astot, C., Sitbon, F., Moritz, T., Olsson, O., Sandberg, G. (2000). Transgenic tobacco plants co-expressing *Agrobacterium iaa* genes have wild type hormone levels but display both auxin- and cytokinin-overproducing phenotypes. *Plant Journal* 23: 279-284

Fan, H.-Y., Tudor, M., Ma, H. (1997). Specific interactions between the K domains of AG and AGLs, members of the MADS domain family of DNA binding proteins. *Plant Journal* 12: 999-1010

Feng, D., Doolittle, R. (1987). Progressive sequence alignment as a prerequisite to correct phylogenetic trees. *Journal of Molecular Evolution* 25: 351-360

Ferrandiz, C., Liljegren, S.J., Yanfosky, M.F. (2000). Negative regulation of the *SHATTERPROOF* genes by *FRUITFULL* during Arabidopsis fruit development. *Science* 289: 436-438

Ferrandiz, C., Pelaz, S., Yanofsky, M. (1999). Control of carpel and fruit development in Arabidopsis. *Annual Review of Biochemistry* 68: 321-354

Ferrario, S., Busscher, J., Franken, J., Angenent, G. 2000. A novel MADS box gene from petunia confers leaf-like features to floral organs. Presented at 6TH International Congress of Plant Molecular Biology, Quebec Canada

Ficcadenti, N., Sestili, S., Pandolfini, T., Cirillo, C., Rotino, G., Spena, A. (1999). Genetic engineering of parthenocarpic fruit development in tomato. *molecular Breeding* 5: 463-470

Fillati, J., Kiser, J., Rose, R., Comai, L. (1987). Efficient transfer of a glyphosate tolerance gene into tomato using a binary *Agrobacterium tumefaciens* vector. *Biotechnology* 5: 726-730

Flanagan, C., Hu, Y., Ma, H. (1996). Specific expression of the AGL1 MADS-box

gene suggests regulatory functions in Arabidopsis gynoecium and ovule development. *Plant Journal* 10: 343-353

Flanagan, C., Ma, H. (1994). Spatially and temporally regulated expression of the MADS-box gene AGL2 in wild-type and mutant Arabidopsis flowers. *Plant Molecular Biology* 26: 581-595

Fos, M., Garcia-Martinez, J. (2000). The *pat-2* gene, which induces natural parthenocarpy, alters gibberellin content in unpollinated tomato ovaries. *Plant Physiology* 122: 471-479

Fos, M., Proano, K., Nuez, F., Garcia-Martinez, J. (2001). Role of gibberellins in parthenocarpic fruit development induced by the genetic system *pat-3/pat-4* in tomato. *Physiologia Plantarum* 111: 545-550

Gandar, P., Hall, A., de Silva, H. (1996). Deterministic models for fruit growth. *Acta Horticulturae* 416: 103-112

Garcia-Maroto, F., Ortega, N., Lozano, R., Carmona, M.-J. (2000). Characterisation of the potato MADS-box gene *STMADS16* and expression analysis in tobacco transgenic plants. *Plant Molecular Biology* 42: 499-513

Gaudin, V., Vrain, T., Jouanin, L. (1994). Bacterial genes modifying hormonal balances in plants. *Plant Physiology and Biochemistry* 32: 11-29

Gillaspy, G., Ben-David, H., Gruissem, W. (1993). Fruits: a developmental perspective. *Plant Cell* 5: 1439-1451

Giovannoni, J. (2001). Molecular Biology of fruit maturation and ripening. *Annual Review of Plant Biology and Plant Molecular Biology* 52: 725-749

Gleave, A. (1992). A versatile binary vector system with a T-DNA organisational structure conducive to efficient integration of cloned DNA into the plant genome. *Plant Molecular Biology* 20: 1203-1207

Goffinet, M., Robinson, T., Lakso, A. (1995). A comparison of 'empire' apple fruit size and anatomy in unthinned and hand-thinned trees. *Journal of Horticultural Science* 70: 375-387

Gonzalez-Bosch, C., Brummell, D., Bennett, A. (1996). Differential expression of two endo-1,4-B-glucanase genes in pericarp and locules of wild type and mutant tomato fruit. *Plant Physiology* 111: 1313-1319

Goto, K., Meyerowitz, E.M. (1994). Function and regulation of the *Arabidopsis* floral homeotic gene *PISTILLATA*. *Genes and Development* 8: 1548-1560

Gray, J., Picton, S., Shabbeer, J., Schuch, W., Grierson, D. (1992). Molecular biology of fruit ripening and its manipulation with antisense genes. *Plant Molecular Biology* 19: 69-87

Grierson, D., Kader, A. (1986). Fruit ripening and quality. In *The Tomato Crop: A scientific basis for improvement*, ed. Atherton, J., Rudich, J., pp. 241-280. London: Chapman & Hall

Gu, Q., Ferrandiz, C., Yanofsky, M., MArtienssen (1998). The *FRUITFULL* MADS-box gene mediates cell differentiation during *Arabidopsis* fruit development. *Development* 125: 1509-1517

Gustafson, F. (1960). Influence of gibberellic acid on setting and development of fruits in tomato. *Plant Physiology* 35: 521-523

Gutierrez, R., MacIntosh, G., Green, P. (1999). Current perspectives on mRNA stability in plants: multiple levels and mechanisms of control. *Trends in Plant Science* 4: 429-438

Hadidi, A., Yang, X. (1990). Detection of pome fruit viroids by enzymatic cDNA amplification. *Journal of Virological Methods* 30: 261-270

Hareven, D., Gutfinger, T., Pneuli, L., Bauch, L., Cohen, O., Lifschitz, E. (1994). The floral system of tomato. *Euphytica* 79: 235-243

Harrison, M., Kaufman, P. (1984). The role of hormone transport and metabolism in apical dominance in oats. *Botanical Gazette* 145: 293-297

Hartmann, U., Hohmann, S., Nettesheim, K., Wisman, E., Saedler, H., Huijser, P. (2000). Molecular cloning of SVP: a negative regulator of the floral transition in *Arabidopsis*. *Plant Journal* 21: 351-360

Hasebe, M., Wen, C.-K., Kato, M., Banks, J. (1998). Characterisation of MADS homeotic genes in the fern *Ceratopteris richardii*. *Proceedings of the National Academy of Sciences of the United States of America* 95: 6222-6227

Heck, G., Perry, S., Nichols, K., Fernandez, D. (1995). AGL15, a MADS domain protein expressed in developing embryos. *Plant Cell* 7: 1271-1282

Hempel, F.D., Welch, D.R., Feldman, L.J. (2000). Floral induction and determination: where is flowering controlled? *Trends in Plant Science* 5: 17-21

Hill, J., Lord, E. (1988). Floral development in *Arabidopsis thaliana*: a comparison of the wild type and the homeotic pistillata mutant. *Canadian Journal of Botany* 67: 2922-2936

Ho, L., Hewitt, J. (1986). Fruit Development. In *The tomato crop*, ed. Atherton, J., Rudich, J., pp. 201-239. London: Chapmann and Hall

Honma, T., Goto, K. (2001). Complexes of MADS-box proteins are sufficient to convert leaves into floral organs. *Nature* 409: 525-529

Hua, X., van de Cotte, B., Montagu, M., Verbruggen, N. (2001). The 5' untranslated region of the *At-P5R* gene is involved in both transcriptional and post-transcriptional regulation. *Plant Journal* 26: 157-169

Huang, H., Mizukami, Y., Hu, Y., Ma, H. (1993). Isolation and characterization of the binding sequences for the product of the Arabidopsis floral homeotic gene AGAMOUS. *Nucleic Acids Research* 21: 4769-4776

Huang, H., Tudor, M., Su, T., Zhang, Y., Hu, Y., Ma, H. (1996). DNA binding properties of two *Arabidopsis* MADS domain proteins: binding consensus and dimer formation. *Plant Cell* 8: 81-94

Huang, H., Tudor, M., Weiss, C., Hu, Y., Ma, H. (1995). The *Arabidopsis* MADS-box gene *AGL3* is widely expressed and encodes a sequence-specific DNA-binding protein. *Plant Molecular Biology* 28: 549-567

Huang, K., Louis, J., Donaldson, L., Lim, F.-L., Sharrocks, A., Clore, G. (2000). Solution structure of the MEF2A-DNA complex: structural basis for the modulation of

DNA bending and specificity by MADS-box transcription factors. *EMBO Journal* 19: 2615-2628

Huijser, P., Klein, J., Lonnig, W.E., Meijer, H., Saedler, H., Sommer, H. (1992). Bracteomania, an inflorescence anomaly, is caused by the loss of the MADS-box gene *squamosa* in *Antirrhinum majus*. *EMBO Journal* 11: 1239-1249

Immink, R., Hannapel, D., Ferrario, S., Busscher, M., Franken, J., Campagne, L., Angenent, G. (1999). A Petunia MADS box gene involved in the transition from vegetative to reproductive development. *Development* 126: 5117-5126

Ingram, G., Doyle, S., Carpenter, R., Schultz, E., Simon, R., Coen, E. (1997). Dual role for *fimbriata* in regulating floral homeotic genes and cell division in *Antirrhinum*. *EMBO Journal* 16: 6521-6534

Irish, E. (1996). Regulation of sex determination in maize. *BioEssays* 18: 363-369

Irish, V., Sussex, I.M. (1990). Function of the apetala-1 gene during *Arabidopsis* floral development. *Plant Cell* 2: 741-753

Ishida, B., Jenkins, S., Say, B. (1998). Induction of *AGAMOUS* gene expression plays a key role in ripening of tomato sepals *in vitro*. *Plant Molecular Biology* 36: 733-739

Itai, A., Tanabe, K., Tamura, F., Tanaka, T. (2000). Isolation of cDNA clones corresponding to genes expressed during fruit ripening in Japanese pear (*Pyrus pyrifolia* Nakai): involvement of the ethylene signal transduction pathway in their expression. *Journal of Experimental Botany* 51: 1163-166

Jack, T. (2001a). Plant development going MADS. *Plant Molecular Biology* 46: 515-520

Jack, T. (2001b). Relearning our ABCs: new twists on an old model. *Trends in Plant Science* 6: 310-316

Jack, T., Brockman, L.L., Meyerowitz, E.M. (1992). The homeotic gene *APETALA3* of Arabidopsis thaliana encodes a MADS box and is expressed in petals and stamens. *Cell* 68: 683-697

Jack, T., Fox, G.L., Meyerowitz, E.M. (1994). Arabidopsis homeotic gene *APETALA3* ectopic expression: transcriptional and posttranscriptional regulation determine floral organ identity. *Cell* 76: 703-716

Jackson, D. (1992). *In situ* hybridisation in plants. In *Molecular Plant Pathology: a practical approach*, ed. Gurr, S., McPherson, M., Bowles, D., pp. 163-174. Great Britain: IRL Press

Janssen, B.-J., Lund, L., Sinha, N. (1998). Overexpression of a homeobox gene, *LeT6*, reveals indeterminate features in the tomato compound leaf. *Plant Physiology* 117: 771-786

Jofuku, K.D., den Boer, B.G., Van Montagu, M., Okamuro, J.K. (1994). Control of *Arabidopsis* flower and seed development by the homeotic gene of *APETALA2*. *Plant Cell* 6: 1211-1225

Jones, D. (1999). Protein secondary structure prediction based on position-specific scoring matrices. *Journal of Molecular Biology* 292: 195-202

Kagan-Zur, V., Livne, D., Mizrahi, Y. (1992). Analysis of effects of auxin on fruit size of tetraploid and diploid tomato fruits. *Journal of Horticultural Science* 67: 817-825

Kang, H., An, G. (1997). Isolation and characterization of a rice MADS box gene belonging to the AGL2 gene family. *Molecular Cells* 7: 45-51

Kang, H., Jang, S., Chung, J., Cho, Y., An, G. (1997). Characterization of two rice MADS box genes that control flowering time. *Molecular Cells* 7: 559-566

Kang, H.-G., Noh, Y.-S., Chung, Y.-Y., Costa, M., An, K., An, G. (1995). Phenotypic alterations of petal and sepal by ectopic expression of a rice MADS box gene in tobacco. *Plant Molecular Biology* 29: 1-10

Kater, M., Colombo, L., Franken, J., Busscher, M., Masiero, S., Campagne, M.-L., Angenent, G. (1998). Multiple *AGAMOUS* homologs from Cucumber and Petunia differ in their ability to induce reproductive organ fate. *Plant Cell* 10: 171-182

Kawaguchi, M., Kobayashi, M., Sakurai, A., Syono, K. (1991). The presence of an

enzyme that converts indole-3-acetamide into IAA in wild and cultivated rice. *Plant Cell Physiology* 32: 143-149

Kelly, A., Bonnlander, M., Meeks-Wagner, D. (1995). NFL, the tobacco homolog of FLORICAULA and LEAFY, is transcriptionally expressed in both vegetative and floral meristems. *Plant Cell* 7: 225-234

Kempin, S., Mandel, M., Yanofsky, M. (1993). Conversion of perianth into reproductive organs by ectopic expression of the tobacco floral homeotic gene *NAG1*. *Plant Physiology* 103: 1041-1046

Kempin, S.A., Savidge, B., Yanofsky, M.F. (1995). Molecular basis of the *cauliflower* phenotype in *Arabidopsis*. *Science* 267: 522-525

Kim, Y.-S., Lee, H.-S., Lee, M.-H., Yoo, O.-J., Liu, J.-R. (1998). A MADS box gene homologous to *AG* is expressed in seedlings as well as in flowers of *Ginseng*. *Plant Cell Physiology* 39: 836-845

Kimura, M. (1983) *The neutral theory of evolution*. Cambridge: Cambridge University Press.

Kotilainen, M., Elomaa, P., Uimari, A., Albert, V.A., Deyue, Y., Teeri, T.H. (2000). *GRCD1*, an *AGL2*-like MADS Box gene, participates in the C function during stamen development in *Gerbera hybrida*. *Plant Cell* 12: 1893-1902

Kramer, E., Dorit, R., Irish, V. (1998). Molecular evolution of genes controlling petal and stamen development: duplication and divergence within the *APETALA3* and *PISTILLATA* MADS-box gene lineages. *Genetics* 149: 765-783

Kramer, E., Irish, V. (1999). Evolution of genetic mechanisms controlling petal development. *Nature* 399: 144-148

Krizek, B., Meyerowitz, E. (1996). Mapping the protein regions responsible for the functional specificities of the *Arabidopsis* MADS domain organ identity proteins. *Proceedings of the National Academy of Sciences of the United States of America* 93: 4063-4070

Krizek, B., Riechmann, J., Meyerowitz, E. (1999). Use of the *APETALA1* promoter to

assay the in vivo function of chimeric MADS box genes. *Sexual Plant Reproduction* 12: 14-26

Krysan, P., Young, J., Sussman, M. (1999). T-DNA as an insertional mutagen in *Arabidopsis. Plant Cell* 11: 2283-2290

Kuhn, J., Tengler, U., Binder, S. (2001). Transcript lifetime is balanced between stabilizing stem-loop structures and degradation-promoting polyadenylation in plant mitochondria. *Molecular Cell Biology* 21: 731-742

Kvarnheden, A., Yao, J., Zhan, X., O'Brien, I., Morris, B.A.M. (2000). Isolation of three distinct *CycD3* genes expressed during fruit development in tomato. *Journal of Experimental Botany* 51: 1-9

Lanahan, M., Yen, H.-C., Giovannoni, J., Klee, H. (1994). The Never Ripe mutation blocks ethylene perception in tomato. *Plant Cell* 6: 521-530

Langridge, W., Fitzgerald, K., Koncz, C., Schell, J., Szalay, A. (1989). Dual promoter of Agrobacterium tumefaciens mannopine synthase genes is regulated by plant growth hormones. *Proceedings of the National Academy of Sciences of the United States of America* 86: 3219-3223

Lawton-Rauh, A., Alvarez-Buylla, E., Purugganan, M. (2000). Molecular evolution of flower development. *Trends in Ecology and Evolution* 4: 144-149

Lee, H., Suh, S.-S., Park, E., Cho, E., Ahn, J., Kim, S.-G., Lee, J., Kwon, Y., Lee, I. (2000). The AGAMOUS-LIKE 20 MADS domain protein integrates floral inductive pathways in *Arabidopsis. Genes and Development* 14: 2366-2376

Lee, T.-H., Kato, T., Kanayama, Y., Ohno, H., Takeno, K., Yamaki, S. (1997a). The role of indole acetic acid and acid invertase in the development of mwlon (*Cucumis melo* L. cv Prince) fruit. *Journal of Japanese Society of Horticultural Science* 65: 723-729

Lee, T.-H., Sugiyama, A., Takeno, K., Ohno, H., Yamaki, S. (1997b). Changes in content of indole-3-acetic acid and in activities of sucrose-metabolizing enzymes during fruit growth in eggplant (*Solanum melongena* L.). *Journal of Plant Physiology* 150: 292-

Lelievre, J.-M., Latche, A., Jones, B., Bouzayen, M., Pech, J.-C. (1997). Ethylene and fruit ripening. *Physiologia Plantarum* 101: 717-739

Levy, Y., Dean, C. (1998a). Control of flowering time. *Current Opinion in Plant Biology* 1: 49-54

Levy, Y., Dean, C. (1998b). The transition to flowering. *Plant Cell* 10: 1973-1989

Lewis, H., Burge, G., Schmierer, D., Jameson, P. (1996). Cytokinnins and fruit development in the kiwifruit (*Actinidia deliciosa*). I. Changes during fruit development. *Physiologia Plantarum* 98: 179-186

Liljegren, S.J., Ditta, G.S., Eshed, Y., Savidge, B., Bowman, J.L., Yanofsky, M.F. (2000). SHATTERPROOF MADS-box genes control seed dispersal in Arabidopsis. *Nature* 404: 766-770

Lincoln, J., Corde, S., Read, E., Fischer, R. (1987). Regulation of of gene expression by ethylene during *Lycopersicum esculentum* (tomato) fruit development. *Proceedings of the National Academy of Sciences of the United States of America* 84: 2793-2797

Llop-Tous, I., Barry, C., Grierson, D. (2000). Regulation of ethylene biosynthesis in response to pollination in tomato flowers. *Plant Physiology* 123: 971-978

Llop-Tous, I., Dominguez-Puigjaner, E., Palomer, X., Vendrell, M. (1999). Characterisation of two divergent endo-B-1,4-glucanase cDNA clones highly expressed in the nonclimacteric strawberry fruit. *Plant Physiology* 119: 1415-1421

Lozano, R., Angosto, T., Gomez, P., Payan, C., Capel, J., Huijser, P., Salinas, J., Martinez-Zapater, J. (1998). Tomato flower abnormalities induced by low temperatures are associated with changes of expression of MADS-box genes. *Plant Physiology* 117: 91-100

Ma, H. (1994). The unfolding drama of flower development: recent results from genetic and molecular analyses. *Genes and Development* 8: 745-756

Ma, H. (1998). To be, or not to be, a flower- control of floral mersitem identity. *Trends*

in Genetics 14: 26-32

Ma, H., dePamphilis, C. (2000). The ABCs of floral evolution. *Cell* 101: 5-8

Ma, H., Yanofsky, M.F., Meyerowitz, E.M. (1991). *AGL1-AGL6*, an *Arabidopsis* gene family with similarity to floral homeotic and transcription factor genes. *Genes and Development* 5: 484-495

Mandel, M., Bowman, J., Kempin, S., Ma, H., Meyerowitz, E., Yanofsky, M. (1992a). Manipulation of flower structure in transgenic tobacco. *Cell* 71: 133-143

Mandel, M., Yanofsky, M. (1995). The Arabidopsis *AGL8* MADS box gene is expressed in inflorescence meristems and is negativel regulated by *APETALA1*. *Plant Cell* 7: 1763-1771

Mandel, M.A., Gustafson-Brown, C., Savidge, B., Yanfosky, M.F. (1992b). Molecular characterisation of the *Arabidopsis* floral homeotic gene *APETALA1*. *Nature* 360: 1992

Mandel, M.A., Yanofsky, M.F. (1998). The Arabidopsis AGL9 MADS box gene is expressed in young flower primordia. *Sexual Plant Reproduction* 11: 22-28

Manning, K. (1998). Isolation of a set of ripening-related genes from strawberry: their identification and possible relationship to fruit quality traits. *Planta* 205: 622-631

Mao, L., Begum, D., Chuang, H., Budiman, M., Szymkowiak, E., Irish, E., Wing, R. (2000). JOINTLESS is a MADS-box gene controlling tomato flower abscission zone development. *Nature* 406: 910-913

Mapelli, S., Torti, G., Badino, M., Soressi, G. (1979). Effects of GA3 on flowering and fruit set in a mutant of tomato. *HortScience* 14: 736-737

Marcelis, L. (1993). Effect of assimilate supply on the growth of individual cucumber fruits. *Physiologia Plantarum* 87: 313-320

Marcelis, L., Hofman-Eijer, L. (1993). Effect of temperature on the growth of individual cucumber fruits. *Physiologia Plantarum* 87: 321-328

Marcelis, L., Hofman-Eijer, L. (1993). Cell division and expansion in the cucumber

fruit. *Journal of Horticultural Science* 68: 665-671

Martin, D., Proebsting, W., Parks, T., Dougherty, W., Lange, T., Lewis, M., Gaskin, P., Hedden, P. (1996). Feed-back regulation of gibberellin biosynthesis and gene expression in *Pisum sativum. Planta* 200: 159-166

Martin, G. (1998). Gene discovery for crop improvement. *Current Opinion in Biotechnology* 9: 220-226

Masia, A., Zanchin, A., Rascio, N., Ramina, A. (1992). Some biochemical and ultrastructural aspects of peach fruit development. *Journal of American Society of Horticultural Science* 117: 808-815

Mazzucato, A., Taddei, A., Soressi, G. (1998). The parthenocarpic fruit (*pat*) mutant of tomato (*Lycopersicum esculentum* Mill.) sets seedless fruits and has aberrant anther and ovule development. *Development* 125: 107-114

McKenzie, M., Mett , V., Reynolds, P., Jameson, P. (1998). Controlled cytokinin production in transgenic tobacco using a copper-inducible promoter. *Plant Physiology* 116: 969-977

Mcsteen, P., Laudencia-Chingcuanco, D., Colasanti, J. (2000). A floret by any other name: control of meristem identity in maize. *Trends in Plant Science* 5: 61-66

Meissner, R., Jacobson, Y., Melamed, S., Levyatuv, S., Shalev, G., Ashri, A., Elkind, Y., Levy, A. (1997). A new model system for tomato genetics. *Plant Journal* 12: 1465-1472

Mena, M., Ambrose, B., Meeley, R., Briggs, S., Yanfosky, M.F., Schmidt, R. (1996). Diversification of C-function activity in maize flower development. *Science* 274: 1537-1540

Mena, M., Mandel, M.A., Lerner, D., Yanfosky, M.F., Schmidt, R. (1995). A characterization of the MADS-box gene family in maize. *Plant Journal* 8: 845-854

Meyer, P. (1996). Homology-dependent gene silencing in plants. *Annual Review of Plant Physiology and Plant Molecular Biology* 47: 23-48

Michaels, S., Amasino, R. (1999). *FLOWERING LOCUS C* encodes a novel MADS domain protein that acts as a repressor of flowering. *Plant Cell* 11: 949-956

Michaels, S., Amasino, R. (2001). Loss of *FLOWERING LOCUS C* activity eliminates the late-flowering phenotype of *FRIGIDA* and autonomous-pathway mutations, but not responsiveness to vernalization. *Plant Cell* 13: 935-942

Mizukami, Y., Huang, H., Tudor, M., Hu, Y., Ma, H. (1996). Functional domains of the floral regulator AGAMOUS: characterisation of the DNA binding domain and analysis of dominant negative mutations. *Plant Cell* 8: 831-845

Mizukami, Y., Ma, H. (1992). Ectopic expression of the floral homeotic gene *AGAMOUS* in transgenic Arabidopsis plants alters floral organ identity. *Cell* 71: 119-131

Mizukami, Y., Ma, H. (1995). Separation of AG function in floral meristem determinacy from that in reproductive organ identity by expressing antisense AG RNA. *Plant Molecular Biology* 28: 767-784

Mizukami, Y., Ma, H. (1997). Determination of Arabidopsis floral meristem identity by AGAMOUS. *Plant Cell* 9: 393-408

Molinero-Rosales, N., Jamilena, M., Zurita, S., Gomez, P., Capel, J., Lozano, R. (1999). FALSIFLORA, the tomato orthologue of FLORICAULA and LEAFY, controls flowering time and floral meristem identity. *Plant Journal* 20: 685-693

Mouradov, A., Glassick, T., Hamdorf, B., Murphy, L., Marla, S., Yang, Y., Teasdale, R. (1998). Family of MADS-box genes expressed early in male and female reproductive structures of Monterey pine. *Plant Physiology* 117: 55-61

Mouradov, A., Hamdorf, B., Teasdale, R., Kim, J., Winter, K.-U., TheiBen, G. (1999). A *DEF/GLO*-like MADS-box gene from a gymnosperm: *Pinus radiata* contains an ortholog of angiosperm B class floral homeotic genes. *Developmental Genetics* 25: 245-252

Munster, T., Pahnke, J., Rosa, A., Kim, J., Martin, W., Saedler, H., Theissen, G. (1997). Floral homeotic genes were recruited from homologousMADS-box genes

preexisting in the common ancestor of ferns and seed plants. *Proceedings of the National Academy of Sciences of the United States of America* 94: 2415-2420

Murashige, T., Skoog, F. (1962). A revised medium for rapid growth and bioassays with tobacco tissue culture. *Physiologia Plantarum* 15: 473-497

Nam, Y.-W., Tichit, L., Leperlier, M., Cuerq, B., Marty, I., Lelievre, J. (1999). Isolation and characterisation of mRNAs differentially expressed during ripening of wild strawberry (*Fagaria vesca* L.) fruits. *Plant Molecular Biology* 39: 629-636

Napoli, C., Lemieux, C., Jorgensen, R. (1990). Introduction of chimeric chalcone synthase gene into petunia results in reversible co-suppression of homologous genes in *trans*. *Plant Cell* 2: 279-289

Narita, J., Gruissem, W. (1989). Tomato hydroxymethylglutaryl-CoA reductase is required early in fruit development but not during ripening. *Plant Cell* 1: 181-190

Nitsch, J. (1970). Hormonal factors in growth and development. In *The biochemistry of fruits and their products*, ed. Hulme, A., pp. 428-472. London: Academic Press

Norman, C., Runswick, M., Pollock, R., Treisman, R. (1988). Isolation and properties of cDNA clones encoding SRF, a transcription factor that binds to the c-fos serum response element. *Cell* 55: 989-1003

O'Brien, T.P., McCully, M.E. (1981) *The study of plant structure. Principles and selected methods*. Victoria, Australia: Termarcarphi Pty Ltd.

Ohara, O., Dorit, R., Gilbert, W. (1989). One-sided polymerase chain reaction: the amplification of cDNA. *Proceedings of the National Academy of Sciences of the United States of America* 86: 5673-5677

Okamuro, J.K., Caster, B., Villarroel, R., Montagu, M., Jofuku, K.D. (1997). The AP2 domain of *APETALA2* defines a large new family of DNA binding proteins in *Arabidopsis*. *Proceedings of the National Academy of Sciences of the United States of America* 94: 7076-7081

Okamuro, J.K., den Boer, B.G.W., Lotys-Prass, C., Szeto, W., Jofuku, K.D. (1996). Flowers into shoots: Photo and hormonal control of a meristem identity switch in

Arabidopsis. *Proceedings of the National Academy of Sciences of the United States of America* 93: 13831-13836

O'Neill, S. (1997). Pollination regulation of flower development. *Annual Review of Plant Physiology and Plant Molecular Biology* 48: 547-574

Ozga, J., Reinecke, D. (1999). Interaction of 4-chloroindole-3-acetic acid and gibberellins in early pea fruit development. *Plant Growth Regulation* 27: 33-38

Page, R.D.M. (1996). TREEVIEW: An application to display phylogenetic trees on personal computers. *Computer Applications in the Biosciences* 12: 357-358

Passmore, S., Maine, G., Elble, R., Christ, C., Tye, B. (1988). A Saccharomyces cerevisiae protein involved in plasmid maintenance is necessary for mating of MATa cells. *Journal of Molecular Biology* 204: 593-606

Pelaz, S., Ditta, G.S., Baumann, E., Wisman, E., Yanofsky, M.F. (2000). B and C floral organ identity functions require *SEPALLATA* MADS-box genes. *Nature* 405: 200-203

Pelaz, S., Gustafson-Brown, C., Kohalmi, S., Crosby, W., Yanofsky, M.F. (2001). *APETALA1* and *SEPALLATA3* interact to promote flower development. *Plant Journal* 26: 385-394

Pelaz, S., Tapia-Lopez, R., Alvarez-Buylla, E., Yanofsky, M. (2001). Conversion of leaves into petals in Arabidopsis. *Current Biology* 11: 182-184

Pellegrini, L., Tan, S., Richmond, T. (1995). Structure of serum response factor core bound to DNA. *Nature* 376: 490-498

Perl-Treves, R., Kahana, A., Rosenman, N., Xiang, Y., Silberstein, L. (1998). Expression of multiple *AGAMOUS*-like genes in male and female flowers oc cucumber (*Cucumis sativus* L.). *Plant and Cell Physiology* 39: 701-710

Picken, A. (1984). A review of pollination and fruit set in the tomato (*Lycopersicum esculentum* Mill.). *Journal of Horticultural Science* 59: 1-13

Pineiro, M., Coupland, G. (1998). The control of flowering time and floral identity in

Arabidopsis. *Plant Physiology* 117: 1-8

Pneuli, L., Abu-Abeid, M., Zamir, D., Nacken, W., Schwarz-Sommer, Z., Lifschitz (1991). The MADS box gene family in tomato: temporal expression during floral development, conserved secondary structures and homology with homeotic genes from *Antirrhinum* and *Arabidopsis*. *Plant Cell* 1: 255-266

Pneuli, L., Carmel-Goren, L., Hareven, D., Gutfinger, T., Alvarez, J., Ganal, M., Zamir, D., Lifschitz, E. (1998). The SELF-PRUNING gene of tomato regulates vegetative to reproductive switching of sympodial meristems and is the ortholog of *CEN* and *TFL1*. *Development* 125: 1979-1989

Pneuli, L., Hareven, D., Broday, L., Hurwitz, C. (1994a). The *TM5* MADS box gene mediates organ differentiation in the three inner whorls of tomato flowers. *Plant Cell* 6: 175-186

Pneuli, L., Hareven, D., Rounsley, S., Yanfosky, M., Lifschitz, E. (1994b). Isolation of the tomato *AGAMOUS* gene *TAG1* and analysis of its homeotic role in transgenic plants. *Plant Cell* 6: 163-173

Pollock, R., Treisman, R. (1991). Human SRF-related proteins: DNA binding properties and potential regulatory targets. *Genes and Development* 5: 2327-2341

Pouteau, S., Nicholls, D., Tooke, F., Coen, E., Battey, N. (1997). The induction and maintenance of flowering in *Impatiens*. *Development* 124: 3343-3351

Pouteau, S., Nicholls, D., Tooke, F., Coen, E., Battey, N. (1998). Transcription pattern of a FIM homologue in Impatiens during floral development and reversion. *Plant Journal* 14: 235-246

Pouteau, S., Tooke, F., Battey, N. (1998). Quantitative control of inflorescence formation in Impatiens balsamina. *Plant Physiology* 118: 1191-1201

Pratt, C. (1988). Apple flower and fruit: morphology and anatomy. *Horticultural Review* 10: 273-308

Purugganan, M., Rounsley, S., Schmidt, R., Yanofsky, M. (1995). Molecular evolution of flower development: diversification of the plant MADS-box regulatory

gene family. *Genetics* 140: 345-356

Ray, A., Robinson-Beers, K., Ray, S., Baker, S., Lang, J., Preuss, D., Milligan, S., Gasser, C. (1994). *Arabidopsis* floral homeotic gene BELL (*BEL1*) controls ovule development through negative regulation of AGAMOUS gene (*AG*). *Proceedings of the National Academy of Sciences of the United States of America* 91: 5761-5765

Rhodes, M. (1971). The climacteric and ripening of fruits. In *The biochemistry of fruits and their products*, ed. Hulme, A., pp. 521-535. London: Academic Press

Riechmann, J., Krizek, B., Meyerowitz, E. (1996). Dimerization specificity of *Arabidopsis* MADS domain homeotic proteins APETALA1, APETALA3, PISTILLATA, and AGAMOUS. *Proceedings of the National Academy of Sciences of the United States of America* 93: 4793-4798

Riechmann, J., Meyerowitz, E. (1997). MADS domain proteins in plant development. *Biological Chemistry* 378: 1079-1101

Riechmann, J.L., Heard, J., Martin, G., Reuben, L., Jiang, C.-Z., Keddie, J., Adam, L., Pineda, O., Ratcliffe, O., Samaha, R., Creelman, R., Pilgrim, M., Broun, P., Zhang, J., Ghandehari, D., Sherman, B., Yu, G.-L. (2000). *Arabidopsis* transcription factors: Genome-wide comparative analysis among eukaryotes. *Science* 290: 2105-2110

Romano, C., Hein, M., Klee, H. (1991). Inactivation of auxin in tobacco transformed with the indoleacetic acid-lysine synthetase gene of *Pseudomonas savastanoi*. *Genes and Development* 5: 438-446

Rotino, G., Perri, E., Zottini, M., Sommer, H., Spena, A. (1997). Genetic engineering of parthenocarpic plants. *Nature Biotechnology* 15: 1398-1401

Rounsley, S., Ditta, G., Yanofsky, M. (1995). Diverse roles for MADS box genes in Arabidopsis development. *Plant Cell* 7: 1259-1269

Rutledge, R., Rean, S., Nicolas, O., Fobert, P., Cote, C., Bosnich, W., Kauffeldt, C., Sunohara, G., Seguin, A., Stewart, D. (1998). Characterisation of an *AGAMOUS* homologue from the conifer black spruce (*Picea mariana*) that produces floral homeotic

conversions when expressed in *Arabidopsis*. *Plant Journal* 15: 625-634

Saitou, N., Nei, M. (1987). The neighbor-joining method: a new method for reconstructing phylogenetic trees. *Molecular Biology and Evolution* 4: 406-425

Samach, A., Onouchi, H., Gold, S., Ditta, G., Schwarz-Sommer, Z., Yanofsky, M.F., Coupland, G. (2000). Distinct roles of CONSTANT target genes in reproductive development of *Arabidopsis*. *Science* 288: 1613-1616

Sambrook, J., Fritsch, E.F., Maniatis, T. (1989) *Molecular cloning. A laboratory manual*. Cold Spring Harbor: CSH Laboratory Press.

Sanders, P., Bui, A., Weterings, K., McIntire, K., Hsu, Y.-C., Lee, P., Truong, M., Beals, T., Goldberg, R. (1999). Anther developmental defects in *Arabidopsis thaliana* male-sterile mutants. *Sexual Plant Reproduction* 11: 297-322

Sano, H., Seo, S., Orudgev, E., Youssefian, S., Ishizuka, K., Ohashi, Y. (1994). Expression of the gene for a small GTP binding protein in transgenic tobacco elevates endogenous cytokinin levels, abnormally induces salicylic acid in response to wounding, and increases resistance to tobacco mosaic virus infection. *Proceedings of the National Academy of Sciences of the United States of America* 91: 10556-10560

Savidge, B., Rounsley, S.D., Yanofsky, M.F. (1995). Temporal relationship between the transcription of two Arabidopsis MADS box genes and the floral organ identity genes. *Plant Cell* 7: 721-733

Schmitz, G., Theres, K. (1999). Genetic control of branching in Arabidopsis and tomato. *Current Opinion in Biology* 2: 51-55

Schuch, W., Bird, C., Ray, J., Smith, C., Watson, C., Morris, P., Gray, J., Arnold, C., Seymour, G., Tucker, G., Grierson, D. (1989). Control and manipulation of gene expression during tomato fruit ripening. *Plant Molecular Biology* 13: 303-311

Schwarz-Sommer, Z., Huijser, P., Nacken, W., Saedler, H., Sommer, H. (1990). Genetic control of flower development by homeotic genes in *Antirrhinum majus*. *Science* 50: 931-936

Schwechheimer, C., Zourelidou, M., Bevan, M. (1998). Plant transcription factor

studies. *Annual Review of Plant Physiology and Plant Molecular Biology* 49: 127-150

Scortecci, K., Michaels, S., Amasino, R. (2001). Identification of MADS-box gene, *FLOWERING LOCUS M*, that represses flowering. *Plant Journal* 26: 229-236

Sekhar, K., Sawhney, V. (1984). A scanning electron microscope study of the development and surface features of floral organs of tomato (*Lycopersicon esculentum*). *Canadian Journal of Botany* 62: 2403-2413

Sekhar, K., Sawhney, V. (1987). Ontogenic study of the fusion of floral organsin the normal and "solanifolia" mutant of tomato (*Lycopersicon esculentum*). *Canadian Journal of Botany* 65: 215-221

Shannon, S., Meeks-Wagner, D.R. (1993). Genetic interactions that regulate inflorescence development in Arabidopsis. *Plant Cell* 5: 639-655

Sheldon, C., Rouse, D., Finnegan, E., Peacock, W., Dennis, E. (2000). The molecular basis of vernalization: The central role of *FLOWERING LOCUS C (FLC)*. *Proceedings of the National Academy of Sciences of the United States of America* 97: 3753-3758

Shore, P., Sharrocks, A. (1995). The MADS-box family of transcription factors. *European Journal of Biochemistry* 229: 1-13

Smyth, D. (2000). A reverse trend-MADS functions revealed. *Trends in Plant Science* 5: 315-317

Smyth, D., Bowman, J.L., Meyerowitz, E.M. (1990). Early flower development in *Arabidopsis*. *Plant Cell* 2: 755-767

Sommer, H., Beltran, J.-P., Huijser, P., Pape, H., Lonnig, W.-E., Saedler, H., Schwarz-Sommer, Z. (1990). *Deficiens*, a homeotic gene involved in the control of flower morphogenesis in *Antirrhinum majus*: the protein shows homology to transcription factors. *EMBO Journal* 9: 605-613

Stam, M., de Bruin, R., van Blokland, R., van der Hoorn, R.A.L., Mol, J.N.M., Kooter, J.M. (2000). Distinct features of post-transcriptional gene silencing by antisense transgenes in single copy and inverted T-DNA repeat loci. *Plant Journal* 21: 27-42

Sung, S., Yu, G., Nam, J., Jeong, D., An, G. (2000). Developmentally regulated expression of two MADS-box genes, MdMADS3 and MdMADS4, in the morphogenesis of flower buds and fruits in apple. *Planta* 210: 519-528

Sung, S.-K., An, G. (1997). Molecular cloning and characterisation of a MADS-box cDNA clone of the Fuji apple. *Plant Cell Physiology* 38: 484-489

Surridge, C. (2001). Plant development. De-pipping the pippin. *Nature Reviews Molecular Cell Biology* 2: 162-163

Takeno, K., Ise, H., Minowa, H., Dounowaki, T. (1992). Fruit growth induced by benzyladenine in *Cucumis sativus* L.: influence of benzyladenine on cell division, cell enlargement and indole-3-acetic acid content. *Journal of Japanese Society of Horticultural Science* 60: 915-920

Tan, S., Richmond, T. (1998). Crystal structure of the yeast MATalpha2/MCM1/DNA ternary complex. *Nature* 391: 660-666

Tandre, K., Svenson, M., Svensson, M., Engstrom, P. (1998). Conservation of gene structure and activity in the regulation of reproductive organ development of conifers and angiosperms. *Plant Journal* 15: 615-623

Theißen, G. (2001a). Development of floral organ identity: stories from the MADS house. *Current Opinion in Plant Biology* 4: 75-85

Theißen, G., Saedler, H. (2001b). Plant biology. Floral quartets. *Nature* 409: 469-471

Theissen, G., Becker, A., Rosa, A., Kanno, A., Kim, J., Munster, T., Winter, K.-U., Saedler, H. (2000). A short history of MADS-box genes inplants. *Plant Molecular Biology* 42: 115-149

Thompson, J.D., Higgins, D.G., Gibson, T.J. (1994). CLUSTAL W: improving the sensitivity of progressive multiple sequence alignment through sequence weighting, position-specific gap penalties and weight matrix choice. *Nucleic Acids Research* 22: 4673-4680

Tooke, F., Battey, N.H. (2000). A leaf-derived signal is a quantitative determinant of floral form in *Impatiens*. *Plant Cell* 12: 1837-1847

van der Krol, A.R., Mur, L.A., Beld, M., Mol, J., Stuitje, A.R. (1990). Flavonoid genes in Petunia: addition of a limiting number of copies may lead to a suppression of gene expression. *Plant Cell* 2: 291-299

Varga, A., Bruinsma, J. (1986). Tomato. In *Handbook of fruit set and development*, ed. Monselise, S., pp. 461-481. Florida: CRC Press

Vivian-Smith, A., Luo, M., Chaudhury, A., Koltunow, A. (2001). Fruit development is actively restricted in the absence of fertilization in *Arabidopsis*. *Development* 128: 2321-2331

Wassenegger, M., Pelissier, T. (1998). A model of RNA-mediated gene silencing in higher plants. *Plant Molecular Biology* 37: 349-362

Weigel, D., Ahn, J., Blazquez, M., Borevitz, J., Christensen, S., Fankhauser, C., Ferrandiz, C., Kardailsky, I., Malancharuvil, E., Neff, M., Nguyen, J., Sato, S., Wang, Z.-Y., Xia, Y., Dixon, R., Harrison, M., Lamb, C., Yanfosky, M.F., Chory, J. (2000). Activation tagging in Arabidopsis. *Plant Physiology* 122: 1003-1013

Weigel, D., Akvarez, J., Smyth, D.R., Yanofsky, M.F., Meyerowitz, E.M. (1992). *LEAFY* controls floral meristem identity in Arabidopsis. *Cell* 69: 843-859

Weigel, D., Meyerowitz, E.M. (1994). The ABCs of floral homeotic genes. *Cell* 78: 203-209

Western, T., Haughn, G. (1999). *BEL1* and *AGAMOUS* genes promote ovule identity in *Arabidopsis thaliana*. *Plant Journal* 18: 329-336

Whittaker, D., Smith, G., Gardner, R. (1997). Expression of ethylene biosynthetic genes in *Actinidia chinensis* fruit. *Plant Molecular Biology* 34: 45-55

Wilson, R.N., Heckman, J.W., Sommerville, C.R. (1992). Gibberellin is required for flowering in *Arabidopsis thaliana* under short days. *Plant Physiology* 100: 403-408

Yang, W.-C., Sundaresan, V. (2000). Genetics of gametophyte biogenesis in *Arabidopsis*. *Current Opinion in Plant Biology* 3: 53-57

Yanofsky, M., Ma, H., Bowman, J., Drews, G., Feldmann, K., Meyerowitz, E. (1990). The protein encoded by the *Arabidopsis* homeotic gene *agamous* resembles transcription factors. *Nature* 346: 35-39

Yao, J., Dong, Y., Morris, B.A. (2001). Parthenocarpic apple fruit production conferred by transposon insertion mutations in a MADS-box transcription factor. *Proceedings of the National Academy of Sciences of the United States of America* 98: 1306-1311

Yao, J.-L., Dong, Y.-H., Kvarnheden, A., Morris, B. (1999). Seven MADS-box genes in apple are expressed in different parts of the fruit. *Journal of American Society of Horticultural Science* 124: 8-13

Yu, D., Kotilainen, M., Pollanen, E., Mehto, M., Elomaa, P., Helariutta, Y., Albert, V., Teeri, T. (1999). Organ identity genes and modified patterns of flower development in *Gerbera hybrida* (Asteraceae). *Plant Journal* 17: 51-62

Zhang, H., Forde, B. (1998). An *Arabidopsis* MADS box gene that controls nutrient-induced changes in root architecture. *Science* 279: 407-409

Appendix A: GenBank accession numbers of protein sequences

Protein name	Accession numbers
AGAMOUS (AG)	P17839
AGL1	P29381
AGL11	Q38836
AGL12	Q38841
AGL15	Q38847
AGL17	Q38840
AGL20	T00879
AGL3	P29383
AGL8	Q38876
APETALA1	S27109
APETALA3	P35632
DEFH49	S78015
DEFICIENS	P23706
FBP2	Q03489
FBP20	AAK21251
GLOBOSA	Q03378
JOINTLESS	AAG09811
PISTILLATA	P48007
SEP1	P29382
SEP2	P29384
SEP3	O22456
SQUAMOSA	S20886
STMADS16	AAB94005
TAG1	Q40168
TM29	CAC83066
TM3	S23729
TM4	Q40170
TM5	Q42464
TM6	S23731
TM8	S23732
TOBGLO	Q03416

Appendix B: pART7 cloning vector

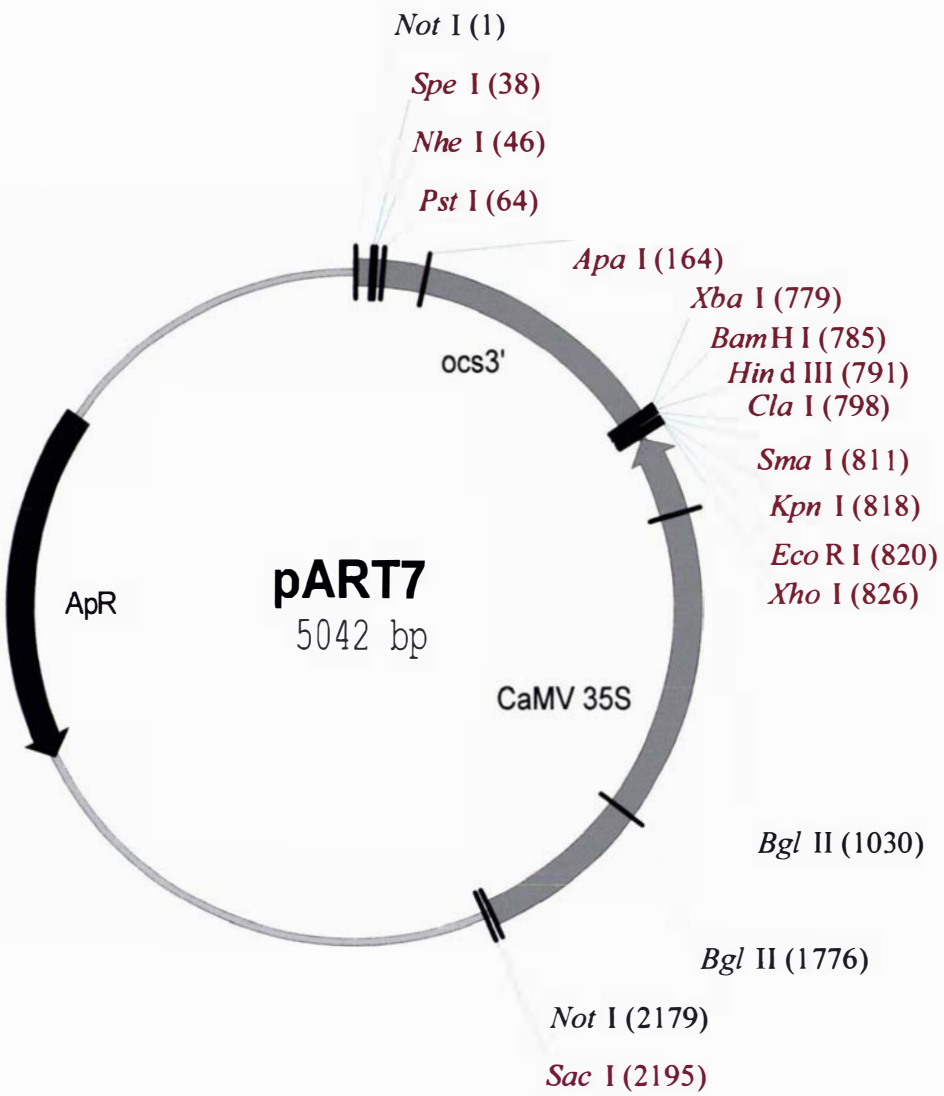

Appendix C: pART27 binary vector

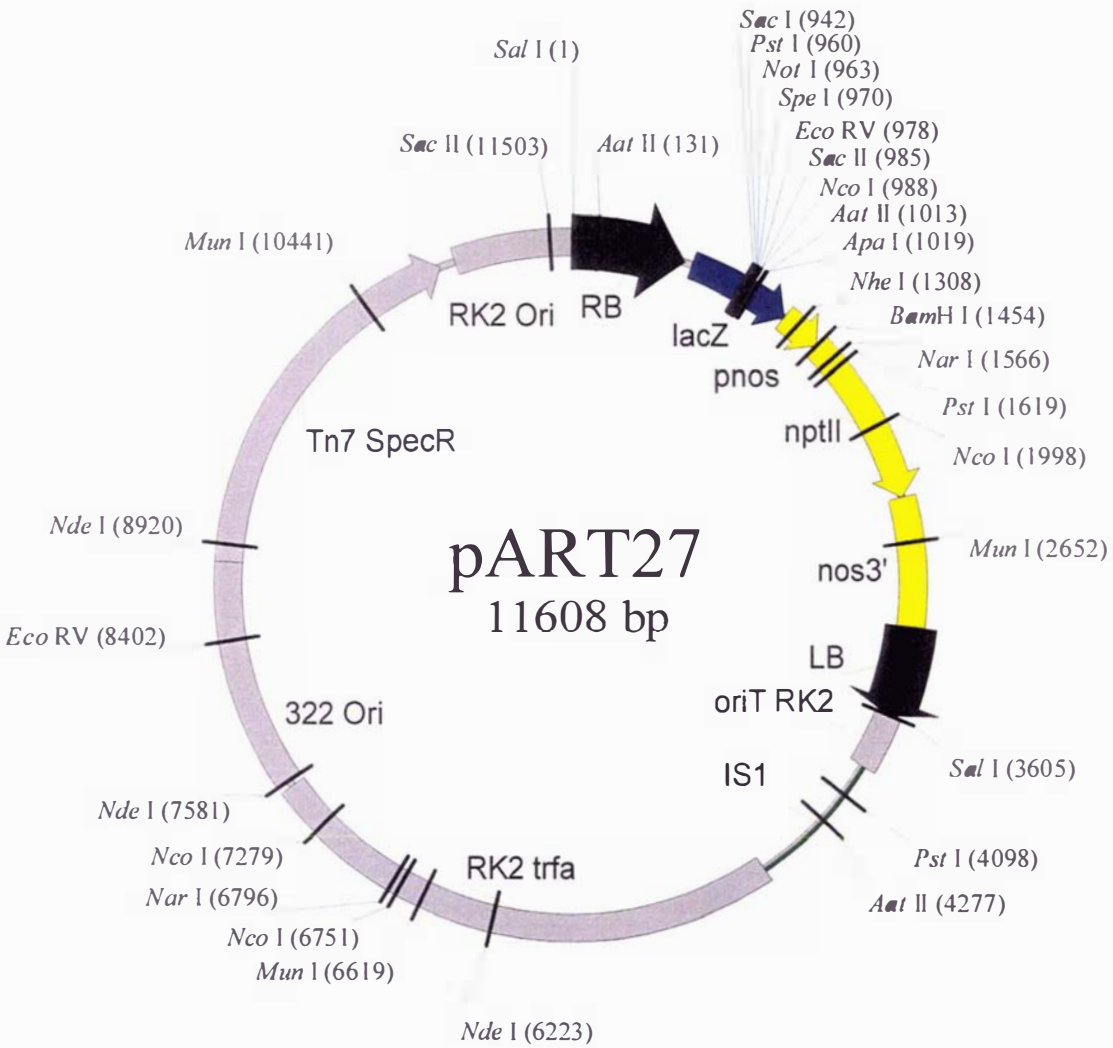

Appendix D: *TM29* genomic DNA sequence[1]

ATGGGTAGAGGAAGAGTTGAGCTGAAGAGGATAGAAAACAAGATAAATAGACAAGTCACTT
TTGCAAAGAGGAGAAATGGATTGCTCAAAAAAGCTTATGAACTATCTGTGCTTTGTGATGC
TGAAGTTGCTCTACTCGTTTTCTCTAATCGTGGAAAACTCTATGAATTCTGCAGCACAAAC
AAGTAATTTTTTTTCTTCTCTATTCTAAGATCTGAAATTAGGATTGAAGCTCTATATTATC
AAAGATCTGTTACATACAACATGAAAAATCATACTCCCATCCTAAAGTTGTTCATAAAATA
AATAAAACATATAGATCTTATGTTTTAGTGCGTTTTTCTAGGAGATCACACTATTTTTGTT
TCCTTAGTGACTCGAATTCACAATTTTAGAGTTGGAGATGGAGGTTTTTTATCATCCGAGC
AACCTCTCGTGTCAGATCCTGAGTTTTAAAATCGAATAAAGTAAGAAAATGCACTTAATAT
TGTTTAGATCGATCATTAGACAATCTCTTCTTATAAAGAAAAGAGTAAATGGACCGAGTAT
AATCGTACCTGCAGATCTGAATAACCAGATAAAACGTCTTCCAGTCCTTAATTCTACACCT
TTTTTGATGATGGCAAATAAGACTGATATGATAAAAGACTCATAATATCCTGTTTTTACCT
CTGTGATCATAGACATTTTGTGATATAAATCAGTCCACCGGGTATTTCTGGCGTGCTTCAT
AAAGTTCATTCACTTTAAAATTTATAGCTAAATATTGACTTTAATTTATAATAATATAGAT
CAGTTCAAATTTTAAGGAAGCCTAGGAAATATCTTTTGGGTAATCTCATGACATGCATATA
TATTTTTTTTTTCATCCGTGAAGCAAATTTCTATTTAGTTATCATTCGAGCTGTGACTTCT
TTAATATGAAAGACTGTAAATTTTCACGGGGGGGAAATTGTATAGAGTACTTGGATTAGTG
TAGTAGTCAAAAATTCATGAAGTTGATTGAGTGGCCTTCAACTTAACATATACGGTTAAAA
GAATTTATGTTATTTATATCGCTAGTGTAAGGACTTATCGGGTCATTAAAAAGATGTGATC
ATTATTGAATATATGCATAATCTTAAAAATAAAAATAATTACAATATACAACAAGTAATGG
TTCTAATGAGGAAGTAGGTCCATTAGTAAGTAGCATTTCCTTCATATCTCTGGGCATTGAA
ACCAGTTTTTGAAACTGTTTTCTACCAAGGATTATGGCTAACTCAAGTCAGGTTGGTAATC
GTAGTTTTAGAATATGATAAAAAATGATTCATTGGTTTACAATAAGTAGAAATTATTTACA
TTGTTTGTCCATCATATAAATGTTGATCCAAATAATTTTACAAAGAGGCGTAGATTTTATC
CTTAATTATCTCTTGAGACATTATTCGAACATGTTTAATATTTTCATCCCGTTTATAGCTT
TTGCATGGCCATATAGGGCAGGCAAAATGTTTTTTTTTTTAAAATAAAAAGAGTTGCGAGC
TAGCACATTTTTTTATCCGTGTTAAATAAAGATGGATCGAATATTTATTTATACTTGCTCA

TATTTGATTCAATCCAATCATTTGAGTATTAATAACTTTTTCCTTTTTATTTATCTTGTGC
AACAGTATGCTCAAAACACTTGATAGGTACCAAAAGTGCAGCTATGGAACATTGGAAGTCA
ATCGATCAATCAAAGATAATGAGGTAACAAATGCTACTAATTTCGTTGACGTCACCTTTTC
AAAGGATGAACGTATGTATGATTTTTACCATAATATAACTTACTATATGTAAGTTAGTTGC
TTTAATTTCTGACATGATCGAATGCTGCTCGATCACAATTTTTTCTGATCGAATTTTTTTC
GCAAATAAAGGAAGAATTTTTTTTTTATATATATAGACCCCTTTTTCCAAGTTATTGATCC
CATCTTGTGAGCCATTGCAGCAAAGCAGCTATAGGGATACTTGAAACTCAAAGCCAAATAT
GAGTCGCTGCAGCGATATCAAAGGTAATTAACTACTAGCTAGAAAGATAATCTATAGGTGT
CAAATGAAACCTAAATATTAGTGACCCGTTCAATTCGTCCAAAATTTTATTCTCAAACATG
GTTCAAGAATGGGCTAAATCATAACACGTTTAGTCAGAATCCATTTGCCAACTTACCGCAG
TTTTTATGCCCAAATTAACCCAACTTTCGACTTGATAATGAAATAGGCGTCGGTGCAGTTA
TGTGATCATCGCGAAATGTCATCAGTTTCTATGATACTTTAGTTTCTCTATTCTGTCTATT
TTAATTTTTTTTAATGTTTAGTGTCGTCTAAAAGCACTAAATAAAATTAGATATATTCATT
TTTTAGTTTAATTTGACTATAAAAAATATTTATCTAAACAACAGTCTAGTAACATTTTATT
AAATCCACAACTTTCGATATATTTATATAATCTTTTATGTACTATGTGGAGGTTTAGAGTA
TCACCAATTAACGGTGTTTATGATGCTATTAATTTCAAAATAAATAAATATACCGACCTAA
ATAAGCTTATATAAGTGACATCTTTGGACGCTCTAGTCACAAATATTGTATTTTCTGGCTT
TTCTTTTTGTTGAGAAATTGGTTTGCCTTTATTAGTTTGGTTTATAAATTACTCTGGTATG
TAAGTATTATTCAAATTAAGTGAGTCGGGTCATGATCTAATCCATTATTTTTGCTCAGCAC
ATATGCTTTTAGTTGGATCAATTATTTATTCAGCCCATTTAAATCCGATTATCCATTTGAT
ACCCCTATGTTAACCATAATCATGCTGTCTAAATTATTTGACATAGAAGGATGTACACAAA
TTGTATTCTTGATAACTTATTATACTTTAACAGACACCTTCTTGGAGATGAGTTGGGGCCT
CTGACTATAGATGATCTTGAGCATCTTGAAGTCCAACTAGATACTTCCCTCAAACACATTA
GGTCCACCAGGGTAAGCTTAACTTATAACAAATTTTTAGACCAATTTCAATTCAAGTATTC
TGATTGTTATCTTCTGGCTGCTCTATAGACACAAATGATGCTTGATCAGCTTTCTGATCTT
CAAACTAAGGTATTCTCATTTGATTCTAAAATGGTCAACATGATGCATGTGTTCAATAGTT
AGTAACTTTACTATTTTATCATAACAGGAGAAATTGTGGAATGAGGCTAACAAGGTTCTTG
AAAGAAAGGTAGGTTGCCCATACATGTGATTCTAACTCATTTTCTAGCTCCATGTATATTA
CTAGTTGTATTGTGATTGATTTTTGTTAGATTAGGTTTATTTTTCGTCAATTTTTTTTTTT
TTACCTAACTAAGTTGCTAAAGTAAAGTATTTCTGTTGAAGAGTCTCACATCGGCTCTTTT
TAAGGAATGGGTATATGGGAAATTGTGAGCTAGTTTTTAGGGTTCAGTAATTATTAAGCCG
AAGATCAATATTCCTTATTGATTGATGTACCAAAGTCATTGAATTGCATATAATTTGTTAG

CAG**ATGGAAGAAATATATGCTGAAAACAACATGCAACAAGCATGGGGTGGTGGTGAGCAAA**
GTCTCAATTATGGTCAGCAGCAACATCCTCAATCTCAGGGTTTCTTCCATCCTCTAGAGTG
CAACTCTTCCTTGCAAATTGGGTAAATTCTACCATATTCATTCTATATATATCTTAATTTT
TAATTTATCCTATCTATTTGACATCTGCCCATTAGTTCACAAGTGAGATTTTTTGAAAAAA
AAAAGGAAGAAGCAAACCAAATATAGCTTTTCATACTCTAGAGATATCGATGAAAGTTATT
CACACAATTAAAGTGCTTGGCTAAAACAAAAATGTTATTGTTTTGATTTAATGCAGGTA**CG**
ATCCAATAACAACTTCAAGCCAAATAACAGCAGTAACAAATGCCCAAAACGTGAATGGTAT
GATACCTGGTTGGATGCTGTGA

[1] The translational start and stop codons are underlined. The exons are in black letters while the intron sequences are in red.

Appendix E: Alignment of short MADS-box sequences